

THEORY OF CONTROL OF QUANTUM SYSTEMS

by


SONJA G. SCHIRMER

A DISSERTATION

Presented to the Department of Mathematics
and the Graduate School of the University of Oregon
in partial fulfillment of the requirements
for the degree of
Doctor of Philosophy


March 2000

'THEORY OF CONTROL OF QUANTUM SYSTEMS', a dissertation prepared by Sonja G. Schirmer in partial fulfillment of the requirements for the Doctor of Philosophy degree in the Department of Mathematics. This dissertation has been approved and accepted by



Dr John Leahy,
Co-chair of the Examining Committee
3/7/00


Date



Dr Marvin Girardeau,
Co-chair of the Examining Committee
3/7/00

Date

- Committee in Charge:
- Dr John Leahy, Co-Chair
 - Dr Marvin Girardeau, Co-Chair
 - Dr Richard Koch
 - Dr Jerry Wolfe
 - Dr Jim Isenberg
 - Dr Jeffrey Cina

Accepted by: 

Dean of the Graduate School



UNIVERSITY OF TORONTO

DIAMOND WHITE CAPSULE

FOR OUTSIDE USE

© 2000 Sonja G. Schirmer

An Abstract of the Dissertation of
Sonja G. Schirmer for the degree of Doctor of Philosophy
in the Department of Mathematics to be taken March 2000
Title: THEORY OF CONTROL OF QUANTUM SYSTEMS

Approved:



Dr John Leahy, Co-chair



Dr Marvin Girardeau, Co-chair

We investigate the problem of optimal control of mixed-state quantum systems using a quantum statistical mechanics model and a Liouville space formulation of Hamiltonian and dissipative dynamics. The problem of optimal control is formulated as a problem of maximization of the ensemble average of an observable of the system, subject to certain constraints.

In chapter two, we address the question of kinematical constraints on the evolution of the system and derive bounds on the expectation value of arbitrary observables for mixed-state quantum systems. The issue of dynamical realizability of the kinematical bounds is discussed and results on controllability of quantum systems are summarized in chapter three. In chapter four, we present an efficient, rapidly convergent feedback algorithm for constructing optimal controls numerically and prove its convergence properties.

Finally, we apply our results on kinematical bounds and controllability, as well as the algorithm presented in chapter four, to several optimal control problems, including maximization of the vibrational energy of a molecular bond, maximization of the top-level population for a three-level system with and without dissipation, and maximization of the energy for systems consisting of non-interacting subsystems, and discuss the results.

CURRICULUM VITAE

NAME OF AUTHOR: Sonja G. Schirmer

GRADUATE AND UNDERGRADUATE SCHOOLS ATTENDED:

University of Oregon
University of Stuttgart

DEGREES AWARDED:

Doctor of Philosophy in Mathematics, 2000, University of Oregon
Master of Arts in Mathematics, 1996, University of Oregon

AREAS OF SPECIAL INTEREST:

Quantum Systems
Control Theory and Optimization
Numerical Methods

PROFESSIONAL EXPERIENCE:

Graduate Teaching Fellow, Department of Mathematics, University
of Oregon, Eugene, 1995-2000

Teaching Assistant, Department of Chemistry, University of
Oregon, Eugene, 1998-1999

AWARDS AND HONOURS:

University of Oregon Scholarship, 1994
Fulbright Professional Enhancement Grant, 1995
Mathematical Sciences Research Institute, Berkeley, Summer
Grant, 1999
Johnson Research Fellowship, 1999

PUBLICATIONS:

Girardeau, M.D., M. Ina, S. G. Schirmer, T. Gulsrud, Phys. Rev.
A 55, R1565 (1997)

Girardeau, M.D., S.G. Schirmer, J.V. Leahy, R.M. Koch, Phys. Rev. A 58, 2684 (1998)

Schirmer, S.G., M.D. Girardeau, J.V. Leahy, Phys. Rev. A. 61, 012101 (2000)

ACKNOWLEDGEMENTS

The author expresses sincere appreciation to Professors John V. Leahy and Marvin D. Girardeau for their assistance with this research and their significant contributions to my professional development. Thanks are also due to Professor Richard M. Koch for the many valuable discussions on various topics of mathematics and science, which so greatly promoted my development as a mathematical scientist. Furthermore, I would like to express my gratitude to all the members of my Ph.D. committee for their valuable input and encouragement with this research.

Finally, I would like to express my sincere appreciation to Professor Herschel Rabitz from the Chemistry Department of Princeton University, for his valuable suggestions and inspiration for future research in this exciting area.

Last but not least, I would like to thank all my personal friends, but in particular Frank Langbein, Kelly Pearson and Tan Zhang, for being my friends when I needed them most, for encouraging me to pursue my dream, and for making me enjoy life.

TABLE OF CONTENTS

Chapter	Page
I. INTRODUCTION.....	1
Motivation and Outline.....	1
Quantum Statistical Mechanics Model.....	2
Liouville Space Formulation and Dissipative Dynamics.....	5
The Optimal Control Problem.....	7
II. BOUNDS ON OPTIMIZATION OF OBSERVABLES.....	11
Kinematical Attainability of Target States.....	11
Kinematical Bounds on the Expectation Values of Observables.....	11
Proof of Kinematical Bounds Theorem.....	13
Improved Bounds for 'Decoupled Systems'.....	16
III. CONTROLLABILITY OF QUANTUM SYSTEMS.....	21
Dynamical Realizability of Kinematical Bounds.....	21
Algebraic Condition for Controllability.....	22
Controllability Calculations.....	24
IV. CONSTRUCTING OPTIMAL CONTROLS.....	32
Euler-Lagrange Equations.....	32
Entangled Feedback Algorithm.....	34
Convergence Behaviour of the Control Algorithm.....	35
Numerical Implementation.....	40
V. ILLUSTRATIVE COMPUTATIONS.....	43
Energy Maximization for a Four-Level Morse Oscillator Model of a Diatomic Molecule.....	43
Energy Maximization for 'Decoupled' Systems.....	58
Maximization of the Top Level Population for a Three-Level System.....	62
VI. CONCLUSION.....	74
APPENDIX	
A. INTERACTIVE QUANTUM CONTROL MATLAB MAIN PROGRAM.....	76

	Page
B. MATLAB SUBROUTINE TO DETERMINE KINEMATICAL BOUNDS....	79
C. MATLAB SUBROUTINE TO DETERMINE CONTROLLABILITY.....	80
D. MATLAB SUBROUTINE TO FIND OPTIMAL CONTROL.....	81
E. AUXILLARY SUBROUTINES.....	87
BIBLIOGRAPHY.....	98

LIST OF FIGURES

Figure	Page
1. Final Yield as a Function of λ	47
2. Energy Maximization for a Four-Level Morse Oscillator initially in the Ground State with Control Parameters $J = 400, \lambda = 4$	48
3. Energy Maximization for a Four-Level Morse Oscillator Initially in the Ground State with Control Parameters $J = 400, \lambda = 4$	49
4. Energy Maximization for a Four-Level Morse Oscillator Initially in the Ground State with Control Parameters $J = 400, \lambda = 2$	50
5. Energy Maximization for a Four-Level Morse Oscillator Initially in the Ground State with Control Parameters $J = 400, \lambda = 1$	51
6. Energy Maximization for a Four-Level Morse Oscillator Initially in the Ground State with Control Parameters $J = 400, \lambda = 8$	52
7. Energy Maximization for a Four-Level Morse Oscillator Initially in Thermal Equilibrium with Control Parameters $J = 800, \lambda = 4$	53
8. Energy Maximization for a Four-Level Morse Oscillator Initially in Thermal Equilibrium with Control Parameters $J = 400, \lambda = 4$	54
9. Energy Maximization for a Four-Level Morse Oscillator Initially in Thermal Equilibrium with Control Parameters $J = 400, \lambda = 2$	55
10. Energy Maximization for a Four-Level Morse Oscillator Initially in Thermal Equilibrium with Control Parameters $J = 400, \lambda = 1$	56
11. Energy Maximization for a Four-Level Morse Oscillator Initially in Thermal Equilibrium with Control Parameters $J = 400, \lambda = 8$	57

	Page
12. Energy Maximization for a Decoupled Four-Level System (Case A) Initially in Thermal Equilibrium with Control Parameters $J = 400, \lambda = 4 \dots$	60
13. Energy Maximization for a Decoupled Four-Level System (Case B) Initially in Thermal Equilibrium with Control Parameters $J = 400, \lambda = 4 \dots$	61
14. Maximization of the Top-Level Population for a Three-Level System Initially in the Ground State with Control Parameters $J = 400, \lambda = 4 \dots$	64
15. Maximization of the Top-Level Population for a Three-Level System Initially in the Ground State with Control Parameters $J = 400, \lambda = 8 \dots$	65
16. Maximization of the Top-Level Population for a Three-Level System Initially in the Ground State with Control Parameters $J = 400, \lambda = 10 \dots$	66
17. Maximization of the Top-Level Population for a Three-Level System Initially in the Ground State with Control Parameters $J = 400, \lambda = 12 \dots$	67
18. Maximization of the Top-Level Population for a Three-Level System Initially in the Ground State with Control Parameters $J = 4000, \lambda = 30 \dots$	68
19. Maximization of the Top-Level Population for a Three-Level System Initially in the Ground State with Control Parameters $J = 400, \lambda = 4 \dots$	69
20. Maximization of the Top-Level Population for a Three-Level System Initially in the Ground State with Control Parameters $J = 400, \lambda = 8 \dots$	70
21. Maximization of the Top-Level Population for a Dissipative Three-Level System Initially in the Ground State with Control Parameters $J = 800, \lambda = 10 \dots$	71
22. Maximization of the Top-Level Population for a Dissipative Three-Level System Initially in the Ground State with Control Parameters $J = 800, \lambda = 10 \dots$	72
23. Maximization of the Top-Level Population for a Dissipative Three-Level System Initially in the Ground State with Control Parameters $J = 4000, \lambda = 30 \dots$	73

LIST OF TABLES

Table		Page
1.	Dimensions of the Lie Algebras for Model System (111.9) for various N	27
2.	Dimensions of the Lie Algebras for Various Model Systems for N = 4	28
3.	Dimensions of the Lie Algebras for Various Model Systems for N = 6	29
4.	Dimensions of the Lie Algebras for Various Model Systems for N = 8	30

CHAPTER I INTRODUCTION

I.1 Motivation and Outline

Recent advances in laser technology have opened up new possibilities for laser control of quantum phenomena [1], such as control of molecular quantum states, chemical reaction dynamics or quantum computers to mention only a few, and if the history of macro-scale engineering is any indication, then achieving control of micro-scale systems and quantum phenomena will lead to substantial technological breakthroughs and new applications, many of which we cannot even conceive today.

The limited success of initially advocated control schemes based largely on physical intuition in both theory and experiment [1, 2, 3, 4, 5, 6], has prompted researchers in recent years to systematically study these systems using control theory. In line with this work, we investigate in this dissertation the problem of optimal control of quantum systems using control theory, quantum statistical mechanics and Liouville space theory.

In chapter one, we describe the quantum statistical mechanics model, the Liouville space formulation of dissipative dynamics, and formulate the problem of optimal control for mixed-state quantum systems. The mixed-state quantum system formulation, while slightly more complicated than the pure-state formulation, allows us to consider applications that require controlling systems initially in thermal equilibrium, or dissipative systems, which can not be treated using pure-state dynamics.

The problem of optimal control is usually formulated as a problem of maximization (or minimization) of the expectation value of an observable of the system, subject to certain constraints. Since the actual value of the desired maximum may not be known, it is important to at least have bounds on the expectation value of observables. This problem is addressed in chapter two, where we focus on finding bounds on the expectation value

of observables that are independent of the specifics of the control problem, arising purely from kinematical constraints.

The question of whether the kinematical bounds derived can be dynamically realized by controlling the system leads to an investigation of the problem of dynamical reachability of target states and in particular of controllability of quantum systems in chapter three.

Once controllability, or at least the dynamical realizability of the aim of control, is established, the main problem that needs to be solved, is the construction of an optimal control that steers the system from its initial state to a target state, for which the aim of control is achieved. In chapter four, we therefore present an efficient, rapidly convergent feedback algorithm for finding optimal controls and prove its convergence properties.

In chapter five, we apply our results on kinematical bounds and controllability, as well as the algorithm presented in chapter four, to several optimal control problems, including maximization of the vibrational energy of a molecular bond, maximization of the top-level population for a three-level system with and without dissipation, and maximization of the energy for systems consisting of non-interacting subsystems, and discuss the results.

1.2 Quantum Statistical Mechanics Model

Our model is a mixed-state quantum system. A *mixed state*, not to be confused with a superposition state, is an ensemble of independent (pure) quantum states $|\Psi_n(t)\rangle$ together with a discrete probability distribution that assigns each of these pure states a certain probability w_n so that

$$0 \leq w_n \leq 1 \quad \forall n, \quad \sum_n w_n = 1. \quad (\text{I.1})$$

A mixed state can always be represented by a density operator $\hat{\rho}(t)$ on the Hilbert space of pure states \mathcal{H} [7]

$$\hat{\rho}(t) = \sum_n w_n |\Psi_n(t)\rangle\langle\Psi_n(t)|, \quad (\text{I.2})$$

where $|\Psi_n(t)\rangle$ are orthonormal states in \mathcal{H} and $|\Psi_n(t)\rangle\langle\Psi_n(t)|$ is the projector onto the subspace spanned by $|\Psi_n(t)\rangle$. We shall always assume that the set $\{|\Psi_n(t)\rangle : n = 1, 2, \dots\}$ forms an orthonormal basis of \mathcal{H} . If the set of independent pure states $|\Psi_n(t)\rangle$ with non-zero probability w_n is not a complete set then we simply extend it by adding independent quantum states with zero probability.

The pure states $|\Psi_n(t)\rangle$ satisfy the *Schrödinger equation*

$$i\hbar \frac{\partial}{\partial t} |\Psi_n(t)\rangle = \hat{H} |\Psi_n(t)\rangle, \quad (\text{I.3})$$

where \hat{H} is the total Hamiltonian of the system. We define the time-evolution operator or propagator $\hat{U}(t, t_0)$ by requiring that for any arbitrary element $|\Psi_n(t)\rangle$ in \mathcal{H} ,

$$|\Psi_n(t)\rangle \equiv \hat{U}(t, t_0) |\Psi_n(t_0)\rangle. \quad (\text{I.4})$$

Substituting equation (I.4) into the Schrödinger equation (I.3) leads to

$$i\hbar \frac{\partial}{\partial t} \hat{U}(t, t_0) = \hat{H} \hat{U}(t, t_0), \quad (\text{I.5})$$

i.e., the propagator satisfies the Schrödinger equation as well. Since the Hamiltonian \hat{H} is Hermitian, it immediately follows that the propagator is a unitary operator.

Taking the adjoint of both sides of equation (I.4) leads to

$$\langle\Psi_n(t)| = \langle\Psi_n(t_0)| \hat{U}(t, t_0)^\dagger, \quad (\text{I.6})$$

where $\hat{U}(t, t_0)^\dagger$ denotes the adjoint of $\hat{U}(t, t_0)$. Thus, given a mixed initial state

$$\hat{\rho}_0 = \hat{\rho}(t_0) = \sum_n w_n |\Psi_n(t_0)\rangle\langle\Psi_n(t_0)|, \quad (\text{I.7})$$

the time-evolved state $\hat{\rho}(t)$ is given by

$$\begin{aligned}
 \hat{\rho}(t) &= \sum_n w_n |\Psi_n(t)\rangle \langle \Psi_n(t)| \\
 &= \sum_n w_n \hat{U}(t, t_0) |\Psi_n(t_0)\rangle \langle \Psi_n(t_0)| \hat{U}(t, t_0)^\dagger \\
 &= \hat{U}(t, t_0) \left[\sum_n w_n |\Psi_n(t_0)\rangle \langle \Psi_n(t_0)| \right] \hat{U}(t, t_0)^\dagger \\
 &= \hat{U}(t, t_0) \hat{\rho}_0 \hat{U}(t, t_0)^\dagger
 \end{aligned} \tag{I.8}$$

Differentiating this identity with respect to time leads to

$$\frac{\partial}{\partial t} \hat{\rho}(t) = \left[\frac{\partial}{\partial t} \hat{U}(t, t_0) \right] \hat{\rho}_0 \hat{U}(t, t_0)^\dagger + \hat{U}(t, t_0) \hat{\rho}_0 \left[\frac{\partial}{\partial t} \hat{U}(t, t_0)^\dagger \right]. \tag{I.9}$$

Inserting equation (I.5) and its adjoint

$$-i\hbar \frac{\partial}{\partial t} \hat{U}(t, t_0)^\dagger = \hat{U}(t, t_0)^\dagger \hat{H}^\dagger \tag{I.10}$$

into the previous equation, multiplying both sides by $i\hbar$ and noting that $\hat{H} = \hat{H}^\dagger$, we obtain

$$\begin{aligned}
 i\hbar \frac{\partial}{\partial t} \hat{\rho}(t) &= \hat{H} \hat{U}(t, t_0) \hat{\rho}_0 \hat{U}(t, t_0)^\dagger - \hat{U}(t, t_0) \hat{\rho}_0 \hat{U}(t, t_0)^\dagger \hat{H} \\
 &= \hat{H} \hat{\rho}(t) - \hat{\rho}(t) \hat{H} = [\hat{H}, \hat{\rho}(t)]
 \end{aligned}$$

Thus, in a non-dissipative quantum system, a mixed state represented by $\hat{\rho}(t)$ satisfies the dynamical law

$$i\hbar \frac{\partial}{\partial t} \hat{\rho}(t) = [\hat{H}, \hat{\rho}(t)], \tag{I.11}$$

called the *quantum Liouville* or Liouville-von Neumann equation.

Observables are represented by Hermitian operators \hat{A} on \mathcal{H} . Their *expectation value* or ensemble average is defined by

$$\langle \hat{A}(t) \rangle = \text{Tr} (\hat{A} \hat{\rho}(t)), \tag{I.12}$$

where $\text{Tr} ()$ denotes the trace.

I.3 Liouville Space Formulation and Dissipative Dynamics

The set of bounded linear operators \hat{A} on \mathcal{H} forms itself Hilbert space, in the literature often called Liouville space. We assign to each operator \hat{A} on \mathcal{H} a Liouville ket $|A\rangle\rangle$ denoting its representation in Liouville space. Given a matrix representation of \hat{A} with respect to a basis $\{|n\rangle, n = 1, 2, \dots, \}$ for \mathcal{H} , we obtain the corresponding Liouville space representation with respect to the associated Liouville basis by rearranging the matrix elements into a column vector. The dual of $|A\rangle\rangle$ is the Liouville bra $\langle\langle A|$, whose matrix representation is a row vector. The inner product in this Liouville space is defined by

$$\langle\langle A|B\rangle\rangle = \text{Tr}(\hat{A}^\dagger \hat{B}), \quad (\text{I.13})$$

where \hat{A}^\dagger denotes the Hermitian conjugate of \hat{A} . It is easy to verify that if $|A\rangle\rangle \doteq (A_1, \dots, A_{N^2})^T$ and $|B\rangle\rangle \doteq (B_1, \dots, B_{N^2})^T$, where T denotes the transpose, then

$$\langle\langle A|B\rangle\rangle = (A_1, \dots, A_{N^2})^* \cdot \begin{pmatrix} B_1 \\ \vdots \\ B_{N^2} \end{pmatrix}, \quad (\text{I.14})$$

where a^* denotes the complex conjugate of a .

Let $|\rho(t)\rangle\rangle$ be the Liouville space representation of the density operator $\hat{\rho}(t)$ for a given mixed-state quantum system. If the system is Hamiltonian then equation (I.11) implies that $|\rho(t)\rangle\rangle$ satisfies the quantum Liouville equation

$$i\hbar \frac{\partial}{\partial t} |\rho(t)\rangle\rangle = \mathcal{L} |\rho(t)\rangle\rangle \quad (\text{I.15})$$

with some initial condition $|\rho(t_0)\rangle\rangle = |\rho_0\rangle\rangle$, where \mathcal{L} is the Liouville operator defined by the dual correspondence

$$\mathcal{L} |\rho(t)\rangle\rangle \leftrightarrow [\hat{H}, \hat{\rho}(t)]. \quad (\text{I.16})$$

Equation (I.16) determines the matrix elements of \mathcal{L} . With respect to the standard

Liouville space basis $|mn\rangle\rangle$ related to the Hilbert space basis $|n\rangle$ by the bijective correspondence $|mn\rangle\rangle \leftrightarrow |m\rangle\langle n|$, we have

$$\begin{aligned}
 \mathcal{L}_{jk,mn} &= \langle\langle jk|\mathcal{L}|mn\rangle\rangle \\
 &= \text{Tr}(|k\rangle\langle j|[\hat{H}, |m\rangle\langle n|]) \\
 &= \sum_i \langle i|k\rangle\langle j|\hat{H}|m\rangle\langle n|i\rangle - \langle i|k\rangle\langle j|m\rangle\langle n|\hat{H}|i\rangle \\
 &= \langle j|\hat{H}|m\rangle\delta_{nk} - \langle n|\hat{H}|k\rangle\delta_{jm} \\
 &= H_{jm}\delta_{kn} - H_{kn}^*\delta_{jm}
 \end{aligned} \tag{I.17}$$

We observe that $H_{kn}^* = H_{nk}$ and thus the (super-) operator \mathcal{L} is Hermitian:

$$\mathcal{L}_{jk,mn}^* = H_{jm}^*\delta_{kn} - H_{kn}\delta_{jm} = \mathcal{L}_{mn,jk}. \tag{I.18}$$

The Liouville space formulation is especially useful since it can easily be adapted to dissipative quantum systems by adding a non-Hermitian dissipation operator Γ to the Liouville operator \mathcal{L} so that the equation of motion becomes

$$i\hbar \frac{\partial}{\partial t} |\rho(t)\rangle\rangle = [\mathcal{L} - i\hbar\Gamma] |\rho(t)\rangle\rangle. \tag{I.19}$$

For instance, to account for dephasing between the k th and ℓ th level, we must modify the equation of motion for the matrix element $\rho_{k\ell}$ by adding a term $i\hbar\gamma_{k\ell}^d\rho_{k\ell}$, where $\gamma_{k\ell}^d$ is the dephasing rate between the k th and the ℓ th level, to the equation of motion for $\rho_{k\ell}$:

$$i\hbar \frac{\partial}{\partial t} \rho_{k\ell}(t) = ([\hat{H}, \hat{\rho}])_{k\ell} - i\hbar\gamma_{k\ell}^d\rho_{k\ell} \tag{I.20}$$

If population transfers occur, we have to modify the equation of motion for the diagonal elements of the density matrix as well:

$$i\hbar \frac{\partial}{\partial t} \rho_{kk}(t) = ([\hat{H}, \hat{\rho}])_{kk} - i\hbar \sum_{m \neq k} \underbrace{\gamma_{mk}\rho_{kk}}_{\substack{\text{population} \\ \text{loss through} \\ \text{transitions} \\ k \rightarrow m}} + i\hbar \sum_{m \neq k} \underbrace{\gamma_{km}\rho_{mm}}_{\substack{\text{population} \\ \text{gain through} \\ \text{transitions} \\ m \rightarrow k}} \tag{I.21}$$

In order for equations (I.20) and (I.21) to be equivalent to (I.19), the non-vanishing matrix elements of Γ must be

$$\begin{aligned}\Gamma_{k\ell, k\ell} &= \gamma_{k\ell}^d & k \neq \ell \\ \Gamma_{kk, mm} &= -\gamma_{km} & k \neq m \\ \Gamma_{kk, kk} &= \sum_{m \neq k} \gamma_{mk}\end{aligned}\quad (\text{I.22})$$

Thus, in the dissipative case, the total Liouville operator is

$$\mathcal{L}_{tot} = \mathcal{L} - i\hbar\Gamma, \quad (\text{I.23})$$

Notice that it is not Hermitian (unless $\Gamma = -\Gamma^\dagger$)

$$\mathcal{L}_{tot}^\dagger = \mathcal{L} + i\hbar\Gamma^\dagger. \quad (\text{I.24})$$

In this setting, the expectation value of an observable of the system, represented by the Hermitian operator \hat{A} on the Hilbert space \mathcal{H} , is determined by Liouville inner product

$$\langle \hat{A}(t) \rangle = \langle \langle A | \rho(t) \rangle \rangle, \quad (\text{I.25})$$

where $\langle \langle A |$ is the dual of the Liouville ket associated with \hat{A} .

I.4 The Optimal Control Problem

If the system is subject to external control then the Hamiltonian of the system depends on one or more *control functions*

$$\vec{f}(t) = (f_1(t), f_2(t), \dots, f_M(t)). \quad (\text{I.26})$$

We shall assume that the number M of external controls is finite and that the system is control-linear, i.e., that the total Hamiltonian of the system can be decomposed as follows:

$$\hat{H} = \hat{H}_0 + \sum_{m=1}^M f_m(t) \hat{H}_m. \quad (\text{I.27})$$

In this case, the corresponding Liouville operator also decomposes:

$$\mathcal{L} = \mathcal{L}_0 + \sum_{m=1}^M f_m(t) \mathcal{L}_m. \quad (\text{I.28})$$

The restrictions imposed on the controls depend on the particular system studied. However, a reasonable minimum requirement for the control functions $f_m(t)$ is that they should be bounded, measurable, real-valued functions defined on a time-interval $[t_0, t_F]$ that depends on the application.

The goal of optimal control is the maximization (or minimization) of the expectation value of a given observable, e.g., the population of a particular energy level or subspace of quantum states, the energy of a molecular bond, etc., at some target time $t = t_F$ subject to certain constraints. To make this statement mathematically rigorous, we define a functional (similar to the functionals used in [8, 9, 10])

$$W(\vec{f}, \rho_v, A_v) = W_1(\rho_v) - W_2(\vec{f}, \rho_v, A_v) - W_3(\vec{f}), \quad (\text{I.29})$$

whose value at a certain target time t_F we would like to maximize. Our functional consists of three parts. W_1 is the expectation value of \hat{A} , which we wish to maximize at the target time t_F ,

$$W_1(\rho_v) = \langle A(t_F) \rangle = \langle \langle A | \rho_v(t_F) \rangle \rangle; \quad (\text{I.30})$$

W_2 and W_3 are constraint functionals, which we define as follows:

$$W_2(\vec{f}, \rho_v, A_v) = \int_{t_0}^{t_F} \langle \langle A_v(t) | \frac{\partial}{\partial t} + \frac{i}{\hbar} \mathcal{L}_{tot}(\vec{f}, t) | \rho_v(t) \rangle \rangle dt, \quad (\text{I.31})$$

$$W_3(\vec{f}) = \sum_{m=1}^M \frac{\lambda_m}{2\hbar} \int_{t_0}^{t_F} f_m^2(t) dt. \quad (\text{I.32})$$

W_2 ensures that the quantum Liouville equation is satisfied. W_3 constrains the fluence, i.e., the total energy of the pulse. $\rho_v(t)$ and $A_v(t)$ are variational trial functions that must satisfy the boundary conditions

$$\rho_v(t_0) = \rho(t_0) = \rho_0, \quad A_v(t_F) = A. \quad (\text{I.33})$$

The solution of this control problem requires finding an admissible control $\vec{f}(t)$ such that W and thus $\langle \hat{A}(t) \rangle$ will attain its global maximum at time $t = t_F$. Several interesting questions arise. What is the global maximum? Is it dynamically attainable, i.e., is there a control that steers the system to a state where the global maximum is assumed? If there is such a control, how can we find it, at least numerically? These questions shall be addressed in the following chapters.

We would like to point out that in absence of dissipation, i.e., for $\hat{\Gamma} = 0$, our variational functional (I.29) is the mixed-state equivalent of the variational functional used by many other authors [11, 12, 13, 14, 15] for pure-state quantum systems:

$$W = \langle \psi_v(t_F) | A | \psi_v(t_F) \rangle - 2 \operatorname{Re} \int_{t_0}^{t_F} \langle \chi_v(t) | [\frac{\partial}{\partial t} + \frac{i}{\hbar} \hat{H}(\vec{f}, t)] | \varphi_v(t) \rangle dt - \sum_{m=1}^M \frac{\lambda_m}{2\hbar} \int_{t_0}^{t_F} f_m^2(t) dt. \quad (\text{I.34})$$

To see this, set $\hat{\rho}_v(t) = |\psi_v(t)\rangle\langle\psi_v(t)|$ where $|\psi_v(t)\rangle$ is a normalized wave-function representing a pure state of the system. We can find a time-dependent complete orthonormal set $\{|\psi_n(t)\rangle : n = 1, 2, \dots\}$ such that $|\psi_1(t)\rangle = |\psi_v(t)\rangle$ for all t . Hence we have

$$\begin{aligned} W_1 &= \operatorname{Tr}(\hat{A}\hat{\rho}_v(t_F)) \\ &= \sum_n \langle \psi_n(t_F) | \hat{A}_v(t_F) | \psi_v(t_F) \rangle \langle \psi_v(t_F) | \psi_n(t_F) \rangle \\ &= \sum_n \langle \psi_v(t_F) | \psi_n(t_F) \rangle \langle \psi_n(t_F) | \hat{A}_v(t_F) | \psi_v(t_F) \rangle \\ &= \langle \psi_v(t_F) | A | \psi_v(t_F) \rangle. \end{aligned}$$

Furthermore, setting $|\chi_v(t)\rangle = \hat{A}_v(t)|\psi_v(t)\rangle$ and $\partial_t \equiv \frac{\partial}{\partial t}$, we obtain

$$\begin{aligned} \langle \langle \hat{A}_v(t) | \partial_t \rho_v(t) \rangle \rangle &= \operatorname{Tr}(\hat{A}_v(t) \partial_t \hat{\rho}_v(t)) \\ &= \sum_n \langle \psi_n(t) | \hat{A}_v(t) (\partial_t |\psi_v(t)\rangle) \rangle \langle \psi_v(t) | \psi_n(t) \rangle \\ &\quad + \sum_n \langle \psi_n(t) | \hat{A}_v(t) | \psi_v(t) \rangle (\partial_t \langle \psi_v(t) |) | \psi_n(t) \rangle \\ &= \langle \psi_v(t) | \hat{A}_v(t) \partial_t |\psi_v(t)\rangle + \sum_n (\partial_t \langle \psi_v(t) |) | \psi_n(t) \rangle \langle \psi_n(t) | \hat{A}_v(t) | \psi_v(t) \rangle \end{aligned}$$

$$\begin{aligned}
&= \langle \psi_v(t) | \hat{A}_v(t) \partial_t | \psi_v(t) \rangle + (\partial_t \langle \psi_v(t) |) \hat{A}_v(t) | \psi_v(t) \rangle \\
&= \langle \psi_v(t) | \hat{A}_v(t) \partial_t | \psi_v(t) \rangle + (\langle \psi_v(t) | \hat{A}_v(t) \partial_t | \psi_v(t) \rangle)^* \\
&= 2 \operatorname{Re} \langle \psi_v(t) | \hat{A}_v(t) \partial_t | \psi_v(t) \rangle \\
&= 2 \operatorname{Re} \langle \chi_v(t) | \partial_t \psi_v(t) \rangle
\end{aligned}$$

as well as

$$\begin{aligned}
\langle \langle A_v(t) | \frac{i}{\hbar} \mathcal{L}(\vec{f}, t) \rho_v(t) \rangle \rangle &= \frac{i}{\hbar} \operatorname{Tr} \left(\hat{A}_v(t) [\hat{H}(\vec{f}, t), \hat{\rho}_v(t)] \right) \\
&= \frac{i}{\hbar} \sum_n \langle \psi_n(t) | \hat{A}_v(t) \hat{H}(\vec{f}, t) | \varphi_v(t) \rangle \langle \psi_v(t) | \psi_n(t) \rangle \\
&\quad - \frac{i}{\hbar} \sum_n \langle \psi_n(t) | \hat{A}_v(t) | \varphi_v(t) \rangle \langle \psi_v(t) | \hat{H}(\vec{f}, t) | \psi_n(t) \rangle \\
&= \frac{i}{\hbar} \langle \psi_v(t) | \hat{A}_v(t) \hat{H}(\vec{f}, t) | \varphi_v(t) \rangle \\
&\quad - \frac{i}{\hbar} \sum_n \langle \psi_v(t) | \hat{H}(\vec{f}, t) | \psi_n(t) \rangle \langle \psi_n(t) | \hat{A}_v(t) | \varphi_v(t) \rangle \\
&= \langle \chi_v(t) | \frac{i}{\hbar} \hat{H}(\vec{f}, t) | \varphi_v(t) \rangle - \langle \psi_v(t) | \frac{i}{\hbar} \hat{H}(\vec{f}, t) | \chi_v(t) \rangle \\
&= \langle \chi_v(t) | \frac{i}{\hbar} \hat{H}(\vec{f}, t) | \varphi_v(t) \rangle + (\langle \chi_v(t) | \frac{i}{\hbar} \hat{H}(\vec{f}, t) | \varphi_v(t) \rangle)^* \\
&= 2 \operatorname{Re} \langle \chi_v(t) | \frac{i}{\hbar} \hat{H}(\vec{f}, t) | \varphi_v(t) \rangle.
\end{aligned}$$

Hence, if $\hat{\rho}_v(t) = |\psi_v(t)\rangle\langle\psi_v(t)|$ then

$$W_2 = \int_{t_0}^{t_F} \langle \langle A_v(t) | \partial_t + \frac{i}{\hbar} \mathcal{L}(\vec{f}, t) | \rho_v(t) \rangle \rangle dt = 2 \operatorname{Re} \int_{t_0}^{t_F} \langle \chi_v(t) | [\partial_t + \frac{i}{\hbar} \hat{H}(\vec{f}, t)] | \varphi_v(t) \rangle dt.$$

CHAPTER II

BOUNDS ON OPTIMIZATION OF OBSERVABLES

II.1 Kinematical Attainability of Target States

Consider a mixed-state quantum system whose dynamical evolution is determined by the quantum Liouville equation (I.11). Equation (I.8) implies that a mixed initial state $\hat{\rho}(t_0)$ can only evolve into target states $\hat{\rho}(t_F)$ related to the initial state $\hat{\rho}(t_0)$ by

$$\hat{\rho}(t_F) = \hat{U}(t_F, t_0)\hat{\rho}(t_0)\hat{U}^\dagger(t_F, t_0), \quad (\text{II.1})$$

where $\hat{U}(t, t_0)$ is the propagator of the system as defined by equation (I.4).

If the system is Hamiltonian, i.e., non-dissipative, then the propagator satisfies the Schrödinger equation (I.5). Hence, for any Hamiltonian system, the propagator must be unitary, no matter what the concrete dynamical law is, and no matter what control we choose. Therefore, only target states $\hat{\rho}(t_F)$ that are related to $\hat{\rho}(t_0)$ by (II.1) for some unitary operator $\hat{U}(t_F, t_0)$ can possibly be reached. This motivates the following:

DEFINITION II.1 : Given any Hamiltonian quantum system, a target state $\hat{\rho}(t_F)$ is *kinematically attainable* from a given initial state $\hat{\rho}(t_0)$ only if there exists a unitary transformation $\hat{U}(t_F, t_0)$ such that equation (II.1) is satisfied.

II.2 Kinematical Bounds on the Expectation Values of Observables

The kinematical restriction on the reachable target states for Hamiltonian quantum systems discussed in the previous section has important implications for the expectation values (ensemble averages) of observables [16].

THEOREM II.1 : Let \mathcal{H} be a fixed N -dimensional subspace of the Hilbert space of pure quantum states of the system and let \hat{A} be a Hermitian operator on \mathcal{H} with eigenvalue decomposition

$$\hat{A} = \sum_{i=1}^m a_i \hat{I}(a_i), \quad (\text{II.2})$$

where $\hat{I}(a_i)$ is the projector onto the eigenspace $E(a_i)$. Let λ_i be the eigenvalues a_i , counted with multiplicity, and ordered

$$\lambda_1 \geq \lambda_2 \geq \cdots \geq \lambda_N. \quad (\text{II.3})$$

If the initial state is

$$\hat{\rho}_0 = \hat{\rho}(t_0) = \sum_{n=1}^N w_n |n\rangle\langle n|, \quad (\text{II.4})$$

where $\{|n\rangle : n = 1, \dots, N\}$ is a basis for \mathcal{H} , and the initial weights w_n are ordered

$$w_1 \geq w_2 \geq \cdots \geq w_n \geq \cdots \geq 0, \quad (\text{II.5})$$

then the expectation value of \hat{A} is bounded by

$$\sum_{n=1}^N \lambda_{N-n+1} w_n \leq \text{Tr}(\hat{A}\hat{\rho}(t)) \leq \sum_{n=1}^N \lambda_n w_n. \quad (\text{II.6})$$

Furthermore, $\langle A(t_F) \rangle$ assumes its upper bound if

$$\text{span}_{j=1, \dots, d(n)} |\Psi_{r(n,j)}(t_F)\rangle = E(a_n), \quad n = 1, \dots, m, \quad (\text{II.7})$$

and $\langle A(t_F) \rangle$ assumes its lower bound if

$$\text{span}_{j=1, \dots, d(n)} |\Psi_{r(n,j)}(t_F)\rangle = E(a_{N-n+1}), \quad n = 1, \dots, m, \quad (\text{II.8})$$

where $d(n) = \dim E(a_n)$ and $r(n, j) = d(1) + \cdots + d(n-1) + j$.

This theorem is an extension of our previous work [17], which enables one to determine kinematical bounds for arbitrary Hermitian operators, i.e., real observables, provided that the space of pure states, of which any ensemble may be comprised, is restricted to a

finite dimensional subspace of the possibly infinite-dimensional true state space. This assumption is necessary for computations and in many cases good approximations can be made by choosing finite dimensional subspaces carefully.

EXAMPLE II.1 : Consider a N -level Morse or harmonic oscillator model for a diatomic molecule with energy levels

$$E_1 < E_2 < \dots < E_N. \quad (\text{II.9})$$

Notice that the energy levels are ordered in an increasing sequence, i.e., we have $\lambda_i = E_{N-i+1}$. If the system is initially in thermal equilibrium, i.e., in particular

$$w_1 \geq w_2 \geq \dots \geq w_N, \quad (\text{II.10})$$

then the kinematical bounds on the expectation value of the (vibrational) energy of the bond are

$$\sum_{n=1}^N w_n E_n \leq \langle \hat{H}_0(t) \rangle \leq \sum_{n=1}^N w_{N-n+1} E_n. \quad (\text{II.11})$$

The kinematical bounds also restrict the population of any k -dimensional subspace $\hat{P}_k \mathcal{H}$:

$$w_N + w_{N-1} + \dots + w_{N-k+1} \leq \langle \hat{P}_k \rangle \leq w_1 + w_2 + \dots + w_k. \quad (\text{II.12})$$

In particular, this shows that the population of any one-dimensional subspace of the system can never exceed w_1 or drop below w_N . Hence, if the system is initially in a mixed-state then it can never reach a pure state (without dissipation).

II.3 Proof of Kinematical Bounds Theorem

LEMMA II.1 (Necessary Condition for Extrema): If the map $\hat{U} \mapsto \text{Tr}(\hat{A}\hat{U}\hat{\chi}\hat{U}^\dagger)$ has an extremum at the identity $\hat{1} \in \mathcal{U}(N)$ then \hat{A} and $\hat{\chi}$ commute.

PROOF : In order for $\text{Tr}(\hat{A}\hat{U}\hat{\chi}\hat{U}^\dagger)$ to be maximal when $\hat{U} = \hat{1}$ we must have

$$\left. \frac{d}{d\tau} \text{Tr}(\hat{A}\hat{U}(\tau)\hat{\chi}\hat{U}^\dagger(\tau)) \right|_{\tau=0} = 0$$

for an arbitrary path $\hat{U}(\tau)$ in $\mathcal{U}(N)$ with $\hat{U}(0) = \hat{1}$. Since the trace operator is a linear, this is equivalent to

$$\text{Tr} \left(\hat{A} \hat{U}'(0) \hat{\chi} \hat{U}^\dagger(0) + \hat{A} \hat{U}(0) \hat{\chi} [\hat{U}^\dagger]'(0) \right) = 0.$$

Observing that $\hat{U}(0) = \hat{1}$, and setting $\frac{d}{d\tau} \hat{U}(\tau)|_{\tau=0} = \hat{U}'(0) \equiv \hat{B}$, we have thus

$$\text{Tr} \left(\hat{A} \hat{B} \hat{\chi} + \hat{A} \hat{\chi} \hat{B}^\dagger \right) = 0. \quad (\text{II.13})$$

If \hat{B} is the derivative of a path $\hat{U}(\tau)$ in $\mathcal{U}(N)$ at $\tau = 0$ then it is skew-Hermitian, and conversely, every skew-Hermitian operator \hat{B} is the derivative of some path $\hat{U}(\tau)$ in $\mathcal{U}(N)$ at $\tau = 0$, since the Lie-algebra of $\mathcal{U}(N)$ consists of all skew-Hermitian matrices $u(N)$. Therefore condition (II.13) must hold for any skew-Hermitian operator \hat{B} . Using $\hat{B}^\dagger = -\hat{B}$, we can rewrite (II.13) as

$$\text{Tr} \left((\hat{\chi} \hat{A} - \hat{A} \hat{\chi}) \hat{B} \right) = 0.$$

We will show that this condition implies $\hat{M} = [\hat{\chi}, \hat{A}] = 0$. Note that \hat{M} is skew-Hermitian since $\hat{\chi}$ and \hat{A} are Hermitian.

Choosing $\hat{B} = (b_{k\ell})$ with

$$b_{k\ell} = \begin{cases} i & \text{for } k = s, \ell = s \\ 0 & \text{otherwise} \end{cases}$$

leads to

$$\text{Tr} \left(\hat{M} \hat{B} \right) = \sum_{j,k=1}^N m_{jk} b_{kj} = i M_{ss} = 0.$$

This holds for $s = 1, \dots, N$. Hence, all the diagonal elements of \hat{M} must vanish.

If

$$b_{k\ell} = \begin{cases} 1 & \text{for } k = s, \ell = r \\ -1 & \text{for } k = r, \ell = s \\ 0 & \text{otherwise} \end{cases}$$

then

$$\begin{aligned}\text{Tr}(\hat{M}\hat{B}) &= \sum_{j,k=1}^N m_{jk}b_{kj} = m_{rs} - m_{sr} \\ &= m_{rs} + m_{rs}^* = 2\text{Re}(m_{rs}) = 0,\end{aligned}$$

If

$$b_{k\ell} = \begin{cases} i & \text{for } k = s, \ell = r \\ i & \text{for } k = r, \ell = s \\ 0 & \text{otherwise} \end{cases}$$

then

$$\begin{aligned}\text{Tr}(\hat{M}\hat{B}) &= \sum_{j,k=1}^N m_{jk}b_{kj} = i(m_{rs} + m_{sr}) \\ &= i(m_{rs} - m_{rs}^*) = -2\text{Im}(m_{rs}) = 0.\end{aligned}$$

Since this holds for $r, s = 1, \dots, N$, all off-diagonal elements of \hat{M} must be zero. Hence \hat{M} vanishes identically and \hat{A} and $\hat{\chi}$ commute. \square

Since \hat{A} is a Hermitian operator on a finite-dimensional Hilbert space \mathcal{H} , there exists a unique eigenvalue decomposition

$$\hat{A} = \sum_{i=1}^m a_i \hat{I}(a_i), \quad (\text{II.14})$$

where $\hat{I}(a_i)$ denotes the projector onto the eigenspace $E(a_i)$. Moreover, all the eigenvalues a_i are real.

LEMMA II.2 (Kinematical Bounds): *Let \hat{A} be a Hermitian operator on \mathcal{H} with eigenvalue decomposition (II.14) and let $\lambda_1 \geq \lambda_2 \geq \dots \geq \lambda_N$ be the eigenvalues a_i , counted with multiplicity and ordered in a decreasing sequence. Then we have*

$$\sum_{k=1}^N \lambda_{N-k+1} w_k \leq \text{Tr}(\hat{A}\hat{\rho}(t)) \leq \sum_{k=1}^N \lambda_k w_k. \quad (\text{II.15})$$

PROOF : By the previous theorem a necessary condition for $\langle \hat{A}(t) \rangle$ to have an extremum at time t_F is that \hat{A} and $\hat{\chi} = \hat{\rho}(t_F)$ commute. But if they commute then they can be simultaneously diagonalized. Hence

$$\text{Tr}(\hat{A}\hat{\rho}(t_F)) = \sum_{k=1}^N \lambda_k w_{\sigma(k)},$$

where σ is a permutation of $\{1, 2, \dots, N\}$. It is now obvious that

$$\sum_{k=1}^N \lambda_{N-k+1} w_k \leq \text{Tr}(\hat{A}\hat{\rho}(t_F)) \leq \sum_{k=1}^N \lambda_k w_k.$$

□

II.4 Improved Bounds for 'Decoupled Systems'

The kinematical bounds derived in the previous sections are universal, i.e., they apply to any Hamiltonian quantum system, independent of the Hamiltonian \hat{H} and especially of the control \vec{f} . It is therefore not surprising that these bounds on the expectation value of observables can be improved for certain systems. In particular, we shall now consider systems comprised of non-interacting subsystems, which we shall refer to as 'decoupled systems'.

Again we shall restrict ourselves to control-linear, Hamiltonian quantum systems. In addition, we shall assume that there is only one control, i.e.,

$$\hat{H}(f(t)) = \hat{H}_0 + f(t)\hat{V}, \quad (\text{II.16})$$

where \hat{H}_0 is the internal Hamiltonian of the unperturbed system and \hat{V} defines the interaction with the control field $f(t)$. By our definition, the system is decoupled if there exists a basis \mathcal{B} for the Hilbert space \mathcal{H} such that \hat{H}_0 is diagonal and

$$\hat{V} = \hat{V}_1 \oplus \hat{V}_2 \doteq \left(\begin{array}{c|c} \hat{V}_1 & 0 \\ \hline 0 & \hat{V}_2 \end{array} \right). \quad (\text{II.17})$$

Let \mathcal{H}_1 and \mathcal{H}_2 be orthogonal subspaces of \mathcal{H} such that $\mathcal{H} = \mathcal{H}_1 \oplus \mathcal{H}_2$ and each \hat{V}_i maps \mathcal{H}_i to itself,

$$\mathcal{H} = \mathcal{H}_1 \oplus \mathcal{H}_2, \quad \hat{V}_i : \mathcal{H}_i \rightarrow \mathcal{H}_i, \quad i = 1, 2. \quad (\text{II.18})$$

It immediately follows that $\hat{H}(f(t))$ is block-diagonal,

$$\mathcal{H}(f(t)) = \hat{H}_1 \oplus \hat{H}_2 \doteq \left(\begin{array}{c|c} \hat{H}_1 & 0 \\ \hline 0 & \hat{H}_2 \end{array} \right) \quad (\text{II.19})$$

and maps \mathcal{H}_i to itself for $i = 1, 2$. Thus, the two subspaces \mathcal{H}_1 and \mathcal{H}_2 do not interact. Let \mathcal{B}_i be the restriction of the basis \mathcal{B} to the subspace \mathcal{H}_i and \hat{P}_i be the projector onto the subspace \mathcal{H}_i . Let N_i denote the dimension of \mathcal{H}_i .

Given an observable \hat{A} on \mathcal{H} , we define the restricted observables $\hat{A}_i = \hat{P}_i \hat{A}$ for $i = 1, 2$. Note that \hat{A}_i is a Hermitian operator on the subspace \mathcal{H}_i , i.e.,

$$\hat{A}_i = \hat{P}_i \hat{A} \hat{P}_i : \mathcal{H}_i \rightarrow \mathcal{H}_i \quad i = 1, 2. \quad (\text{II.20})$$

Let $\lambda_n^{(i)}$ denote the eigenvalues of \hat{A}_i , counted with multiplicity and ordered

$$\lambda_1^{(i)} \geq \lambda_2^{(i)} \geq \dots \geq \lambda_{N_i}^{(i)}. \quad (\text{II.21})$$

If $\hat{\rho}_i(t_0)$ is the density operator for subsystem i , whose matrix representation with respect to the basis \mathcal{B}_i is given by

$$\hat{\rho}_i(t_0) \doteq \text{diag}(w_1^{(i)}, \dots, w_{N_i}^{(i)}) \quad (\text{II.22})$$

with $w_1^{(i)} \geq w_2^{(i)} \geq \dots \geq w_{N_i}^{(i)}$, we can apply theorem 1 to obtain bounds for the expectation value of \hat{A}_i :

$$\sum_{n=1}^{N_i} w_{N_i-n+1}^{(i)} \lambda_n^{(i)} \leq \langle \hat{A}_i(t) \rangle \leq \sum_{n=1}^{N_i} w_n^{(i)} \lambda_n^{(i)}. \quad (\text{II.23})$$

Notice that the total probability for each subspace is less or equal to one, and that the sum of the subspace probabilities must equal one, i.e.,

$$p_i = \sum_{n=1}^{N_i} w_n^{(i)} \leq 1, \quad p_1 + p_2 = 1. \quad (\text{II.24})$$

If the probability for subspace i is one, then the initial ensemble is restricted to this subspace and since the subspaces do not interact, the ensemble will remain in this subspace forever, i.e., $p_i = 1$ for all times. In this case, $\langle \hat{A}(t) \rangle = \langle \hat{A}_i(t) \rangle$.

If both subspaces are initially occupied, i.e., both p_1 and p_2 are non-zero, then the density operator for the entire space \mathcal{H} is the direct sum of the subspace density operators $\hat{\rho}_1(t_0)$ and $\hat{\rho}_2(t_0)$, i.e.,

$$\hat{\rho}(t_0) = \hat{\rho}_1(t_0) \oplus \hat{\rho}_2(t_0) \doteq \left(\begin{array}{c|c} \hat{\rho}_1(t_0) & 0 \\ \hline 0 & \hat{\rho}_2(t_0) \end{array} \right). \quad (\text{II.25})$$

Since \hat{H} maps each subspace to itself, we can conclude

$$\hat{\rho}(t) = \hat{\rho}_1(t) \oplus \hat{\rho}_2(t) \doteq \left(\begin{array}{c|c} \hat{\rho}_1(t) & 0 \\ \hline 0 & \hat{\rho}_2(t) \end{array} \right) \quad (\text{II.26})$$

for $t > t_0$ and thus

$$\begin{aligned} \langle \hat{A}(t) \rangle &= \text{Tr}(\hat{A}\hat{\rho}(t)) \\ &= \text{Tr} \left(\left(\begin{array}{cc} \hat{A}_1 & * \\ * & \hat{A}_2 \end{array} \right) \left(\begin{array}{cc} \hat{\rho}_1(t) & 0 \\ 0 & \hat{\rho}_2(t) \end{array} \right) \right) \end{aligned} \quad (\text{II.27})$$

$$\begin{aligned} &= \text{Tr} \left(\begin{array}{cc} \hat{A}_1\hat{\rho}_1(t) & * \\ * & \hat{A}_2\hat{\rho}_2(t) \end{array} \right) \\ &= \text{Tr}(\hat{A}_1\hat{\rho}_1(t)) + \text{Tr}(\hat{A}_2\hat{\rho}_2(t)) \end{aligned} \quad (\text{II.28})$$

Since $\hat{\rho}_i(t)$ and \hat{A}_i ($i = 1, 2$) are operators on \hat{H}_i , we can apply (II.23). Thus we have

THEOREM II.2 : *Consider a decoupled quantum system as defined above. If $\hat{\rho}_0$ is given by (II.25), then the expectation value of an observable \hat{A} is bounded by*

$$\sum_{n=1}^{N_1} w_n^{(1)} \lambda_{N_1-n+1}^{(1)} + \sum_{n=1}^{N_2} w_n^{(2)} \lambda_{N_2-n+1}^{(2)} \leq \langle \hat{A}(t) \rangle \leq \sum_{n=1}^{N_1} w_n^{(1)} \lambda_n^{(1)} + \sum_{n=1}^{N_2} w_n^{(2)} \lambda_n^{(2)}, \quad (\text{II.29})$$

where $\lambda_n^{(i)}$ are the eigenvalues of the subspace observable \hat{A}_i , counted with multiplicity and ordered in a decreasing sequence. Furthermore, the upper bound is attained at $t = t_F$ if for all $k = 1, \dots, m_1$

$$\text{span}_{j=1, \dots, d(k)} |\Psi_{r(k,j)}^{(1)}(t_F)\rangle = E(a_k^{(1)}), \quad (\text{II.30})$$

where $d(k) = \dim E(a_k^{(1)})$ and $r(k, j) = d(1) + \dots + d(k-1) + j$, and for $\ell = 1, \dots, m_2$

$$\text{span}_{j=1, \dots, d(\ell)} |\Psi_{r(\ell, j)}^{(2)}(t_F)\rangle = E(a_\ell^{(2)}), \quad (\text{II.31})$$

where $d(\ell) = \dim E(a_\ell^{(2)})$ and $r(\ell, j) = d(1) + \dots + d(\ell-1) + j$. Similarly, the lower bound is realized if for all $k = 1, \dots, m_1$

$$\text{span}_{j=1, \dots, d(k)} |\Psi_{r(k, j)}^{(1)}(t_F)\rangle = E(a_{N_1-k+1}^{(1)}), \quad (\text{II.32})$$

where $d(k) = \dim E(a_k^{(1)})$ and $r(k, j) = d(1) + \dots + d(k-1) + j$, and for $\ell = 1, \dots, m_2$

$$\text{span}_{j=1, \dots, d(\ell)} |\Psi_{r(\ell, j)}^{(2)}(t_F)\rangle = E(a_{N_2-\ell+1}^{(2)}), \quad (\text{II.33})$$

where $d(\ell) = \dim E(a_\ell^{(2)})$ and $r(\ell, j) = d(1) + \dots + d(\ell-1) + j$.

EXAMPLE II.2 : Consider a three level quantum system with energy levels $E_1 < E_2 < E_3$ and corresponding eigenmodes $|n\rangle$ of the Hamiltonian \hat{H}_0 for $n = 1, \dots, 3$. Suppose we start with an initial mixed state

$$\hat{\rho}_0 = \sum_{n=1}^3 w_n |n\rangle\langle n|$$

with $w_1 > w_2 > w_3$, and the only possible transitions when the system is driven are between level one and three, i.e., the interaction operator \hat{V} has the form

$$\hat{V} = |1\rangle\langle 3| + |3\rangle\langle 1|.$$

With respect to the basis $B = \{|1\rangle, |3\rangle, |2\rangle\}$, the matrix representations of the operators above are

$$\hat{H}_0 \doteq \begin{pmatrix} E_1 & 0 & 0 \\ 0 & E_3 & 0 \\ 0 & 0 & E_2 \end{pmatrix}, \quad \hat{V} \doteq \begin{pmatrix} 0 & 1 & 0 \\ 1 & 0 & 0 \\ 0 & 0 & 0 \end{pmatrix}, \quad \hat{\rho}_0 \doteq \begin{pmatrix} w_1 & 0 & 0 \\ 0 & w_3 & 0 \\ 0 & 0 & w_2 \end{pmatrix}.$$

It is now quite obvious that the orthogonal subspaces \mathcal{H}_1 and \mathcal{H}_2 spanned by $\{|1\rangle, |3\rangle\}$ and $\{|2\rangle\}$, respectively, are invariant under $\hat{H} = \hat{H}_0 + f(t)\hat{V}$.

Thus, if our observable is $\hat{A} = \hat{H}_0$ then the induced restricted observables are

$$\hat{A}_1 \doteq \begin{pmatrix} E_1 & 0 \\ 0 & E_3 \end{pmatrix}, \quad \hat{A}_2 \doteq (E_2)$$

with respect to our chosen base. Clearly, \hat{A}_1 is an observable on \mathcal{H}_1 with

$$w_1 E_1 + w_3 E_3 \leq \langle \hat{A}_1(t) \rangle \leq w_1 E_3 + w_3 E_1.$$

\hat{A}_2 is an observable on \mathcal{H}_2 with

$$w_2 E_2 \leq \langle \hat{A}_2(t) \rangle \leq w_2 E_2.$$

Hence, according to theorem 2, we have

$$w_1 E_1 + w_3 E_3 + w_2 E_2 \leq \langle \hat{A}(t) \rangle \leq w_1 E_3 + w_3 E_1 + w_2 E_2.$$

Concretely, if we choose, e.g., $E_n = n$ for $n = 1, 2, 3$ and $w_1 = 0.5$, $w_2 = 0.3$ and $w_3 = 0.2$ then

$$1.7 \leq \langle \hat{H}_0(t) \rangle \leq 2.3,$$

where 1.7 is the global minimum and 2.3 is the global maximum value of the energy for this system.

CHAPTER III

CONTROLLABILITY OF QUANTUM SYSTEMS

III.1 Dynamical Realizability of Kinematical Bounds

The kinematical bounds derived in the previous chapter provide bounds on the expectation value of observables for Hamiltonian quantum systems. A priori knowledge of such bounds is very useful when one tries to control the system such as to maximize the expectation value of an observable. This is especially true if numerical methods are employed to determine an optimal control since most numerical algorithms (e.g., [18, 11]) are based on differential equations that are necessary but not sufficient conditions for a global maximum. Independent knowledge of the global maximum thus enables one to decide if a numerically obtained 'optimal' control is actually optimal in the sense of steering the system to the global maximum.

However, there is a problem. While the kinematical bounds cannot be violated dynamically, the question arises whether these kinematical bounds can always be 'dynamically realized'. To formulate the question precisely, let us define this expression as follows.

DEFINITION III.1 : A kinematical bound for an observable is *dynamically realizable* if there exists an admissible control-trajectory pair that steers the system from the initial state $\hat{\rho}(t_0)$ to a final state $\hat{\rho}(t_F)$, for which the expectation value of the target observable assumes its kinematical maximum or minimum.

For a Hamiltonian quantum system, equation (1.8) implies that the only admissible trajectories are

$$\hat{\rho}(t) = \hat{U}(t, t_0)\hat{\rho}_0\hat{U}(t, t_0)^\dagger, \quad (\text{III.1})$$

where $\hat{\rho}_0$ is the initial state of the system and $\hat{U}(t, t_0)$ is the propagator (1.4) satisfying

the dynamical law

$$i\hbar \frac{\partial}{\partial t} \hat{U}(t, t_0) = \left[\hat{H}_0 + \sum_{m=1}^M f_m(t) \hat{H}_m \right] \hat{U}(t, t_0). \quad (\text{III.2})$$

The set of admissible controls depends on the constraints of the system considered. However, in general we can assume that an admissible control should be at least a bounded measurable function.

Equation (III.2) shows that the problem amounts to deciding whether every unitary operator $\hat{U}(t_F, t_0)$ can be dynamically generated. Since $U(N)$ is a group, it suffices to verify that every unitary operator is accessible from the identity. This motivates the following

DEFINITION III.2 Controllability: A (Hamiltonian) quantum system is (*completely controllable*) if every unitary operator in $U(N)$ is accessible from the identity operator \hat{I} via a path that satisfies the dynamical law (III.2).

If the system is (completely) controllable then every kinematically attainable target state can be reached dynamically from a given initial state. In this case, it is obvious that the kinematical bounds are always dynamically realizable, i.e., the kinematical upper and lower bounds correspond to the global maximum and minimum of $\langle \hat{A}(t_F) \rangle$, respectively, which can be attained if the system is driven with an optimal control $\vec{f}(t)$.

III.2 Algebraic Condition for Controllability

Consider a Hamiltonian quantum system (III.2) defined on the N -dimensional Hilbert space \mathcal{H} and G be the unitary group $U(N)$ and $L(G)$ be the Lie algebra $u(N)$.

THEOREM III.1 : *A necessary and sufficient condition for the system to be completely controllable is that the Lie sub-algebra L_0 of $L(G)$ generated by $\hat{H}_0, \dots, \hat{H}_M$ has (real) dimension N^2 , or equivalently, that the ideal ℓ_0 of $L(G)$ generated by $\hat{H}_1, \dots, \hat{H}_M$ has (real) dimension $N^2 - 1$.*

This result was first formulated and proved for pure-state quantum systems in [19, 20]. The proof uses the results by Jurdjevic and Sussmann on controllability of systems on Lie groups [21]:

THEOREM III.2 : *Let X_0, \dots, X_M be right-invariant vector fields on a Lie group G and $u_m(t)$ be bounded measurable control functions. Suppose*

$$\frac{dx}{dt}(t) = X_0(x(t)) + \sum_{m=1}^M u_m(t)X_m(x(t)) \quad (\text{III.3})$$

for $x(t) \in G$. Let L_0 be the sub-algebra of the Lie algebra $L(G)$ generated by the vector fields $\{X_0, \dots, X_M\}$ and denote the corresponding connected Lie subgroup by S_0 . If S_0 is compact then there exists a time T so that the set of states accessible from the identity $\hat{1} \in S_0$, in time T , is all of S_0 .

PROOF (Theorem 1): Setting $x(t) = \hat{U}(t, t_0)$ and

$$\vec{X}_m(x(t)) = -\frac{i}{\hbar} \hat{H}_m \hat{U}(t, t_0), \quad m = 0, \dots, M, \quad (\text{III.4})$$

equation (III.2) becomes

$$\frac{dx}{dt} = \vec{X}_0(x(t)) + \sum_{m=1}^M f_m(t) \vec{X}_m(x(t)), \quad (\text{III.5})$$

which defines a control system on the Lie group $U(N)$ of the type studied by Jurdjevic and Sussmann. Note that the Lie algebra L_0 generated by $\vec{X}_0, \dots, \vec{X}_M$ is the same as the Lie algebra generated by $\hat{H}_0, \dots, \hat{H}_M$.

$U(N)$ is a connected, compact Lie group. Therefore, the Lie subgroup S_0 associated with the Lie algebra L_0 generated by $\hat{H}_0, \dots, \hat{H}_M$ is also compact. Hence, it follows from theorem 2 that every state in S_0 is accessible from $\hat{1}$ for sufficiently large t_F . All that remains to be shown is that $S_0 = U(N)$.

Since the Lie algebra $L(U(N))$ consists of all skew-Hermitian matrices $u(N)$, its real dimension is

$$2 \left(\sum_{n=1}^{N-1} n \right) + N = N(N-1) + N = N^2, \quad (\text{III.6})$$

because there are $N(N - 1)/2$ off-diagonal elements, which can be arbitrary complex numbers, and N diagonal elements, which must be imaginary.

Since L_0 is a sub-algebra of the Lie algebra $u(N)$, its (real) dimension must be less or equal to N^2 , and $\dim L_0 = N^2$ implies that $L_0 = u(n)$, and consequently that $S_0 = U(N)$. Therefore,

$$\dim_{\mathbb{R}} L_0 = N^2 \quad (\text{III.7})$$

is a sufficient condition for controllability. It is also necessary since if $\dim L_0 < \dim u(N)$ then $S_0 \neq U(N)$. \square

Theorem 1 provides an algebraic condition for controllability of a quantum system that can easily be implemented on a computer and verified numerically.

III.3 Controllability Calculations

Throughout this section, we shall consider the following N -level systems:

$$\hat{H} = \hat{H}_0 + f_1(t)\hat{V}_1 + f_2(t)\hat{V}_2, \quad (\text{III.8})$$

$$\hat{H} = \hat{H}_0 + f(t)\hat{V}, \quad (\text{III.9})$$

$$\hat{H} = \hat{H}_0 + \hat{V}_2 + f(t)\hat{V}_1, \quad (\text{III.10})$$

$$\hat{H} = \hat{H}_0 + \hat{V}_1 + f(t)\hat{V}_2, \quad (\text{III.11})$$

$$\hat{H} = \hat{H}_0 + f(t)\hat{V}_1, \quad (\text{III.12})$$

where the internal Hamiltonian shall be

$$\hat{H}_0 = \sum_{n=1}^N E_n |n\rangle\langle n|, \quad (\text{III.13})$$

and the transition dipole operator shall be of the form

$$\hat{V} = \sum_{n=1}^{N-1} d_n (|n\rangle\langle n+1| + |n+1\rangle\langle n|). \quad (\text{III.14})$$

If N is even we define in addition

$$\hat{V}_1 = \sum_{n=1}^{N/2-1} d_n(|n\rangle\langle n+1| + |n+1\rangle\langle n|) + \sum_{n=N/2+1}^{N-1} d_n(|n\rangle\langle n+1| + |n+1\rangle\langle n|), \quad (\text{III.15})$$

$$\hat{V}_2 = d_{N/2}(|N/2\rangle\langle N/2+1| + |N/2+1\rangle\langle N/2|). \quad (\text{III.16})$$

The energy eigenvalues E_n of the system are either the Morse oscillator values

$$E_n^M = \hbar\omega_0 \left(n - \frac{1}{2}\right) \left[1 - \frac{1}{2} \left(n - \frac{1}{2}\right) B\right], \quad (\text{III.17})$$

or the harmonic oscillator values

$$E_n^H = \hbar\omega_0 \left(n - \frac{1}{2}\right), \quad (\text{III.18})$$

or simply equally spaced

$$E_n^E = n. \quad (\text{III.19})$$

The transition probabilities are either the Morse / harmonic oscillator values

$$d_n^M = \sqrt{n}, \quad n = 1, \dots, N-1, \quad (\text{III.20})$$

or all equal

$$d_n^E = 1, \quad n = 1, \dots, N-1, \quad (\text{III.21})$$

or almost all equal

$$d_n^A = 1, \quad n = 1, \dots, N-2, \quad d_{N-1} = 2. \quad (\text{III.22})$$

First, we computed the dimension of the Lie algebra of model system (III.9) for various different choices of E_n and d_n for N ranging from two to eight. The results of these computations, shown in table 1, suggest that the dimension is N^2 in most cases except when the energy levels are equally spaced and *all* the transition probabilities are equal. In this rather unphysical special case, the dimension drops for $N > 2$. Notice,

however, that it appears to be sufficient to change only one of the transition probabilities to recover controllability. For $N = 4$, the decrease of the dimension from 16 (for $E_n = n$ and $d_1 = d_2 = 1, d_3 = 2$) to 11 (for $E_n = n$ and $d_1 = d_2 = d_3 = 1$) can be explained by comparing the Lie algebras. In both cases, the Lie algebra is generated by

$$\begin{aligned}
 A &= \hat{H}_0, & B &= \hat{V}, \\
 C &= [A, B], \\
 D &= [C, B], \\
 E &= [D, B], & F &= [D, C], \\
 G &= [E, B], & H &= [E, C], & I &= [E, D], & J &= [F, C], & K &= [F, D], & L &= [F, E], \\
 M &= [G, B], & N &= [G, C], & O &= [G, D], & P &= [H, D],
 \end{aligned}
 \tag{III.23}$$

however, for $d_1 = d_2 = 1$ and $d_3 = 2$, these generators are linearly independent while for $d_1 = d_2 = d_3 = 1$

$$I = 2F, \quad K = -2E, \quad L = J - G, \quad O = -2H, \quad P = -6F + 2N, \tag{III.24}$$

i.e., we have five linear dependencies, which explains the drop in the dimension from 16 to 11.

Our second aim was to compare the controllability of the different model systems. (III.9) is the basic Morse oscillator / harmonic oscillator model, in which all the transitions are equally affected by the control field $f(t)$. (III.8) is a modification of this system, in which some of the transitions are assumed to be controlled by a field $f_1(t)$, while others are controlled by another independent field $f_2(t)$. In models (III.10) and (III.11) we go one step further and assume that only some of the transitions can be directly influenced by the control field $f(t)$, while other transitions are not immediately affected by any control field. The main difference between (III.10) and (III.11) is that in (III.10) all but one of the transitions are directly affected by the control field, while in (III.11) the situation is exactly reversed. Finally, in (III.12) we consider a decoupled system consisting of two

TABLE 1: Dimensions of the Lie algebras for model system (III.9) for various N

	$E_n = E_n^M, d_n = \sqrt{n}$	$E_n = E_n^H, d_n = \sqrt{n}$	$E_n = E_n^E, d_n = \sqrt{n}$	$E_n = E_n^M, d_n = 1$	$E_n = E_n^H, d_n = 1$	$E_n = E_n^E, d_n = 1$	$E_n = E_n^M, d_n = 1, d_{N-1} = 2$
$N = 2$	4	4	4	4	4	4	4
$N = 3$	9	9	9	9	4	4	9
$N = 4$	16	16	16	16	11	11	16
$N = 5$	25	25	25	25	11	11	25
$N = 6$	36	36	36	36	22	22	36
$N = 7$	49	49	49	49	22	22	49
$N = 8$	64	64	64	64	37	37	64

TABLE 2: Dimensions of the Lie algebras for various model systems for $N = 4$

$N = 4$	$\hat{H} = \hat{H}_0 + f_1 \hat{V}_1 + f_2 \hat{V}_2$	$\hat{H} = \hat{H}_0 + f \hat{V}$	$\hat{H} = \hat{H}_0 + \hat{V}_2 + f \hat{V}_1$	$\hat{H} = \hat{H}_0 + \hat{V}_1 + f \hat{V}_2$	$\hat{H} = \hat{H}_0 + f \hat{V}_1$
$E_n = E_n^M, d_n = \sqrt{n}$	16	16	16	16	7
$E_n = E_n^M, d_n = 1$	16	16	16	16	7
$E_n = E_n^H, d_n = \sqrt{n}$	16	16	16	16	7
$E_n = E_n^E, d_n = \sqrt{n}$	16	16	16	16	7
$E_n = E_n^H, d_n = 1$	11	11	11	11	4
$E_n = E_n^E, d_n = 1$	11	11	11	11	4
$E_n = E_n^E, d_n = 1, d_{N-1} = 2$	16	16	16	16	7

similar, non-interacting subsystems.

When examining tables 2–4, showing the dimension of the Lie algebra for the various models and choices of the parameters E_n and d_n discussed above, the first striking observation is that for fixed choice of the parameters E_n and d_n , the dimension of the Lie algebra appears to be the same for all the model systems except the last one. In particular, we note that the dimension is almost always N^2 , even if only some transitions are directly influenced by a control field, provided that the system does not decouple into completely non-interacting subsystems. The only noticeable exception occurs again for the special case of equally spaced energy levels and equal transition probabilities. However, even in this case, the dimension of the Lie algebra, although less than N^2 , appears to be same for systems (III.9)–(III.11).

TABLE 3: Dimensions of the Lie algebras for various model systems for $N = 6$

$N = 6$	$\hat{H} = \hat{H}_0 + f_1 \hat{V}_1 + f_2 \hat{V}_2$	$\hat{H} = \hat{H}_0 + f \hat{V}$	$\hat{H} = \hat{H}_0 + \hat{V}_2 + f \hat{V}_1$	$\hat{H} = \hat{H}_0 + \hat{V}_1 + f \hat{V}_2$	$\hat{H} = \hat{H}_0 + f \hat{V}_1$
$E_n = E_n^M, d_n = \sqrt{n}$	36	36	36	36	17
$E_n = E_n^M, d_n = 1$	36	36	36	36	17
$E_n = E_n^H, d_n = \sqrt{n}$	36	36	36	36	17
$E_n = E_n^E, d_n = \sqrt{n}$	36	36	36	36	17
$E_n = E_n^H, d_n = 1$	22	22	22	22	4
$E_n = E_n^E, d_n = 1$	22	22	22	22	4
$E_n = E_n^E, d_n = 1, d_{N-1} = 2$	36	36	36	36	12

TABLE 4: Dimensions of the Lie algebras for various model systems for $N = 8$

$N = 8$	$\hat{H} = \hat{H}_0 + f_1 \hat{V}_1 + f_2 \hat{V}_2$	$\hat{H} = \hat{H}_0 + f \hat{V}$	$\hat{H} = \hat{H}_0 + \hat{V}_2 + f \hat{V}_1$	$\hat{H} = \hat{H}_0 + \hat{V}_1 + f \hat{V}_2$	$\hat{H} = \hat{H}_0 + f \hat{V}_1$
$E_n = E_n^M, d_n = \sqrt{n}$	64	64	64	64	31
$E_n = E_n^M, d_n = 1$	64	64	64	64	31
$E_n = E_n^H, d_n = \sqrt{n}$	64	64	64	64	31
$E_n = E_n^E, d_n = \sqrt{n}$	64	64	64	64	31
$E_n = E_n^H, d_n = 1$	37	37	37	37	11
$E_n = E_n^E, d_n = 1$	37	37	37	37	11
$E_n = E_n^E, d_n = 1, d_{N-1} = 2$	64	64	64	64	26

Examining the dimensions of the Lie algebra for the decoupled system for $N = 4$, $N = 6$ and $N = 8$, furthermore suggests that the dimension is $N^2/2 - 1$ except when the energy levels are equally spaced and all the transition probabilities are equal. This is consistent with our expectations since the system considered consists of two non-interacting subsystems. Hence, the dimension of the ideal ℓ_0 generated by the two subsystems should be the sum of the dimensions of the ideals generated by each of the subsystems. If both subsystems have dimension $N/2$ and are controllable, it thus follows that the dimension of the ideal ℓ_0 of the total system is $2[(N/2)^2 - 1] = N^2/2 - 2$. Hence the dimension of the Lie algebra generated by \hat{H}_0 and \hat{V}_1 should be $N^2/2 - 1$.

CHAPTER IV
CONSTRUCTING OPTIMAL CONTROLS

IV.1 Euler-Lagrange Equations

Once controllability and kinematical bounds are established, the main question is how the external control should be chosen to manipulate the dynamics of the system in the way desired. We shall assume that the goal of optimization is maximization of a target functional $W(\vec{f}, \rho_v, A_v)$ (see Eq. I.29) at a certain target time t_F .

THEOREM IV.1 : *A necessary condition for the target functional $W(\vec{f}, \rho_v, A_v)$ to have a maximum is that the variation of W under independent variations of A_v , ρ_v and f_m is zero. This leads to the Euler-Lagrange equations*

$$\lambda_m f_m(t) = -i \langle \langle A_v(t) | \mathcal{L}_m | \rho_v(t) \rangle \rangle \quad (\text{IV.1})$$

$$i\hbar \partial_t | \rho_v(t) \rangle \rangle = \left[\mathcal{L}_0 + \sum_{m=1}^M f_m(t) \mathcal{L}_m - i\hbar \Gamma \right] | \rho_v(t) \rangle \rangle \quad (\text{IV.2})$$

$$i\hbar \partial_t | A_v(t) \rangle \rangle = \left[\mathcal{L}_0 + \sum_{m=1}^M f_m(t) \mathcal{L}_m + i\hbar \Gamma^\dagger \right] | A_v(t) \rangle \rangle, \quad (\text{IV.3})$$

where $\partial_t \equiv \frac{\partial}{\partial t}$, with mixed boundary conditions

$$| \rho_v(t_0) \rangle \rangle = | \rho_0 \rangle \rangle, \quad | A_v(t_F) \rangle \rangle = | A \rangle \rangle. \quad (\text{IV.4})$$

PROOF : Considering the definitions of W , W_1 , W_2 and W_3 [see equations (I.29)–(I.32)] it is immediately obvious that $\frac{\delta W}{\delta A_v} = \frac{\delta W_2}{\delta A_v}$ and that $\frac{\delta W_2}{\delta A_v} = 0$ leads to

$$\left[\partial_t + \frac{i}{\hbar} \mathcal{L}_{tot}(\vec{f}, t) \right] | \rho_v(t) \rangle \rangle = 0. \quad (\text{IV.5})$$

Recalling the definition of \mathcal{L}_{tot} [see equation (I.23)], this establishes equation (IV.2).

In order to compute $\frac{\delta W}{\delta \rho_v}$, we first re-write W_2 using integration by parts and the fact that the Liouville inner product satisfies the identity $\langle\langle A|B\rangle\rangle = \langle\langle B|A\rangle\rangle^*$:

$$\begin{aligned} W_2 &= \int_{t_0}^{t_F} \langle\langle A_v(t) | \partial_t + \frac{i}{\hbar} \mathcal{L}_{tot}(\vec{f}, t) | \rho_v(t) \rangle\rangle dt \\ &= \langle\langle A_v(t) | \rho_v(t) \rangle\rangle \Big|_{t_0}^{t_F} - \int_{t_0}^{t_F} \langle\langle \partial_t A_v(t) | \rho_v(t) \rangle\rangle dt + \int_{t_0}^{t_F} \langle\langle A_v(t) | \frac{i}{\hbar} \mathcal{L}_{tot}(\vec{f}, t) | \rho_v(t) \rangle\rangle dt \\ &= \langle\langle A_v(t) | \rho_v(t) \rangle\rangle \Big|_{t_0}^{t_F} - \int_{t_0}^{t_F} \langle\langle \rho_v(t) | \partial_t A_v(t) \rangle\rangle^* dt + \int_{t_0}^{t_F} \langle\langle \rho_v(t) | [\frac{i}{\hbar} \mathcal{L}_{tot}(\vec{f}, t)]^\dagger | A_v(t) \rangle\rangle^* dt \\ &= \langle\langle A | \rho_v(t_F) \rangle\rangle - \langle\langle A_v(t_0) | \rho_0 \rangle\rangle - \int_{t_0}^{t_F} \langle\langle \rho_v(t) | \partial_t + \frac{i}{\hbar} \mathcal{L}_{tot}^\dagger(\vec{f}, t) | A_v(t) \rangle\rangle^* dt \end{aligned}$$

The first term in this expression for W_2 cancels out W_1 . Hence, W becomes

$$W = \langle\langle A_v(t_0) | \rho_0 \rangle\rangle + \int_{t_0}^{t_F} \langle\langle \rho_v(t) | \partial_t + \frac{i}{\hbar} \mathcal{L}_{tot}^\dagger(\vec{f}, t) | A_v(t) \rangle\rangle^* dt + \sum_{m=1}^M \frac{\lambda_m}{2\hbar} \int_{t_0}^{t_F} [f_m(t)]^2 dt \quad (\text{IV.6})$$

Thus, $\frac{\delta W}{\delta \rho_v} = 0$ leads to

$$\left[\partial_t + \frac{i}{\hbar} \mathcal{L}_{tot}^\dagger(\vec{f}, t) \right] | A_v(t) \rangle\rangle = 0, \quad (\text{IV.7})$$

which establishes equation (IV.3).

Finally, inserting the definition of \hat{L}_{tot} , i.e.,

$$\mathcal{L}_{tot}(\vec{f}, t) = \mathcal{L}_0 + \sum_{m=1}^M f_m(t) \mathcal{L}_m - i\hbar\Gamma \quad (\text{IV.8})$$

into equation (I.31), we obtain

$$W_2 = \int_{t_0}^{t_F} \langle\langle A_v(t) | \partial_t + \frac{i}{\hbar} \mathcal{L}_0 + \Gamma | \rho_v(t) \rangle\rangle + \frac{i}{\hbar} \sum_{m=1}^M f_m(t) \langle\langle A_v(t) | \mathcal{L}_m | \rho_v(t) \rangle\rangle dt. \quad (\text{IV.9})$$

Thus,

$$\frac{\delta W_2}{\delta f_m} = \frac{i}{\hbar} \langle\langle A_v(t) | \mathcal{L}_m | \rho_v(t) \rangle\rangle. \quad (\text{IV.10})$$

Together with

$$\frac{\delta W_1}{\delta f_m} = 0, \quad \frac{\delta W_3}{\delta f_m} = \frac{\lambda_m}{\hbar} f_m(t), \quad (\text{IV.11})$$

$\frac{\delta W}{\delta f_m} = 0$ leads to

$$\lambda_m f_m(t) = -i \langle\langle A_v(t) | \mathcal{L}_m | \rho_v(t) \rangle\rangle \quad (\text{IV.12})$$

for $m = 1, \dots, M$, which establishes equation (IV.1). \square

IV.2 Entangled Feedback Algorithm

Several optimization techniques including the conjugate gradient method [22, 23], the Krotov method [24] and non-linear eigensystem methods [25, 10] have been developed to solve the problem of finding an optimal control using the Euler-Lagrange equations. However, the realizability and efficiency of these methods leave much to be desired.

Major progress was made when Zhu and Rabitz presented an efficient, rapidly monotonically convergent entangled feedback method for quantum optimal control of the expectation value of a positive definite operator in [11]. This algorithm has since been generalized to mixed-state quantum systems [18] and dissipative quantum systems [26]. In the following we shall present a further generalization of this algorithm for mixed-state quantum systems subject to dissipation and multiple independent controls.

The core of the entangled feedback algorithm are the two coupled differential equations

$$i\hbar\partial_t|\rho_v(t)\rangle\rangle = \left[\mathcal{L}_0 - \sum_{m=1}^M \frac{i\langle\langle A_v(t)|\mathcal{L}_m|\rho_v(t)\rangle\rangle}{\lambda_m} \mathcal{L}_m - i\hbar\Gamma \right] |\rho_v(t)\rangle\rangle \quad (\text{IV.13})$$

$$i\hbar\partial_t|A_v(t)\rangle\rangle = \left[\mathcal{L}_0 - \sum_{m=1}^M \frac{i\langle\langle A_v(t)|\mathcal{L}_m|\rho_v(t)\rangle\rangle}{\lambda_m} \mathcal{L}_m + i\hbar\Gamma^\dagger \right] |A_v(t)\rangle\rangle \quad (\text{IV.14})$$

with mixed boundary conditions

$$|\rho_v(t_0)\rangle\rangle = |\rho_0\rangle\rangle, \quad |A_v(t_F)\rangle\rangle = |A\rangle\rangle, \quad (\text{IV.15})$$

which are derived from the Euler-Lagrange equations by substituting

$$f_m(t) = -\frac{i}{\lambda_m} \langle\langle A_v(t)|\mathcal{L}_m|\rho_v(t)\rangle\rangle,$$

i.e., equation (IV.1) into equations (IV.2) and (IV.3).

As with any iterative method, the entangled feedback algorithm described here requires an independently derived initial control $\vec{f}^{(0)}(t)$ to start the iteration. In many cases, however, it appears to be sufficient to choose random noise or set the initial control to zero. Once the initial control is chosen, we determine an initial $|\rho_v^{(0)}(t)\rangle\rangle$ by solving

$$\partial_t |\rho_v^{(0)}(t)\rangle\rangle = -\frac{i}{\hbar} \left[\mathcal{L}_0 + \sum_{m=1}^M f_m^{(0)}(t) \mathcal{L}_m - i\hbar\Gamma \right] |\rho_v^{(0)}(t)\rangle\rangle \quad (\text{IV.16})$$

with initial condition $|\rho_v^{(0)}(t_0)\rangle\rangle = |\rho_0\rangle\rangle$. Then we define

$$f_m^{(n,k)}(t) \equiv -\frac{i}{\lambda_m} \langle\langle A_v^{(n)}(t) | \mathcal{L}_m | \rho_v^{(n-k)}(t) \rangle\rangle \quad (\text{IV.17})$$

$$\mathcal{L}^{(n,k)} \equiv \mathcal{L}_0 + \sum_{m=1}^M f_m^{(n,k)} \mathcal{L}_m \quad (\text{IV.18})$$

for $n \geq 1$, and iteratively solve the differential equations

$$i\hbar\partial_t |A_v^{(n)}(t)\rangle\rangle = [\mathcal{L}^{(n,1)} + i\hbar\Gamma^\dagger] |A_v^{(n)}(t)\rangle\rangle \quad (\text{IV.19})$$

$$i\hbar\partial_t |\rho_v^{(n)}(t)\rangle\rangle = [\mathcal{L}^{(n,0)} - i\hbar\Gamma] |\rho_v^{(n)}(t)\rangle\rangle \quad (\text{IV.20})$$

with the boundary conditions

$$|A_v^{(n)}(t_F)\rangle\rangle = |A\rangle\rangle, \quad |\rho_0^{(n)}(t_0)\rangle\rangle = |\rho_0\rangle\rangle. \quad (\text{IV.21})$$

Notice the importance of the order in which the equations are solved. In each iteration step we first solve the differential equation for $|A_v(t)\rangle\rangle$ using the solution for $|\rho_v(t)\rangle\rangle$ derived in the previous step. Then we use this information to solve the differential equation for $|\rho_v(t)\rangle\rangle$.

IV.3 Convergence Behaviour of the Control Algorithm

We shall show that in absence of dissipation the algorithm always converges quadratically and monotonically. If dissipation is present, additional assumptions are necessary for convergence:

1. $\|A_v^{(n)}(t)\|_2$ and $\|\rho_v^{(n)}(t)\|_2$ must be uniformly bounded for all n and $t_0 \leq t \leq t_F$, and
2. the propagator $\mathcal{U}(t, t_0)$ must be invertible for $t_0 \leq t \leq t_F$.

If the latter condition fails then the Euler-Lagrange equations (IV.1–IV.3) with two-point boundary conditions (IV.4) can not be solved since equation (IV.3) must be integrated backwards in time to find $|A_v(t)\rangle$. If the propagator is invertible but either $\|A_v^{(n)}(t)\|_2$ or $\|\rho_v^{(n)}(t)\|_2$ is not uniformly bounded for all n and $t_0 \leq t \leq t_F$, then the algorithm is still useful but we can not guarantee quadratic and monotonic convergence.

In the first part of the proof, we establish that

$$\delta W^{(n+1,n)} = W^{(n+1)} - W^{(n)} = \sum_{m=1}^M \frac{\lambda_m}{2\hbar} \int_{t_0}^{t_F} [\delta f_m^{(n+1)}(t)]^2 + [\delta f_m^{(n+1,n)}(t)]^2 dt. \quad (\text{IV.22})$$

This result is true for both Hamiltonian and dissipative systems, provided that the propagator $\mathcal{U}(t, t_0)$ is invertible for $t_0 \leq t \leq t_F$.

The second part will be show that $W^{(n)}$ is a uniformly bounded sequence, which will depend on the requirement that $\|A_v^{(n)}(t)\|$ and $\|\rho_v^{(n)}(t)\|$ be uniformly bounded for all n and $t_0 \leq t \leq t_F$. This condition is always satisfied for Hamiltonian systems, i.e., when $\Gamma = 0$, since in this case the time evolution operator $\mathcal{U}^{(n)}(t, t_0)$ is unitary, i.e.,

$$\|A_v^{(n)}(t)\|_2^2 = \langle\langle A_v^{(n)}(t) | A_v^{(n)}(t) \rangle\rangle = \langle\langle A \mathcal{U}^{(n)}(t_F, t) | \mathcal{U}^{(n)}(t, t_F) A \rangle\rangle = \langle\langle A | A \rangle\rangle = \|A\|_2^2, \quad (\text{IV.23})$$

$$\|\rho_v^{(n)}(t)\|_2^2 = \langle\langle \rho_v^{(n)}(t) | \rho_v^{(n)}(t) \rangle\rangle = \langle\langle \rho_0 \mathcal{U}^{(n)}(t_F, t) | \mathcal{U}^{(n)}(t, t_F) \rho_0 \rangle\rangle = \langle\langle \rho_0 | \rho_0 \rangle\rangle = \|\rho_0\|_2^2. \quad (\text{IV.24})$$

In general, $\|\rho_v^{(n)}(t)\|_2 \leq \|\rho_0\|_2$ for all n and $t_0 \leq t \leq t_F$ even in the dissipative case, i.e., uniform boundedness of $\|\rho_v^{(n)}(t)\|$ is usually satisfied. The norm of $A_v^{(n)}(t)$, however, tends to increase as we integrate $A_v^{(n)}(t)$ backwards in time, i.e., $\|A_v^{(n)}(t)\|_2 \geq \|A\|_2$ for $t < t_F$. Hence, it is not obvious that $\|A_v^{(n)}(t)\|_2$ will be uniformly bounded in the dissipative case.

To establish (IV.22), we observe that the objective functional after the n th iteration step is

$$W^{(n)} = W_1^{(n)} - W_3^{(n)} = \langle\langle A|\rho_v^{(n)}(t_F)\rangle\rangle - \sum_{m=1}^M \frac{\lambda_m}{2\hbar} \int_{t_0}^{t_F} [f_m^{(n,0)}(t)]^2 dt \quad (\text{IV.25})$$

since $W_2^{(n)} = W_2(\vec{f}^{(n,0)}, \rho_v^{(n)}, A_v^{(n)}) = 0$ according to equations (I.31) and (IV.20). Furthermore, we use the following lemmas.

LEMMA IV.1 : If $\mathcal{U}(t, t_0)$ satisfies $i\hbar\partial_t\mathcal{U}(t, t_0) = \mathcal{L}_{tot}\mathcal{U}(t, t_0)$ then

$$|\rho(t)\rangle\rangle = -\frac{i}{\hbar}\mathcal{U}(t, t_0) \int_{t_0}^t \mathcal{U}^{-1}(t', t_0)|\varphi(t')\rangle\rangle dt' \quad (\text{IV.26})$$

is a solution of $i\hbar\partial_t|\rho(t)\rangle\rangle = \mathcal{L}_{tot}|\rho(t)\rangle\rangle + |\varphi(t)\rangle\rangle$ (provided that $\mathcal{U}(t, t_0)$ is invertible for $t_0 \leq t \leq t_F$).

PROOF : Differentiating $|\rho(t)\rangle\rangle$ using

$$\partial_t \int_{t_0}^t \mathcal{U}^{-1}(t', t_0)|\varphi(t')\rangle\rangle dt' = \mathcal{U}^{-1}(t, t_0)|\varphi(t)\rangle\rangle$$

leads to

$$\begin{aligned} \partial_t|\rho(t)\rangle\rangle &= [-\frac{i}{\hbar}\mathcal{L}_{tot}\mathcal{U}(t, t_0)] \int_{t_0}^t \mathcal{U}^{-1}(t', t_0)|\varphi(t')\rangle\rangle dt' - \frac{i}{\hbar}\mathcal{U}(t, t_0)\mathcal{U}^{-1}(t, t_0)|\varphi(t)\rangle\rangle \\ &= -\frac{i}{\hbar}\mathcal{L}_{tot}|\rho(t)\rangle\rangle - \frac{i}{\hbar}|\varphi(t)\rangle\rangle. \end{aligned}$$

□

LEMMA IV.2 : $|\delta\rho_v^{(n)}(t)\rangle\rangle \equiv |\rho_v^{(n+1)}(t)\rangle\rangle - |\rho_v^{(n)}(t)\rangle\rangle$ is formally given by

$$-\frac{i}{\hbar}\mathcal{U}^{(n+1,1)}(t, t_0) \int_{t_0}^t \mathcal{U}^{(n+1,1)}(t', t_0)^{-1} \sum_{m=1}^M \mathcal{L}_m |(\delta f_m^{(n+1)}\rho_v^{(n+1)} + \delta f_m^{(n+1,n)}\rho_v^{(n)})(t')\rangle\rangle dt'. \quad (\text{IV.27})$$

where

$$\mathcal{U}^{(n+1,1)}(t, t_0) \equiv \exp_+ \left[-\frac{i}{\hbar} \int_{t_0}^t \mathcal{L}_{tot}^{(n+1,1)}(\tau) d\tau \right]. \quad (\text{IV.28})$$

PROOF :

$$i\hbar\partial_t|\rho_v^{(n)}(t)\rangle\rangle = \left[\mathcal{L}_0 - i\hbar\Gamma + \sum_{m=1}^M f_m^{(n,0)}(t)\mathcal{L}_m \right] |\rho_v^{(n)}(t)\rangle\rangle \quad (\text{IV.29})$$

leads to

$$i\hbar\partial_t|\delta\rho_v^{(n)}(t)\rangle\rangle = [\mathcal{L}_0 - i\hbar\Gamma]|\delta\rho_v^{(n)}\rangle\rangle + \sum_{m=1}^M \mathcal{L}_m [f_m^{(n+1,0)}(t)|\rho_v^{(n+1)}(t)\rangle\rangle - f_m^{(n+1,0)}(t)|\rho_v^{(n+1)}(t)\rangle\rangle]. \quad (\text{IV.30})$$

Inserting

$$\begin{aligned} & f_m^{(n+1,0)}|\rho_v^{(n+1)}\rangle\rangle - f_m^{(n,0)}|\rho_v^{(n)}\rangle\rangle \quad (\text{IV.31}) \\ &= (f_m^{(n,0)} + \delta f_m^{(n+1,n)} + \delta f_m^{(n)})|\rho_v^{(n)} + \delta\rho_v^{(n)}\rangle\rangle - f_m^{(n,0)}|\rho_v^{(n)}\rangle\rangle \\ &= (\delta f_m^{(n+1,n)} + \delta f_m^{(n)})|\rho_v^{(n)}\rangle\rangle + (f_m^{(n,0)} + \delta f_m^{(n+1,n)} + \delta f_m^{(n)})|\delta\rho_v^{(n)}\rangle\rangle \\ &= (\delta f_m^{(n+1,n)} + \delta f_m^{(n)})|\rho_v^{(n)}\rangle\rangle + (f_m^{(n+1,n)} + \delta f_m^{(n)})|\delta\rho_v^{(n)}\rangle\rangle \\ &= \delta f_m^{(n+1,n)}|\rho_v^{(n)}\rangle\rangle + \delta f_m^{(n)}|\rho_v^{(n+1)}\rangle\rangle + f_m^{(n+1,n)}|\delta\rho_v^{(n)}\rangle\rangle \quad (\text{IV.32}) \end{aligned}$$

and collecting like terms, equation (IV.30) becomes

$$i\hbar\partial_t|\delta\rho_v^{(n)}(t)\rangle\rangle = \mathcal{L}_{tot}^{(n+1,1)}|\delta\rho_v^{(n)}(t)\rangle\rangle + \sum_{m=1}^M \mathcal{L}_m |(\delta f_m^{(n+1)}\rho_v^{(n+1)} + \delta f_m^{(n+1,n)}\rho_v^{(n)})(t)\rangle\rangle \quad (\text{IV.33})$$

According to the previous lemma, the formal solution of this differential equation is (IV.27).

□

To complete part 1 of the proof, we need to simplify the expression

$$\delta W^{(n+1,n)} = W^{(n+1)} - W^{(n)} = \langle\langle A|\delta\rho_v^{(n)}(t_F)\rangle\rangle - \sum_{m=1}^M \frac{\lambda_m}{2\hbar} \int_{t_0}^{t_F} [f_m^{(n+1,0)}(t)]^2 - [f_m^{(n,0)}]^2 dt, \quad (\text{IV.34})$$

i.e., in particular we need to re-write the first term

$$\begin{aligned} \langle\langle A|\delta\rho_v^{(n)}(t_F)\rangle\rangle &= -\frac{i}{\hbar} \int_{t_0}^{t_F} \langle\langle A|\mathcal{U}^{(n+1,1)}(t_F, t_0)\mathcal{U}^{(n+1,1)}(t, t_0)^{-1} \times \\ & \quad \sum_{m=1}^M \mathcal{L}_m |(\delta f_m^{(n+1)}\rho_v^{(n+1)} + \delta f_m^{(n+1,n)}\rho_v^{(n)})(t)\rangle\rangle dt \\ &= -\frac{i}{\hbar} \int_{t_0}^{t_F} \langle\langle A_v^{(n+1)}(t)| \sum_{m=1}^M \mathcal{L}_m |(\delta f_m^{(n+1)}\rho_v^{(n+1)} + \delta f_m^{(n+1,n)}\rho_v^{(n)})(t)\rangle\rangle dt \\ &= -\frac{i}{\hbar} \sum_{m=1}^M \int_{t_0}^{t_F} \delta f_m^{(n+1)}(t) \langle\langle A_v^{(n+1)}(t)| \mathcal{L}_m \rho_v^{(n+1)}(t)\rangle\rangle dt \end{aligned}$$

$$\begin{aligned}
& + \int_{t_0}^{t_F} \delta f_m^{(n+1,n)}(t) \langle \langle A_v^{(n+1)}(t) | \mathcal{L}_m \rho_v^{(n)}(t) \rangle \rangle dt \\
= & \sum_{m=1}^M \frac{\lambda_m}{\hbar} \int_{t_0}^{t_F} \delta f_m^{(n+1)}(t) f_m^{(n+1,0)}(t) + \delta f_m^{(n+1,n)}(t) f_m^{(n+1,1)}(t) dt \\
= & \sum_{m=1}^M \frac{\lambda_m}{\hbar} \int_{t_0}^{t_F} [f_m^{(n+1,0)}(t)]^2 - f_m^{(n+1,1)}(t) f_m^{(n+1,0)}(t) \\
& + [f_m^{(n+1,1)}(t)]^2 - f_m^{(n,0)}(t) f_m^{(n+1,1)}(t) dt. \tag{IV.35}
\end{aligned}$$

Substituting equation (IV.35) into (IV.34) yields

$$\begin{aligned}
\delta W^{(n+1,n)} & = \sum_{m=1}^M \frac{\lambda_m}{2\hbar} \int_{t_0}^{t_F} [f_m^{(n+1,0)}(t)]^2 - 2f_m^{(n+1,1)}(t) f_m^{(n+1,0)}(t) + [f_m^{(n+1,1)}(t)]^2 \\
& \quad + [f_m^{(n+1,1)}(t)]^2 - 2f_m^{(n,0)}(t) f_m^{(n+1,1)}(t) + [f_m^{(n,0)}(t)]^2 dt \\
= & \sum_{m=1}^M \frac{\lambda_m}{2\hbar} \int_{t_0}^{t_F} [\delta f_m^{(n+1)}(t)]^2 + [\delta f_m^{(n+1,n)}(t)]^2 dt, \tag{IV.36}
\end{aligned}$$

which completes part 1 of the proof.

LEMMA IV.3 : If $\|A_v^{(n)}(t)\|_2$ and $\|\rho_v^{(n)}(t)\|_2$ are uniformly bounded then $W^{(n)}$ is uniformly bounded.

PROOF : Applying Cauchy-Schwarz's inequality

$$\begin{aligned}
|\langle \langle A | \rho_v^{(n)}(t) \rangle \rangle|^2 & \leq \|A\|_2^2 \cdot \|\rho_v^{(n)}(t)\|_2^2 \leq \|A\|_2^2, \\
|f_m(t)|^2 & = \left| -\frac{i}{\lambda_m} \langle \langle A_v^{(n)}(t) | \mathcal{L}_m \rho_v^{(n)}(t) \rangle \rangle \right|^2 \\
& \leq \frac{1}{\lambda_m^2} \|A_v^{(n)}(t)\|_2^2 \cdot \|\mathcal{L}_m \rho_v^{(n)}(t)\|_2^2 \\
& \leq \frac{1}{\lambda_m^2} \|A_v^{(n)}(t)\|_2^2 \cdot \|\mathcal{L}_m\| \cdot \|\rho_v^{(n)}(t)\|_2^2 \\
& \leq \frac{1}{\lambda_m^2} \|A_v^{(n)}(t)\|_2^2 \cdot \|\mathcal{L}_m\| \tag{IV.37}
\end{aligned}$$

where $\|\cdot\|$ is the usual operator norm. Thus,

$$|W^{(n)}| \leq |W_1^{(1)}| + |W_3^{(n)}| \leq \|A\|_2 + \sum_{m=1}^M \frac{t_F - t_0}{2\lambda_m} \|A_v^{(n)}(t)\|_2^2 \cdot \|\mathcal{L}_m\| \tag{IV.38}$$

for all n , and since $\|A_v^{(n)}(t)\|_2$ and $\|\rho_v^{(n)}(t)\|_2$ are uniformly bounded by assumption, the claim follows. \square

To complete the proof of the convergence theorem, notice that equation (IV.36) implies that the total variation from $n = 0$ to n_F is

$$\begin{aligned} \delta W^{(n_F,0)} &= W^{(n_F)} - W^{(0)} = \sum_{n=0}^{n_F-1} \delta W^{(n+1,n)} \\ &= \sum_{n=0}^{n_F-1} \sum_{m=1}^M \frac{\lambda_m}{2\hbar} \int_{t_0}^{t_F} [\delta f_m^{(n+1)}(t)]^2 + [\delta f_m^{(n+1,n)}(t)]^2 dt \end{aligned} \quad (\text{IV.39})$$

Since $W^{(n)}$ is uniformly bounded, $W^{(n_F)} - W^{(0)}$ is also uniformly bounded for all n_F and thus the sequence $\{\delta W^{(n_F,0)} : n_F \in \mathbb{N}_0\}$ is uniformly bounded.

$$\int_{t_0}^{t_F} [\delta f_m^{(n+1)}(t)]^2 + [\delta f_m^{(n+1,n)}(t)]^2 dt > 0 \quad (\text{IV.40})$$

for any n implies furthermore that $\delta W^{(n_F,0)}$ is an increasing sequence. Hence,

$\lim_{n_F \rightarrow \infty} \delta W^{(n_F,0)}$ exists and is finite and

$$\lim_{n \rightarrow \infty} \frac{\lambda_m}{2\hbar} \int_{t_0}^{t_F} [\delta f_m^{(n+1)}(t)]^2 + [\delta f_m^{(n+1,n)}(t)]^2 dt = 0, \quad m = 1, \dots, M. \quad (\text{IV.41})$$

IV.4 Numerical Implementation

The differential equations arising from this feedback algorithm must be solved numerically. While there are many methods of integrating differential equations numerically, we employ a symmetric split operator method [27, 11]. The main advantage of this method is that it preserves the norm of the operators if the system is Hamiltonian.

We divide the time interval $[t_0, t_F]$ in subintervals $[t_j, t_{j+1}]$ of a fixed length $\Delta t = t_{j+1} - t_j$ with $t_F = t_J$. On each subinterval $[t_j, t_{j+1}]$ we approximate $f^{(n,k)}(t)$ by the constant $f^{(n,k)}(\tau_j)$ where

$$\tau_j = t_j + \Delta t/2 = t_{j+1} - \Delta t/2. \quad (\text{IV.42})$$

With this approximation the propagator can be written as

$$\mathcal{U}^{(n,k)}(t_{j+1}, t_j) = \exp \left[-\frac{i}{\hbar} \Delta t \left(\mathcal{L}_0 + \sum_{m=1}^M f_m^{(n,k)}(\tau_j) \mathcal{L}_m - i\hbar\Gamma \right) \right]. \quad (\text{IV.43})$$

Unfortunately, this expression is numerically very inefficient since it would require evaluation of a matrix exponential for each time τ_j . However, we can use

$$e^{-i\alpha(A+B)} = e^{-i(\alpha/2)A} e^{-i\alpha B} e^{-i(\alpha/2)A} + O(\alpha^3) \quad (\text{IV.44})$$

to obtain an approximation to (IV.43) that is accurate up to terms of order Δt^2 . Setting

$$\mathcal{U}_D = \exp \left(-\frac{\Delta t}{2} \Gamma \right) \quad (\text{IV.45})$$

$$\mathcal{U}_0 = \exp \left(-\frac{i}{\hbar} \frac{\Delta t}{2} \mathcal{L}_0 \right) \quad (\text{IV.46})$$

$$\mathcal{U}_m^{(n,k)}(\tau_j) = \exp \left(-\frac{i}{\hbar} \frac{\Delta t}{2} f_m^{(n,k)}(\tau_j) \mathcal{L}_m \right) \quad (\text{IV.47})$$

and applying this formula repeatedly leads to

$$\begin{aligned} \mathcal{U}^{(n,k)}(t_{j+1}, t_j) &= \mathcal{U}_D \mathcal{U}_0 \mathcal{U}_1^{(n,k)}(\tau_j) \mathcal{U}_2^{(n,k)}(\tau_j) \cdots \mathcal{U}_M^{(n,k)}(\tau_j) \times \\ &\quad \mathcal{U}_M^{(n,k)}(\tau_j) \cdots \mathcal{U}_2^{(n,k)}(\tau_j) \mathcal{U}_1^{(n,k)}(\tau_j) \mathcal{U}_0 \mathcal{U}_D. \end{aligned} \quad (\text{IV.48})$$

Notice that if there is more than one control, the choice of the order of the terms in (IV.48) is not fixed but rather depends on the order of the controls. This problem could be corrected by averaging over all the possible permutations of the order of the controls but in practice this appears to be too computationally expensive.

(IV.48) is numerically favourable since the matrix exponentials \mathcal{U}_0 and \mathcal{U}_D need to be computed only once and \mathcal{U}_0 and $\mathcal{U}_m^{(n,k)}(\tau_j)$ can be efficiently computed using

$$\mathcal{U}_0 = \sum_{a=1}^N |a\rangle\rangle \exp \left(-\frac{i\Delta t}{2\hbar} a \right) \langle\langle a| \quad (\text{IV.49})$$

$$\mathcal{U}_m^{(n,k)}(\tau_j) = \sum_{b_m=1}^N |b_m\rangle\rangle \exp \left(-\frac{i\Delta t}{2\hbar} f_m^{(n,k)}(\tau_j) b_m \right) \langle\langle b_m|, \quad (\text{IV.50})$$

where $|a\rangle\rangle$ and $|b_m\rangle\rangle$ are the eigenkets of \mathcal{L}_0 and \mathcal{L}_m , respectively; a and b_m are the corresponding (real) eigenvalues. (IV.50) reduces the evaluation of $\mathcal{U}_m^{(n,k)}(\tau_j)$ essentially

to computing a few complex exponentials in each step and summing up the terms. Note that the eigenvalue decomposition of \mathcal{L}_m has to be computed only once.

In order to compute $f_m(\tau_j)$, we note that

$$f_m(t \pm \Delta t) = f_m(t) \pm \Delta t \frac{df_m(t)}{dt} + O(|\Delta t|^2) \quad (\text{IV.51})$$

and hence we have the first order approximation

$$f_m^{(n,0)}(\tau_j) = f_m^{(n,0)}(t_j) + \frac{\Delta t}{2\lambda_m} \langle \langle A_v^{(n)}(t_j) | [\mathcal{L}_0, \mathcal{L}_m] \rho_v^{(n)}(t_j) \rangle \rangle \quad (\text{IV.52})$$

$$f_m^{(n,1)}(\tau_{j-1}) = f_m^{(n,1)}(t_j) - \frac{\Delta t}{2\lambda_m} \langle \langle A_v^{(n)}(t_j) | [\mathcal{L}_0, \mathcal{L}_m] \rho_v^{(n-1)}(t_j) \rangle \rangle. \quad (\text{IV.53})$$

CHAPTER V
ILLUSTRATIVE COMPUTATIONS

V.1 Energy maximization for a four-level Morse oscillator model of a diatomic molecule

We first consider a four-level system (Morse oscillator model for a diatomic molecule) with internal Hamiltonian

$$\hat{H}_0 = \sum_{n=1}^4 E_n |n\rangle\langle n| \quad (\text{V.1})$$

$$\doteq \begin{bmatrix} 0.494762 & 0 & 0 & 0 \\ 0 & 1.45286 & 0 & 0 \\ 0 & 0 & 2.36906 & 0 \\ 0 & 0 & 0 & 3.24336 \end{bmatrix}$$

and interaction Hamiltonian

$$\hat{H}_1 = f(t) \sum_{n=1}^3 d_n (|n\rangle\langle n+1| + |n+1\rangle\langle n|) \quad (\text{V.2})$$

$$\doteq f(t) \begin{bmatrix} 0 & 1.0 & 0 & 0 \\ 1.0 & 0 & 1.41421 & 0 \\ 0 & 1.41421 & 0 & 1.73205 \\ 0 & 0 & 1.73205 & 0 \end{bmatrix},$$

where $f(t)$ is the external control field, which is to be determined. We neglect dissipation, i.e., $\Gamma = 0$. We verified that this system is completely controllable.

The target observable is the energy of the system,

$$\hat{A} = \hat{H}_0. \quad (\text{V.3})$$

and the aim is to maximize the expectation value of \hat{A} at the target time $t_F = 200$ fs, starting at $t_0 = 0$, subject to the constraints that the evolution of the system satisfy the quantum Liouville equation and that the pulse fluence be as small as possible.

We consider two initial states of the system. In the first case, which we shall refer to as the pure-state case, the system is initially in the ground state, i.e.,

$$\begin{aligned}\hat{\rho}_0 &= |1\rangle\langle 1| \\ &\doteq \begin{bmatrix} 1 & 0 & 0 & 0 \\ 0 & 0 & 0 & 0 \\ 0 & 0 & 0 & 0 \\ 0 & 0 & 0 & 0 \end{bmatrix}.\end{aligned}\quad (\text{V.4})$$

and the kinematical bounds for the expectation value of the observable according to theorem II.1 are

$$0.494762 \leq \langle \hat{A}(t) \rangle \leq 3.24336. \quad (\text{V.5})$$

These bounds are dynamically attainable since the system is completely controllable.

Therefore, the relative yield is

$$\text{yield} = \frac{\langle \hat{A}(t_F) \rangle}{3.24336}. \quad (\text{V.6})$$

In the second case, which we shall refer to as the mixed-state case, the system is initially in thermal equilibrium, i.e.,

$$\begin{aligned}\hat{\rho}_0 &= \sum_{n=1}^4 w_n |n\rangle\langle n| \\ &\doteq \begin{bmatrix} w_1 & 0 & 0 & 0 \\ 0 & w_2 & 0 & 0 \\ 0 & 0 & w_3 & 0 \\ 0 & 0 & 0 & w_4 \end{bmatrix}\end{aligned}\quad (\text{V.7})$$

with weights

$$w_n = C \exp\left(-\frac{E_n}{E_4 - E_1}\right). \quad (\text{V.8})$$

This is a Boltzmann distribution with $kT = E_4 - E_1$ and normalization constant

$$C = \left(e^{-E_1/kT} + e^{-E_2/kT} + e^{-E_3/kT} + e^{-E_4/kT}\right)^{-1} \quad (\text{V.9})$$

Concretely, $w_1 = 0.3850$, $w_2 = 0.2758$, $w_3 = 0.1976$ and $w_4 = 0.1416$ and the kinematical bounds for the expectation value of the observable according to theorem II.1 are

$$1.518570 \leq \langle \hat{A}(t) \rangle \leq 2.259226. \quad (\text{V.10})$$

Again these bounds are dynamically attainable. Hence, the relative yield is

$$\text{yield} = \frac{\langle \hat{A}(t_F) \rangle}{2.259226}. \quad (\text{V.11})$$

We performed various control computations for both the mixed-state and the pure-state case. The results of some of these computations are presented in figures 2–11. The first graph in the top left corner of each figure represents the final optimal pulse, i.e., the output of the algorithm, after the number of iterations specified. Its Fourier components are shown in the adjoining graph (top right). The evolution of the energy level populations (middle left) and the ensemble average of the target observable (middle right) that result from driving the system with this control field, are displayed below. Notice the inversion of the energy level populations in all the mixed-state computations, which is predicted by theorem 1, and the almost monotonic increase of the expectation value of the target observable. The bottom left graph depicts the relative yield as a function of the number of iterations. The input field is plotted in the last graph (bottom right).

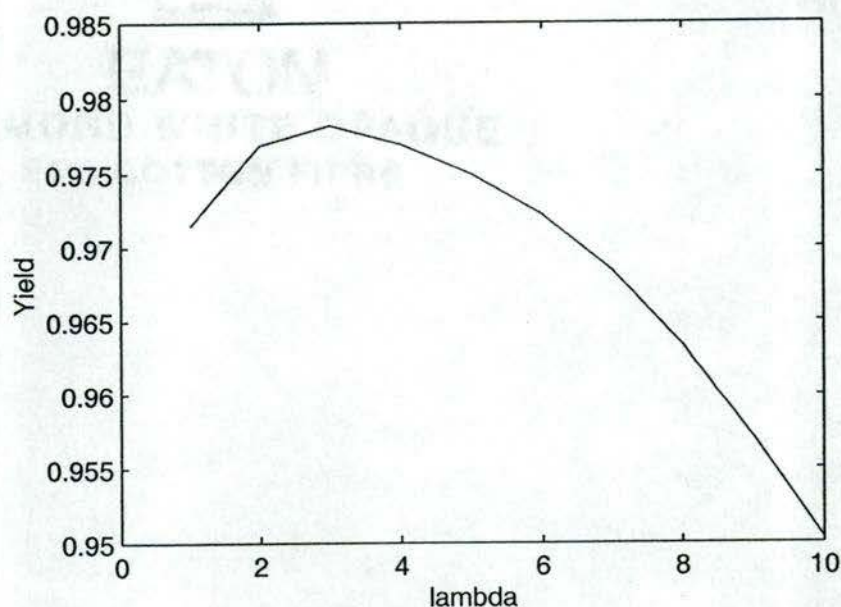
In all these figures, the striking dissimilarity of the initial field (bottom right) and the final optimal pulse (top left) is immediately obvious. A glance at the yield plotted as a function of the number of iterations also demonstrates the rapid, quadratic convergence of the algorithm. The yield usually increases tremendously during the first iteration step and then quickly approaches a limiting value close to one. The rapid convergence of the algorithm is even more impressive when one watches the actual transformation of the input field into the optimal control as the algorithm progresses. Several movies showing the transformation of the input field into the final optimal pulse, as well as the corresponding transformation of the evolution of the energy level populations and

the ensemble average of the target observable, are available online (in mpeg format) at <http://hopf.uoregon.edu/~schirmer/Research/Research.html>

In order to determine the dependence of the outcome of a numerical optimization computation on the input field $f^{(0)}$, we carried out computations for various input fields while keeping the parameters λ and J fixed. We observed that the final optimal control field obtained, changes with the magnitude of the input field, i.e., $\|f^{(0)}\|$, but does not appear to be affected noticeably by small perturbations in the input field. Specifically, we tested the program using 'random noise' as input. In general, we noticed no significant differences in the final pulse shape when performing computations with different random initial functions as long as $\|f^{(0)}\|$ remained essentially the same. Changing the norm of the initial field, however, can affect the result of the computation, as a comparison of figures 2 and 3 shows. The only difference between these computations is that in one case the norm of the initial field is about five times larger than in the other. The resulting final pulse shapes are quite dissimilar, yet, the final yield does not change significantly (94.97% vs 96.39%), which also demonstrates the non-uniqueness of solutions to the optimal control problem.

The choice of the number of subintervals J in the numerical implementation of the algorithm is another important issue since the value of J determines the time-resolution of the field and restricts the Fourier components of the pulse. Increasing the value of J improves the time resolution of the pulse and tends to increase the yield. However, choosing a larger J also increases the computational burden considerably, while the yield improvement may be rather small, as a comparison of figures 7 and 8 shows. Doubling the value of J improves the yield only marginally from 97.82% for $J = 400$ to 98.21% for $J = 800$ after 20 iterations.

We also performed computations for different values of the control parameter λ and fixed values of J and the initial field $f^{(0)}$. Figure 1 shows the dependence of the yield

FIGURE 1: Final yield as a function of λ 

for a mixed-state computation after (at most) 20 iterations as a function of λ . The computations were carried out for $J = 400$ and random noise of magnitude 0.05 (arb. units) as input field. There appears to be a maximum of ca. 97.82% for $\lambda = 3$. When λ is too small, the magnitude of the control field, which is proportional to $\frac{1}{\lambda}$ according to equation (IV.1), becomes too large and the pulse too short, which negatively affects the yield. When λ is too large, the control field does not appear to be strong enough to drive the system, which also seems to lead to a decrease of the final yield.

Moreover, when the magnitude of the field becomes too large, the approximations made to solve the Euler-Lagrange equations numerically break down, resulting in poor performance of the program. An example of such behaviour is shown in figure 5. Notice that the yield increases significantly in the first step and then drops again, which causes the program to terminate immediately. In some cases, it is still possible to obtain convergence by increasing the parameter J , however, in general it appears to be better to adjust the control parameter λ .

FIGURE 2: Energy maximization for a four-level Morse oscillator initially in the ground state with control parameters $J = 400$, $\lambda = 4$

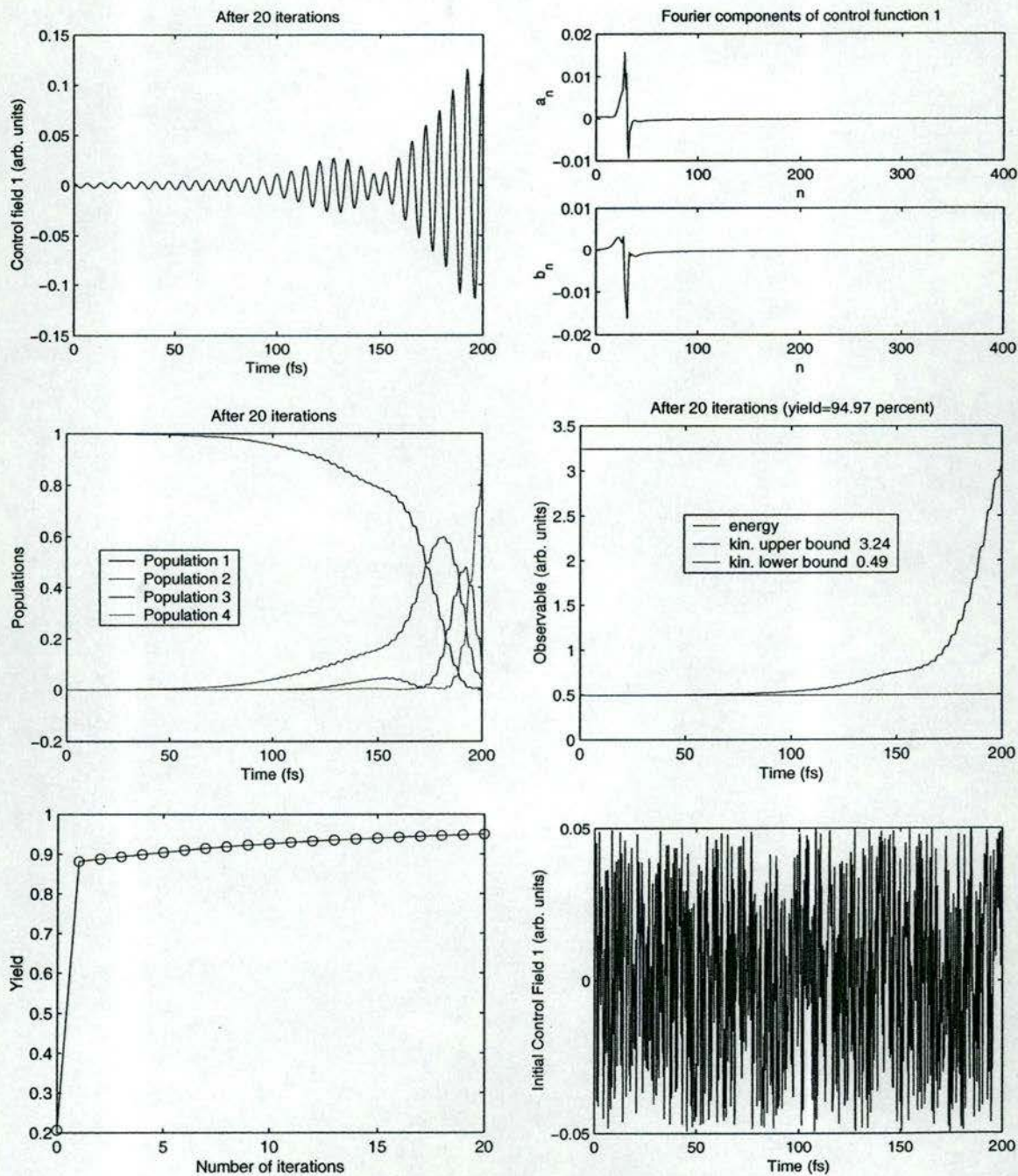


FIGURE 3: Energy maximization for a four-level Morse oscillator initially in the ground state with control parameters $J = 400$, $\lambda = 4$

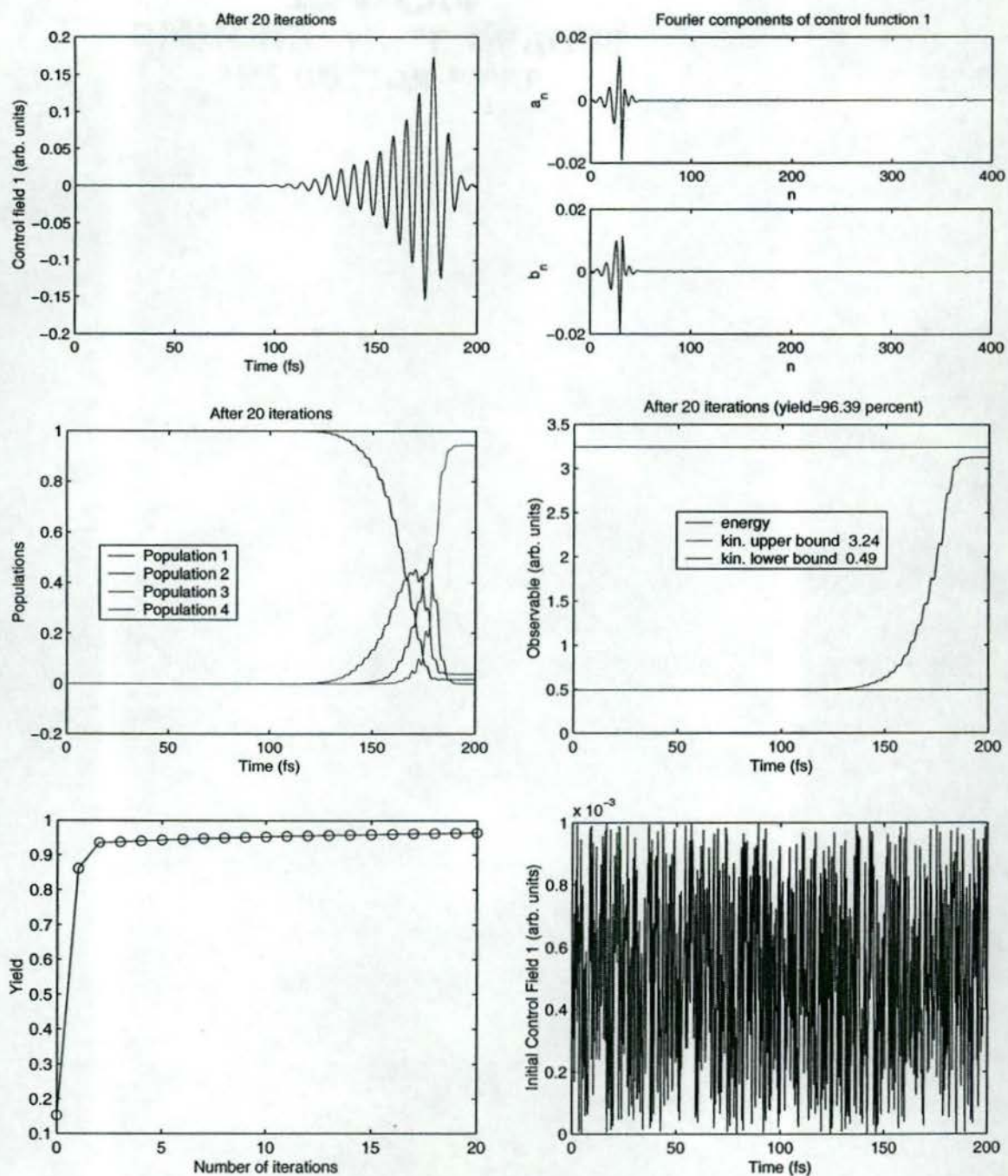


FIGURE 4: Energy maximization for a four-level Morse oscillator initially in the ground state with control parameters $J = 400$, $\lambda = 2$

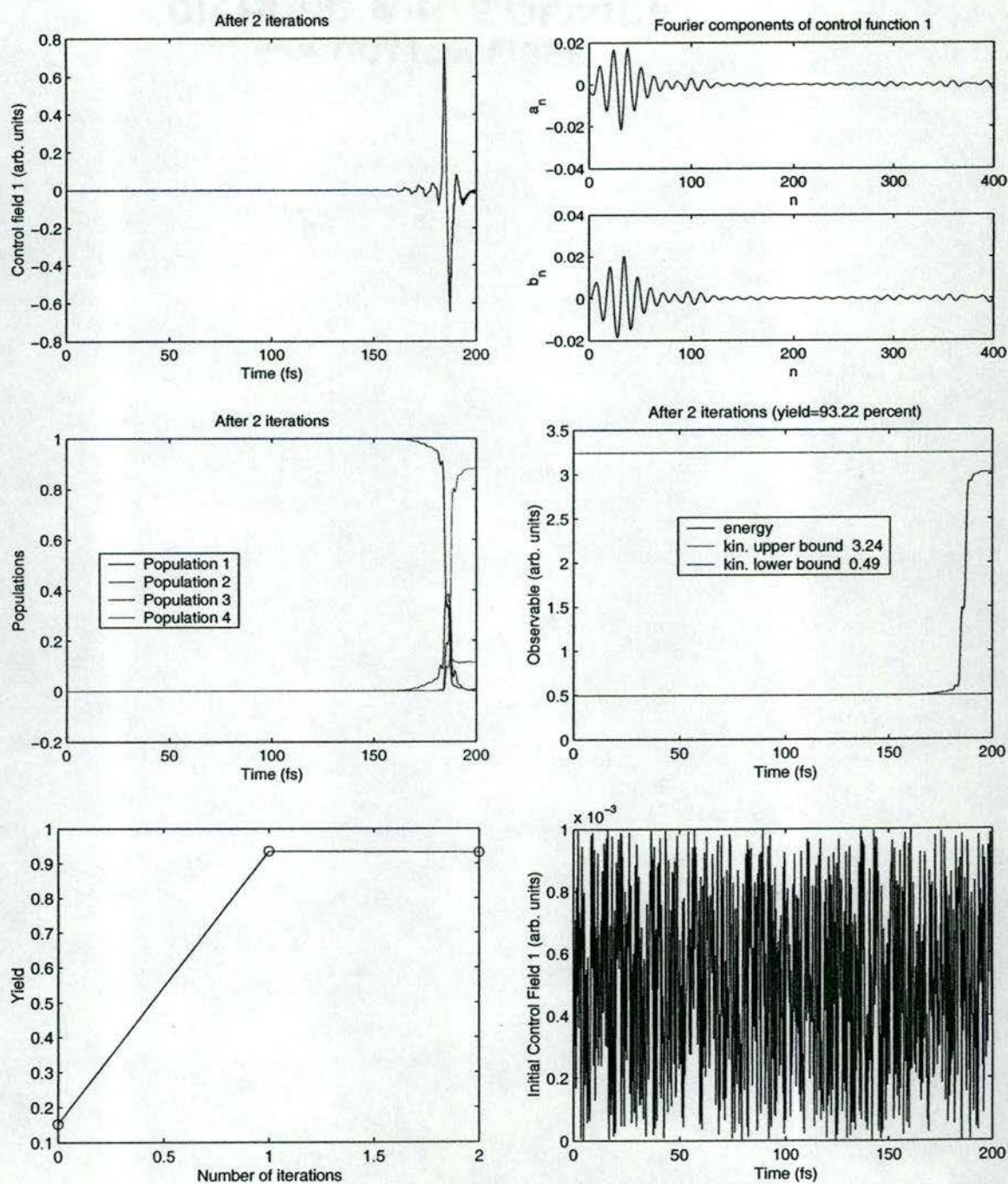


FIGURE 5: Energy maximization for a four-level Morse oscillator initially in the ground state with control parameters $J = 400$, $\lambda = 1$

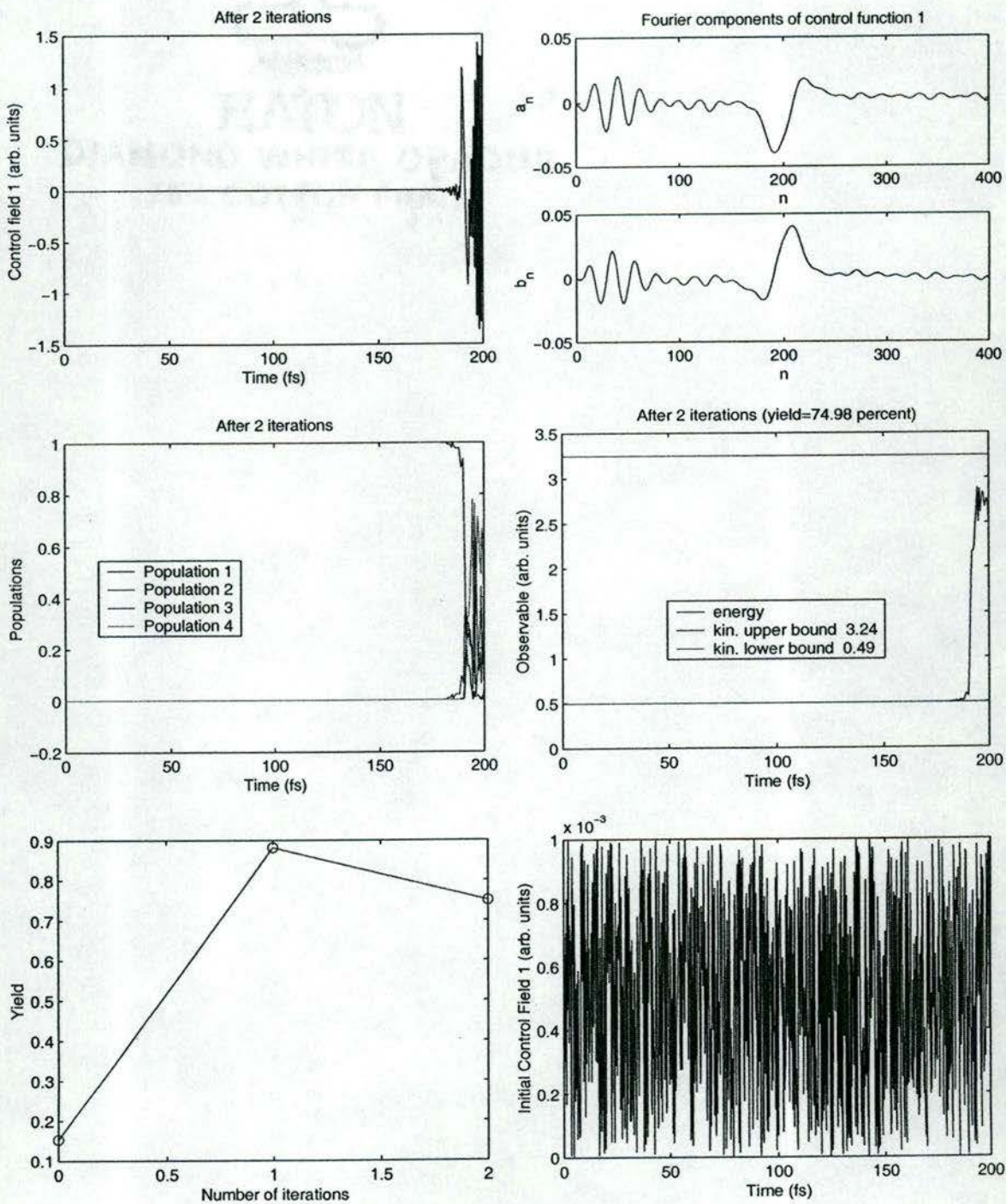


FIGURE 6: Energy maximization for a four-level Morse oscillator initially in the ground state with control parameters $J = 400$, $\lambda = 8$

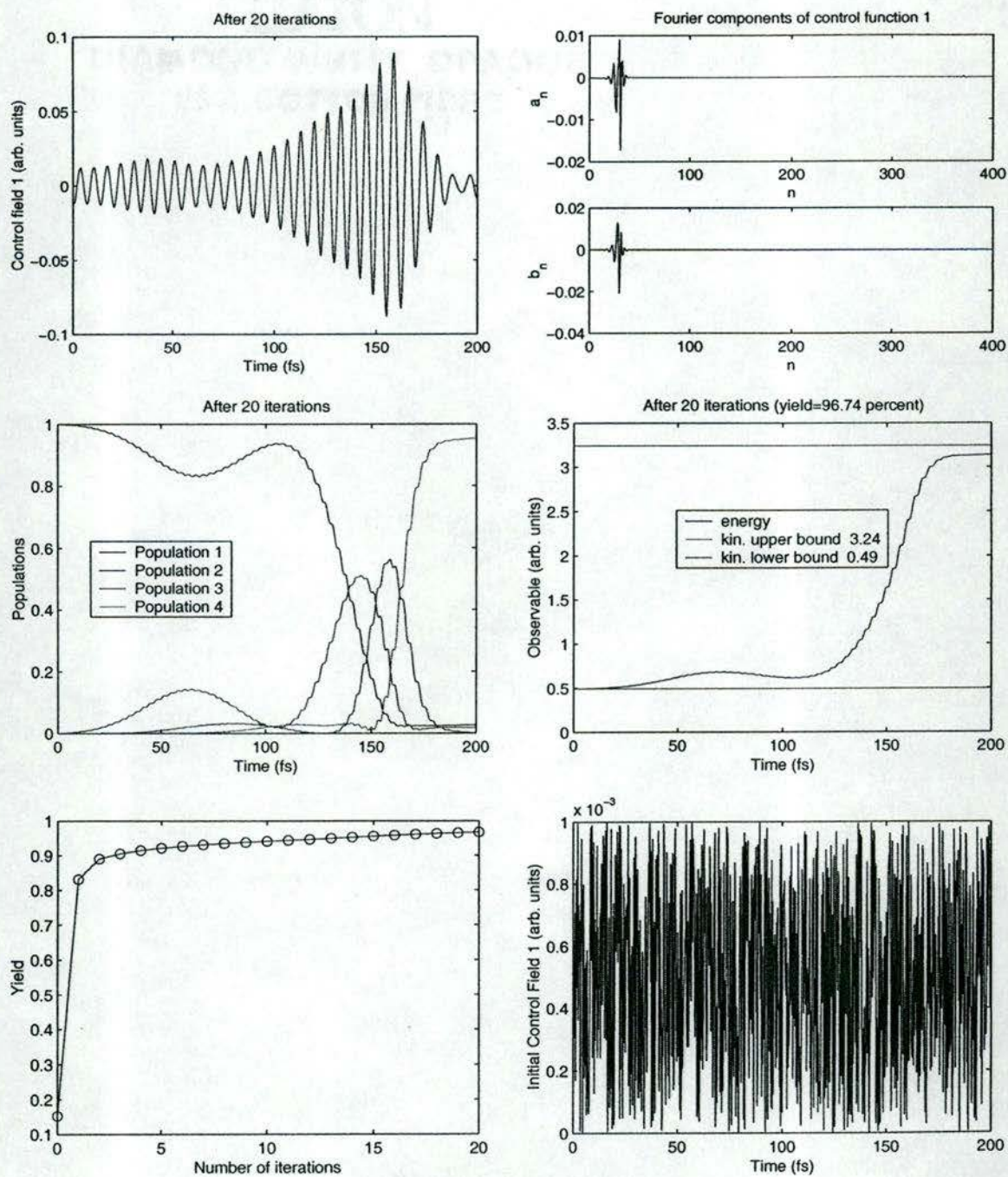


FIGURE 7: Energy maximization for a four-level Morse oscillator initially in thermal equilibrium with control parameters $J = 800$, $\lambda = 4$

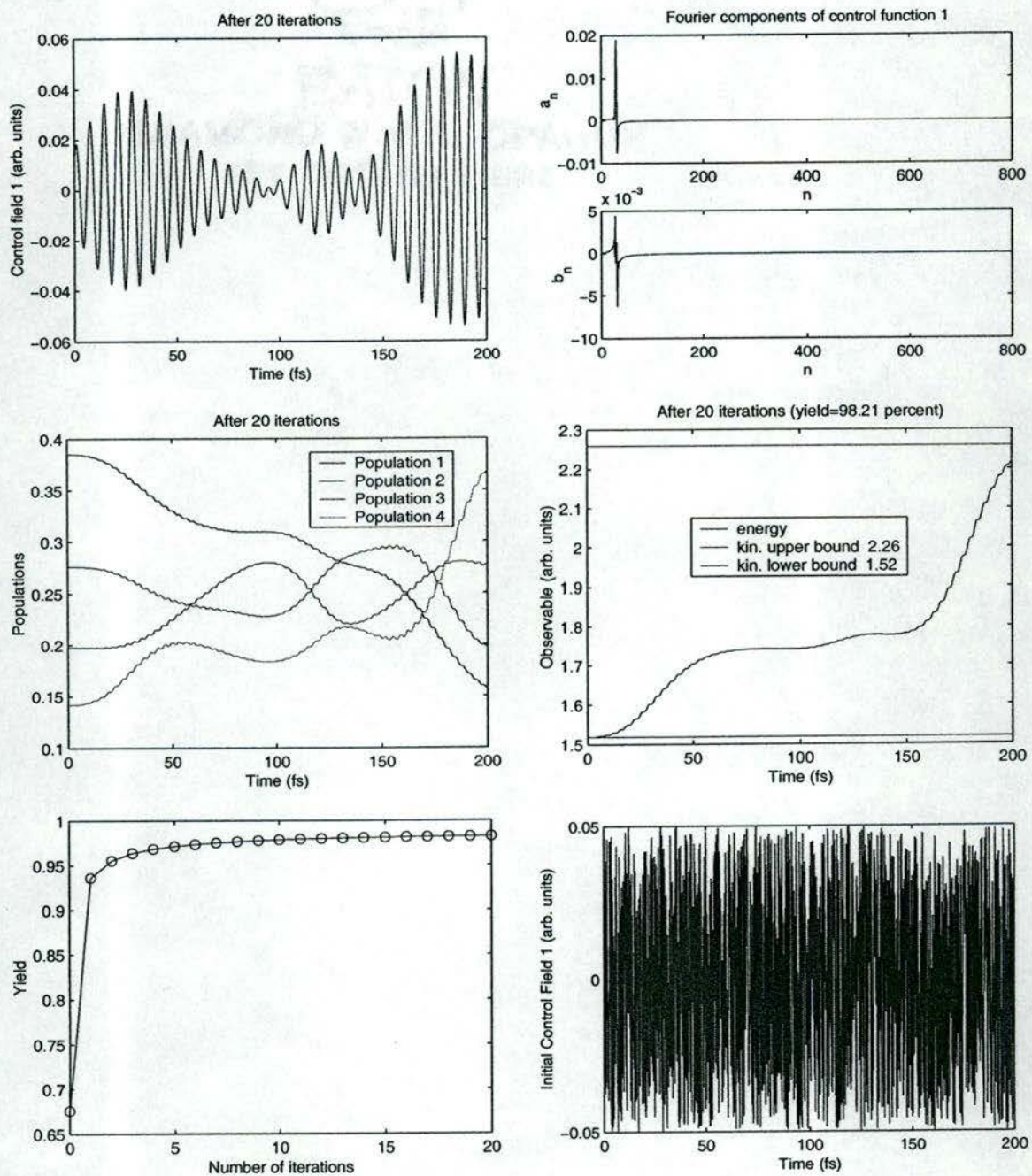


FIGURE 8: Energy maximization for a four-level Morse oscillator initially in thermal equilibrium with control parameters $J = 400$, $\lambda = 4$

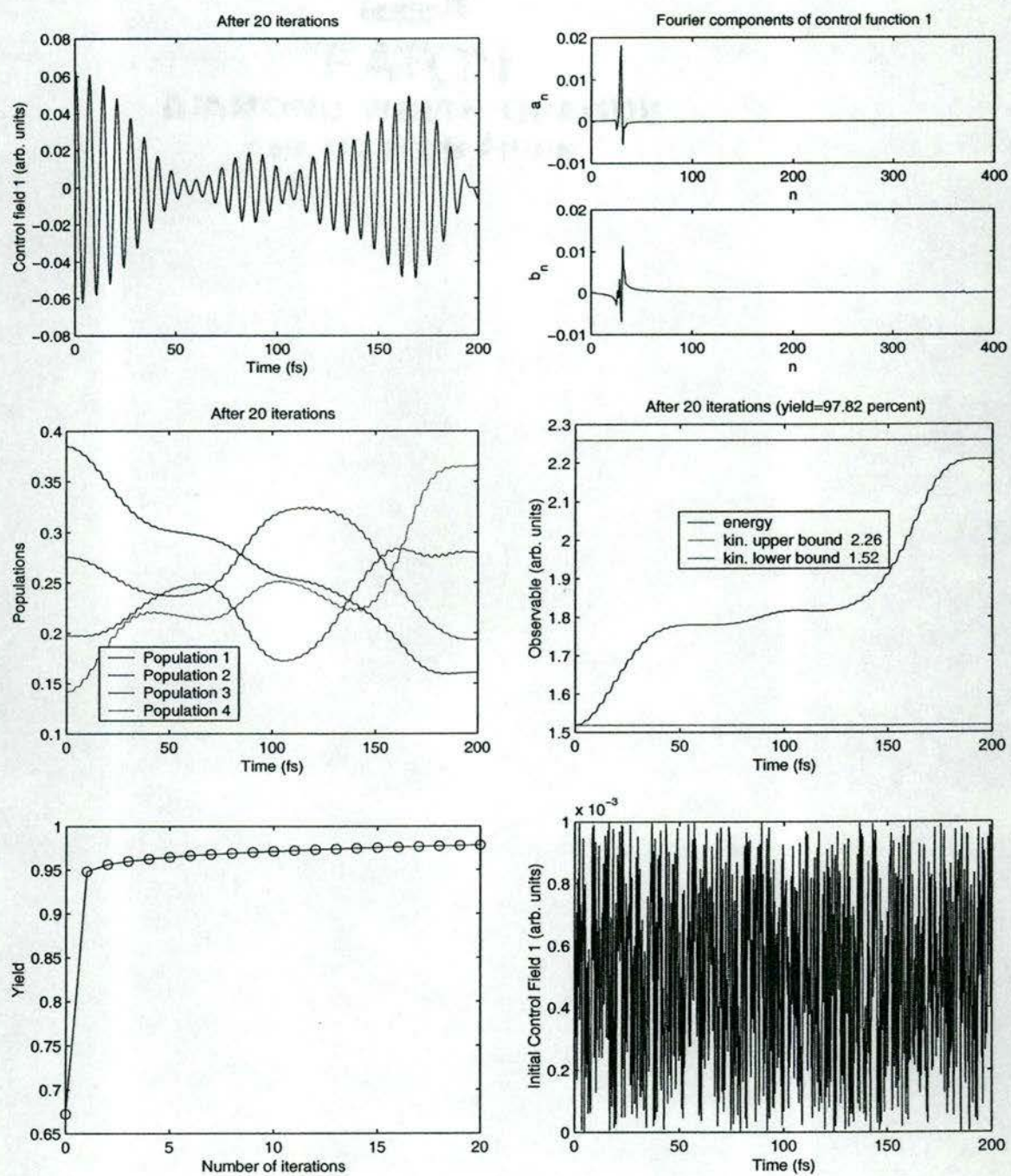


FIGURE 9: Energy maximization for a four-level Morse oscillator initially in thermal equilibrium with control parameters $J = 400$, $\lambda = 2$

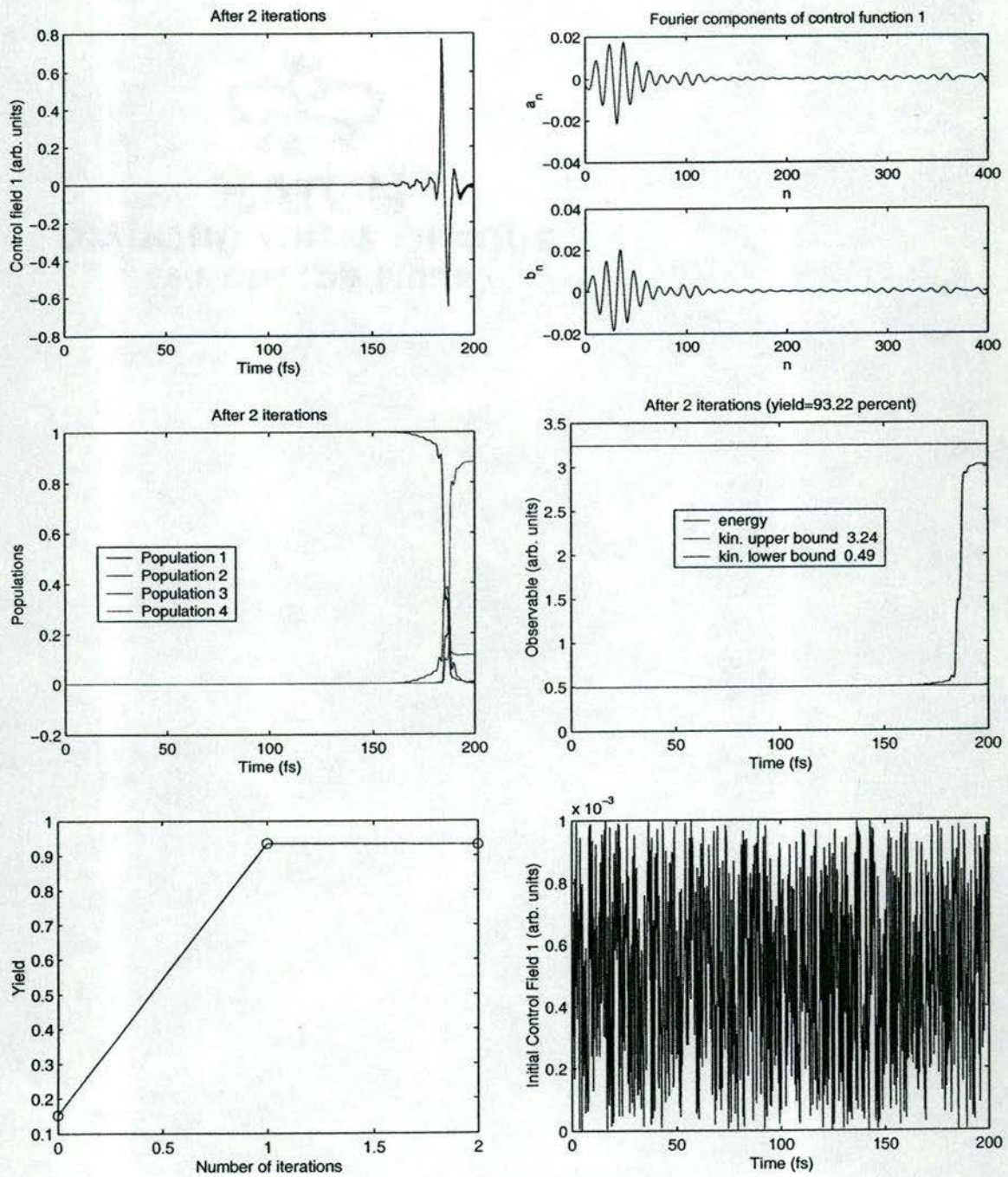


FIGURE 10: Energy maximization for a four-level Morse oscillator initially in thermal equilibrium with control parameters $J = 400$, $\lambda = 1$

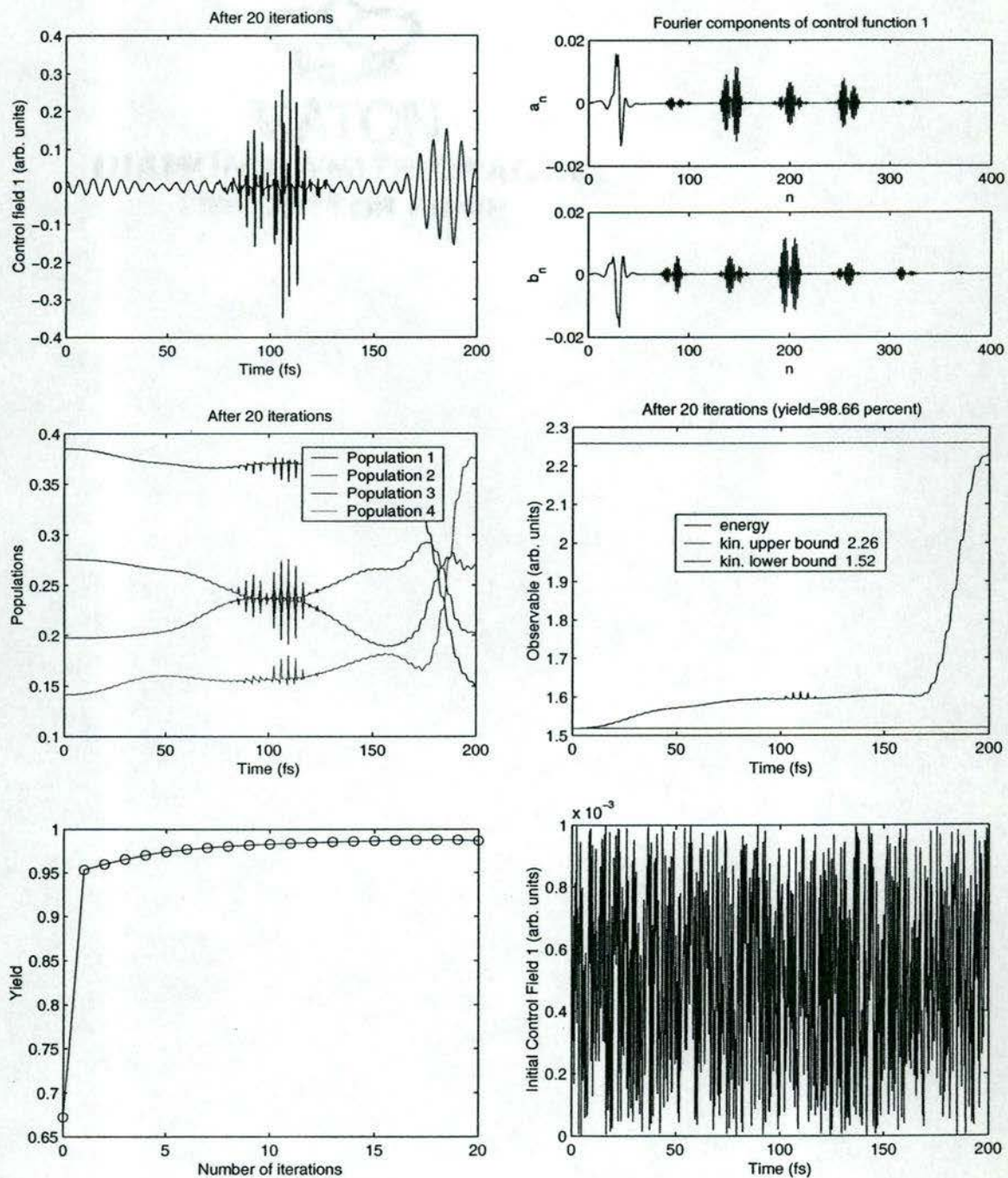
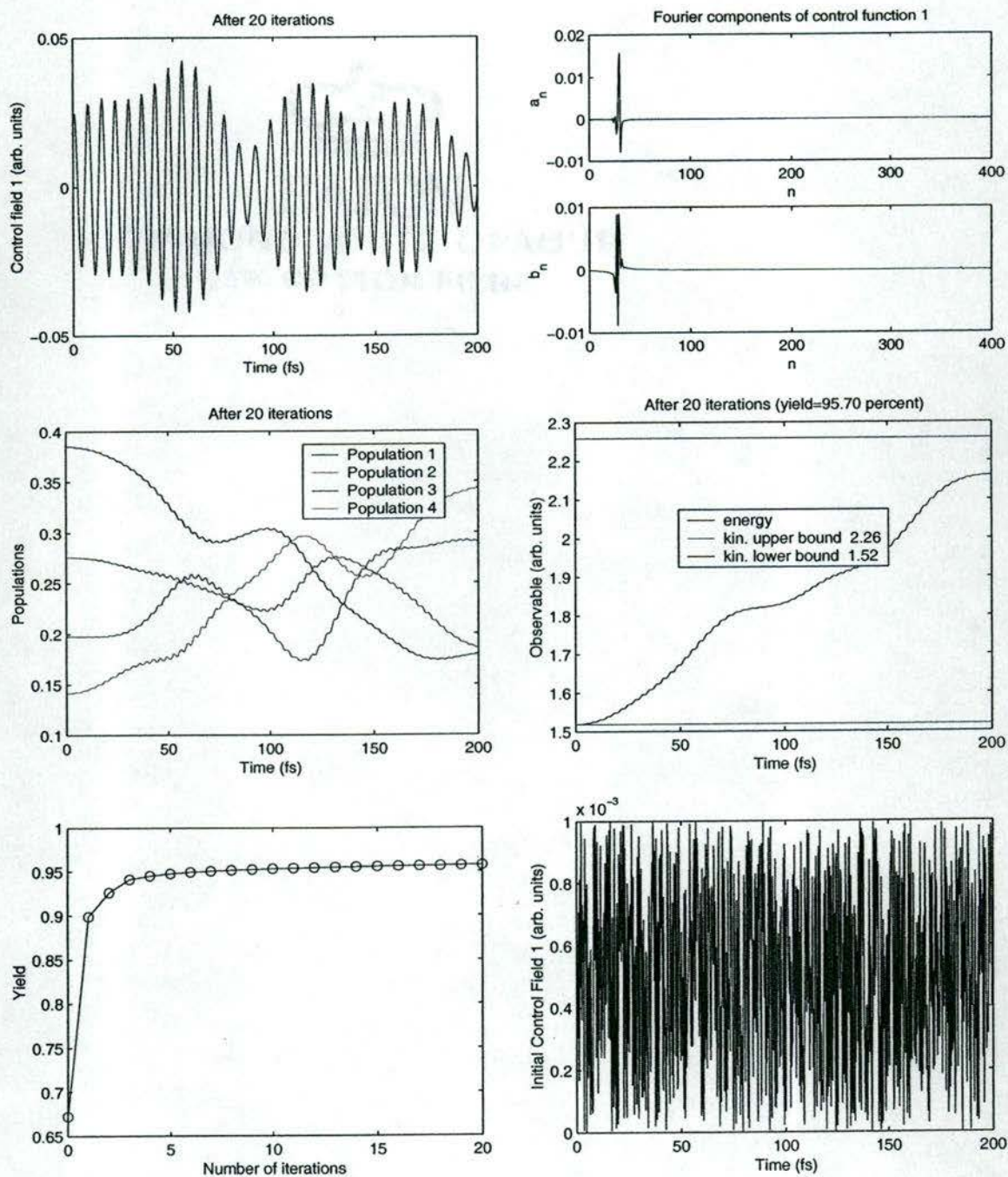


FIGURE 11: Energy maximization for a four-level Morse oscillator initially in thermal equilibrium with control parameters $J = 400$, $\lambda = 8$



V.2 Energy maximization for 'decoupled' Systems

Consider a system whose internal Hamiltonian is given by (V.1). Let the observable be the energy of the system (V.3) and assume the system is initially in thermal equilibrium (V.7). We shall study two cases of interactions.

Case A:

$$\begin{aligned}\hat{H}_1 &= f(t) \sum_{n=1}^3 d_n (|n\rangle\langle n+1| + |n+1\rangle\langle n|) \\ &\doteq f(t) \begin{bmatrix} 0 & 1.0 & 0 & 0 \\ 1.0 & 0 & 0 & 0 \\ 0 & 0 & 0 & 1.73205 \\ 0 & 0 & 1.73205 & 0 \end{bmatrix}.\end{aligned}\quad (\text{V.12})$$

Case B:

$$\begin{aligned}\hat{H}_1 &= f(t) (|1\rangle\langle 4| + |4\rangle\langle 1| + |2\rangle\langle 3| + |3\rangle\langle 2|) \\ &\doteq f(t) \begin{bmatrix} 0 & 0 & 0 & 1 \\ 0 & 0 & 1 & 0 \\ 0 & 1 & 0 & 0 \\ 1 & 0 & 0 & 0 \end{bmatrix},\end{aligned}\quad (\text{V.13})$$

where $f(t)$ is the external control field, which is to be determined. Both of these systems are only partially controllable, as can easily be verified.

In case A, the expectation value of the observable is bounded by

$$1.5186 \leq \langle \hat{A}(t) \rangle \leq 1.6722. \quad (\text{V.14})$$

according to theorem II.2. These bounds are dynamically attainable since each of the subsystems is completely controllable. Hence the relative yield is

$$\text{yield} = \frac{\langle \hat{A}(t_F) \rangle}{1.6722}. \quad (\text{V.15})$$

In case B, the expectation value of the observable is bounded by

$$1.518570 \leq \langle \hat{A}(t) \rangle \leq 2.259226, \quad (\text{V.16})$$

according to theorem II.2. Notice that these bounds are exactly the same as the kinematical bounds for the Morse oscillator model. Although the whole system is not completely controllable, the bounds are also dynamically realizable since both subsystems are controllable. Hence, the relative yield is

$$\text{yield} = \frac{\langle \hat{A}(t_F) \rangle}{2.259226}. \quad (\text{V.17})$$

Figure 12 shows the result of a control computation for case A with $J = 400$ and $\lambda = 4$. Figure 13 shows the result of a control computation for case B with $J = 400$ and $\lambda = 4$. In both cases, the final yield is close to 100% although the system is not completely controllable. Furthermore, observe the simultaneous inversion of populations one/two and three/four in figure 12, as well as the simultaneous inversion of populations one/four and two/three in figure 13, exactly as predicted by theorem 2.

FIGURE 12: Energy maximization for a decoupled four-level system (Case A) initially in thermal equilibrium with control parameters $J = 400$, $\lambda = 4$

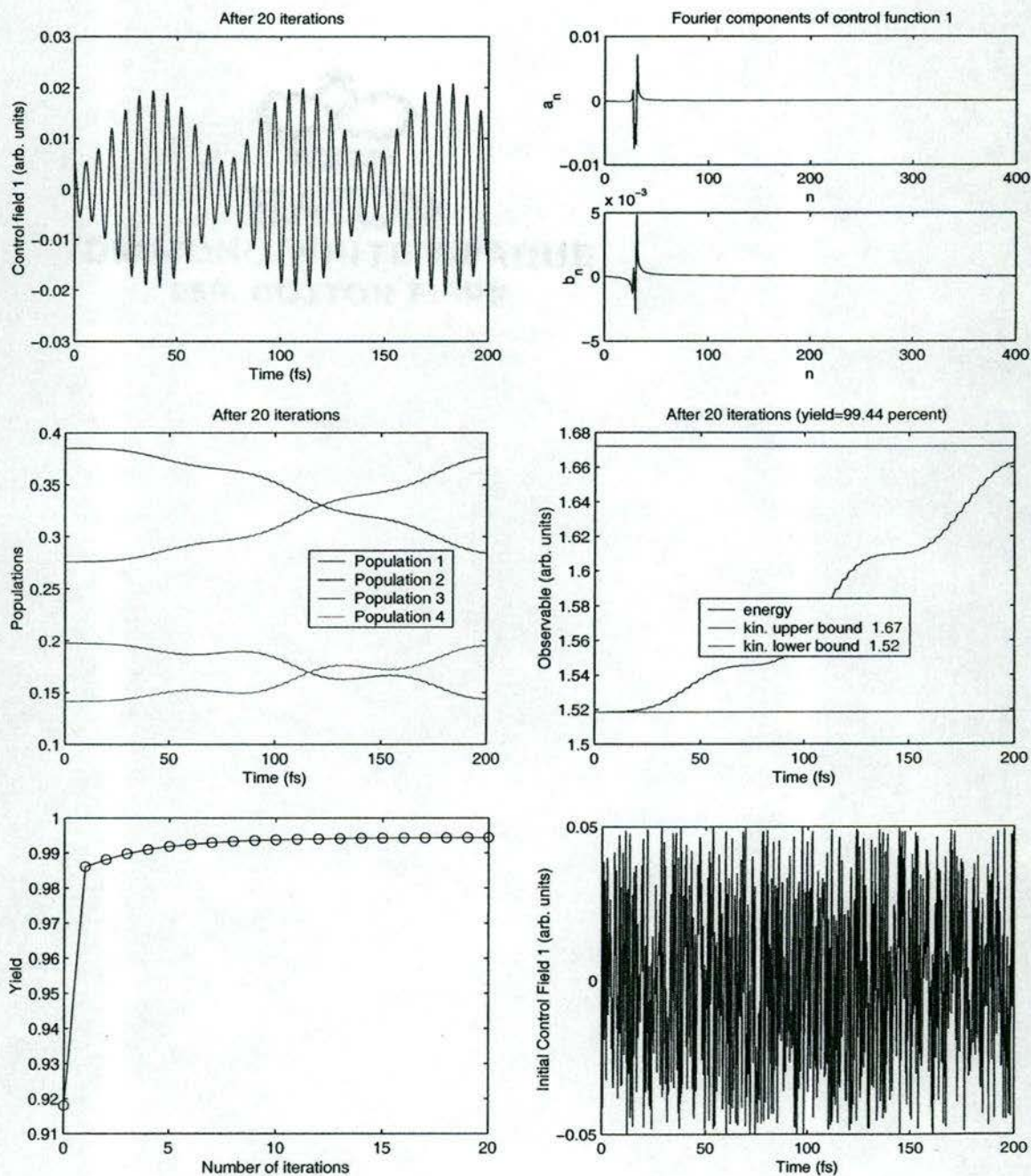
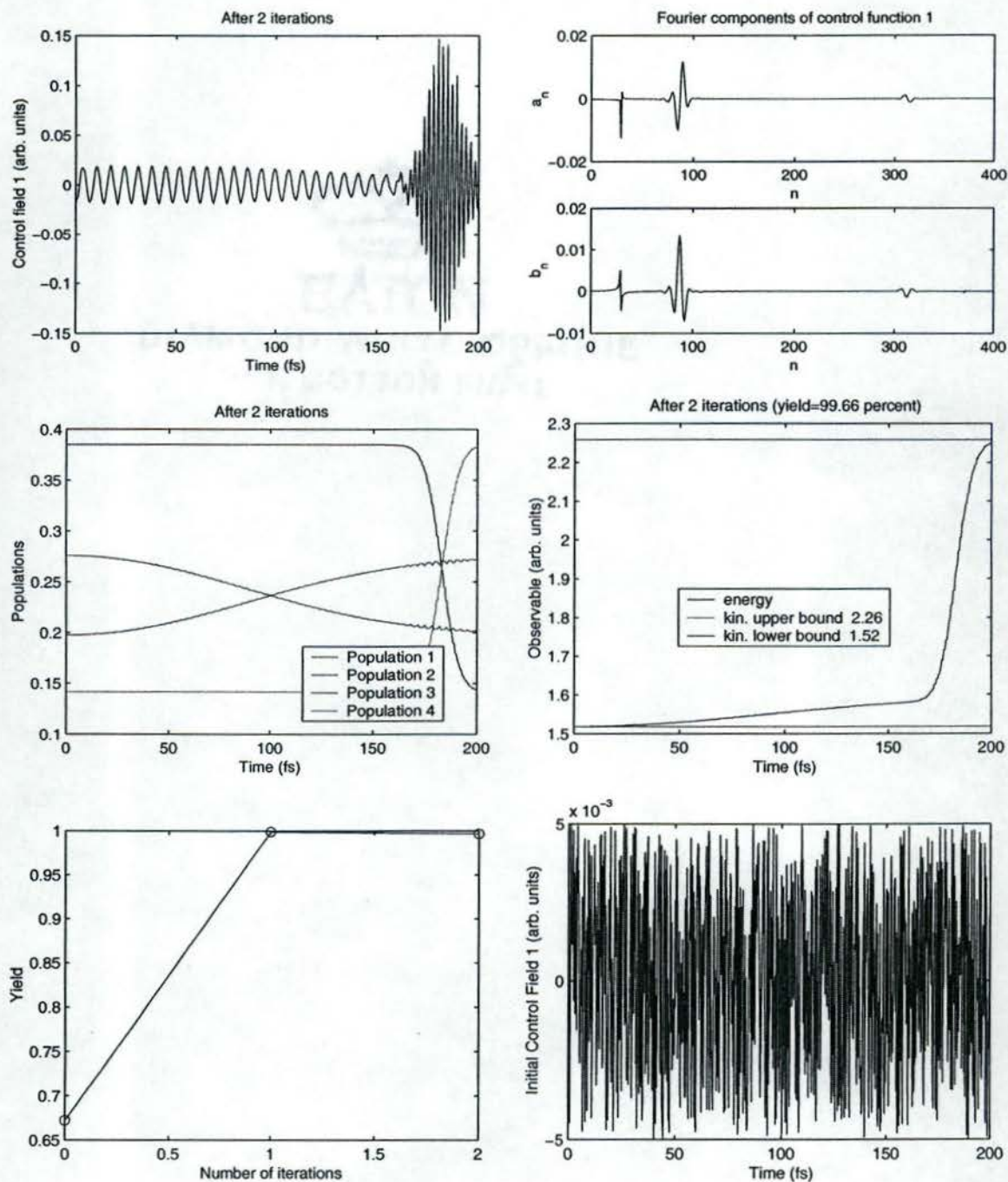


FIGURE 13: Energy maximization for a decoupled four-level system (case B) initially in thermal equilibrium with control parameters $J = 400$, $\lambda = 4$



V.3 Maximization of the top level population for a three-level system

We consider a three-level system initially in state

$$\hat{\rho}_0 = |1\rangle\langle 1| \doteq \begin{bmatrix} 1 & 0 & 0 \\ 0 & 0 & 0 \\ 0 & 0 & 0 \end{bmatrix} \quad (\text{V.18})$$

with internal Hamiltonian

$$\begin{aligned} \hat{H}_0 &= \sum_{n=1}^3 E_n |n\rangle\langle n| \\ &\doteq \begin{bmatrix} 0.5 & 0 & 0 \\ 0 & 1.5 & 0 \\ 0 & 0 & 2.4 \end{bmatrix} \end{aligned} \quad (\text{V.19})$$

and interaction Hamiltonian

$$\begin{aligned} \hat{H}_1 &= f(t) \sum_{n=1}^2 d_n (|n\rangle\langle n+1| + |n+1\rangle\langle n|) \\ &\doteq f(t) \begin{bmatrix} 0 & 1 & 0 \\ 1 & 0 & 1 \\ 0 & 1 & 0 \end{bmatrix}, \end{aligned} \quad (\text{V.20})$$

where $f(t)$ is the external control field, which is to be determined. The observable is the population of level three,

$$\hat{A} = |3\rangle\langle 3| \doteq \begin{bmatrix} 0 & 0 & 0 \\ 0 & 0 & 0 \\ 0 & 0 & 1 \end{bmatrix}, \quad (\text{V.21})$$

which is to be maximized at $t_F = 400$ fs.

We performed computations with and without dissipation. In the dissipative case the dephasing operator is

$$\hat{\gamma}^d = \begin{bmatrix} 0 & 0.01 & 0.01 \\ 0 & 0 & 0.01 \\ 0 & 0 & 0 \end{bmatrix} \quad (\text{V.22})$$

and the population relaxation operator is

$$\hat{\gamma} = \begin{bmatrix} 0 & 0.005 & 0 \\ 0 & 0 & 0.005 \\ 0 & 0 & 0 \end{bmatrix}. \quad (\text{V.23})$$

The dissipative terms give rise to the Liouville space dissipation operator

$$\Gamma = \begin{bmatrix} 0 & 0 & 0 & 0 & -0.005 & 0 & 0 & 0 & 0 & 0 \\ 0 & 0 & 0 & 0 & 0 & 0 & 0 & 0 & 0 & 0 \\ 0 & 0 & 0 & 0 & 0 & 0 & 0 & 0 & 0 & 0 \\ 0 & 0 & 0 & 0.01 & 0 & 0 & 0 & 0 & 0 & 0 \\ 0 & 0 & 0 & 0 & 0.005 & 0 & 0 & 0 & 0 & -0.005 \\ 0 & 0 & 0 & 0 & 0 & 0 & 0 & 0 & 0 & 0 \\ 0 & 0 & 0 & 0 & 0 & 0 & 0.01 & 0 & 0 & 0 \\ 0 & 0 & 0 & 0 & 0 & 0 & 0 & 0.01 & 0 & 0 \\ 0 & 0 & 0 & 0 & 0 & 0 & 0 & 0 & 0 & 0.005 \end{bmatrix}. \quad (\text{V.24})$$

Figures 14, 15, 16 and 17 show the results of computations performed for the non-dissipative case with $J = 400$, $\lambda \in \{4, 8, 10, 12\}$ and a sinusoidal initial field. For comparison, 19 and 20 show the results of computations for the same case with $J = 400$ and $\lambda \in \{4, 8\}$ but random noise as initial field. We also performed computations with $J = 4000$ and $\lambda = 30$, presented in figures 18.

Finally, figures 21 and 22 show the results of computations for the dissipative case with $J = 800$ and $\lambda = 10$. Figure 23 shows the results for $J = 4000$ and $\lambda = 30$. The final yield for these three computations varies considerably. Since the kinematical bounds are generally not dynamically realizable for dissipative systems, this is to be expected. Dynamically-realizable bounds on the expectation value of the observable for dissipative systems would be desirable.

FIGURE 14: Maximization of the top-level population for a three-level system initially in the ground state with control parameters $J = 400$, $\lambda = 4$

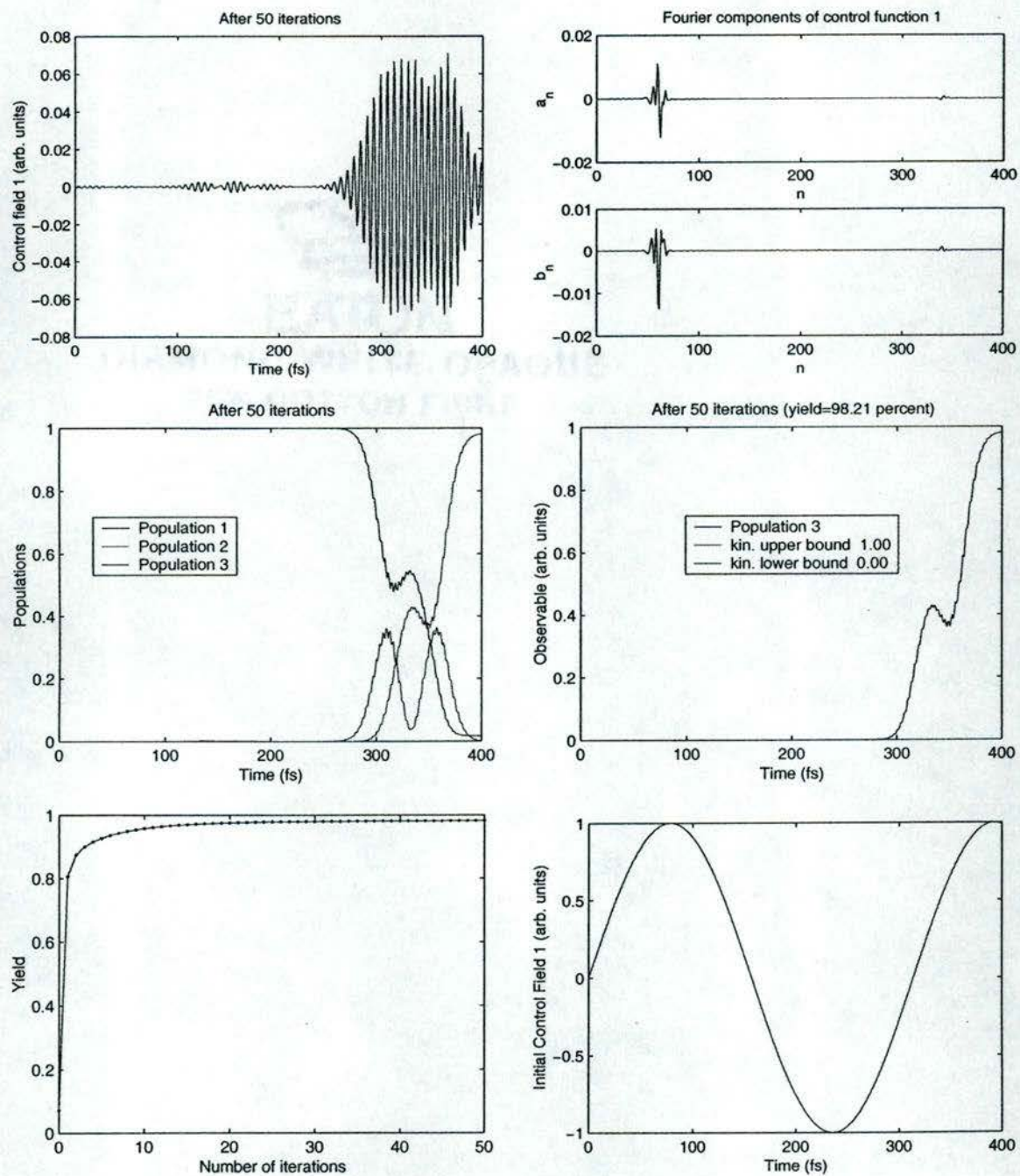


FIGURE 15: Maximization of the top-level population for a three-level system initially in the ground state with control parameters $J = 400$, $\lambda = 8$

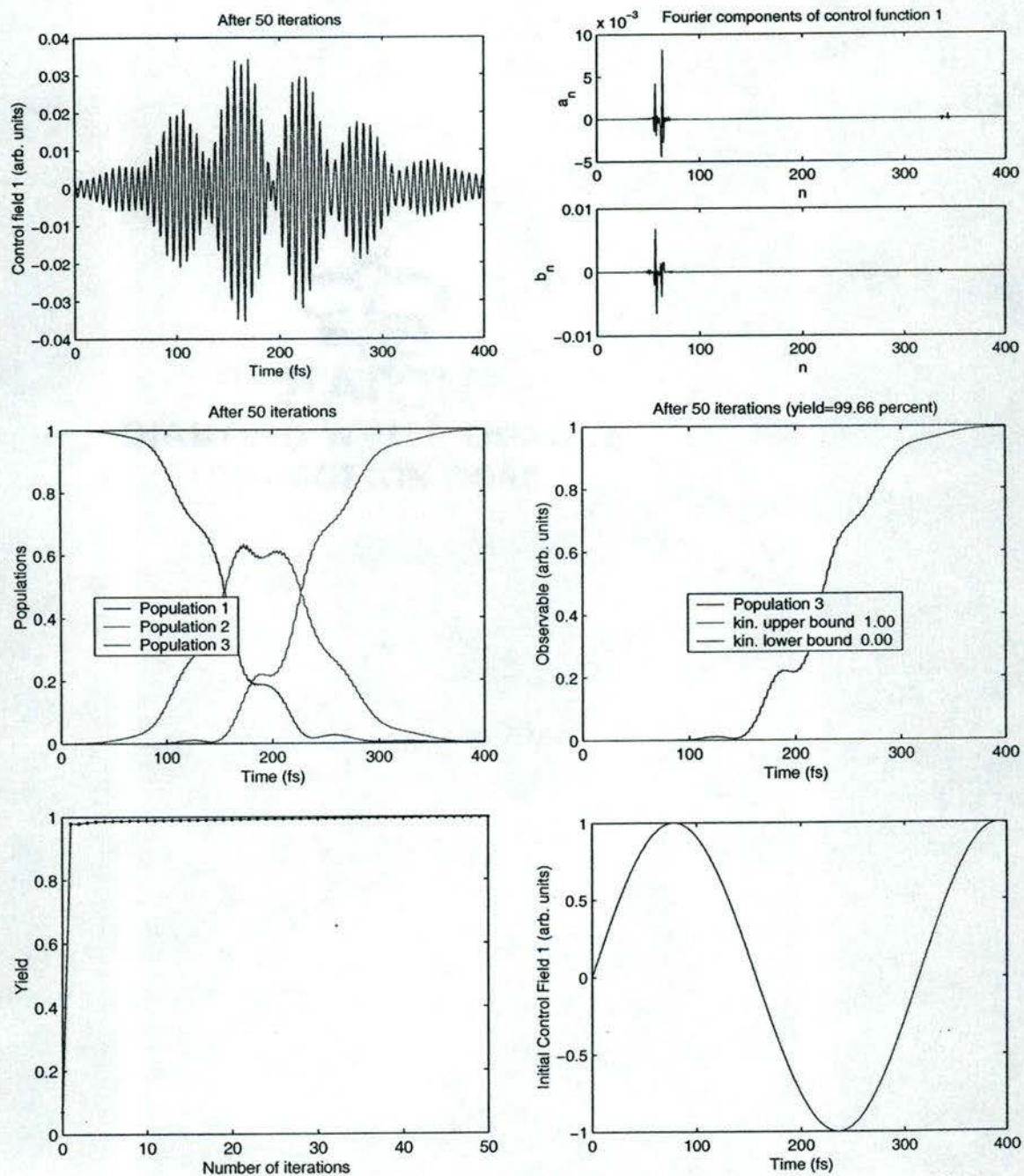


FIGURE 16: Maximization of the top-level population for a three-level system initially in the ground state with control parameters $J = 400$, $\lambda = 10$

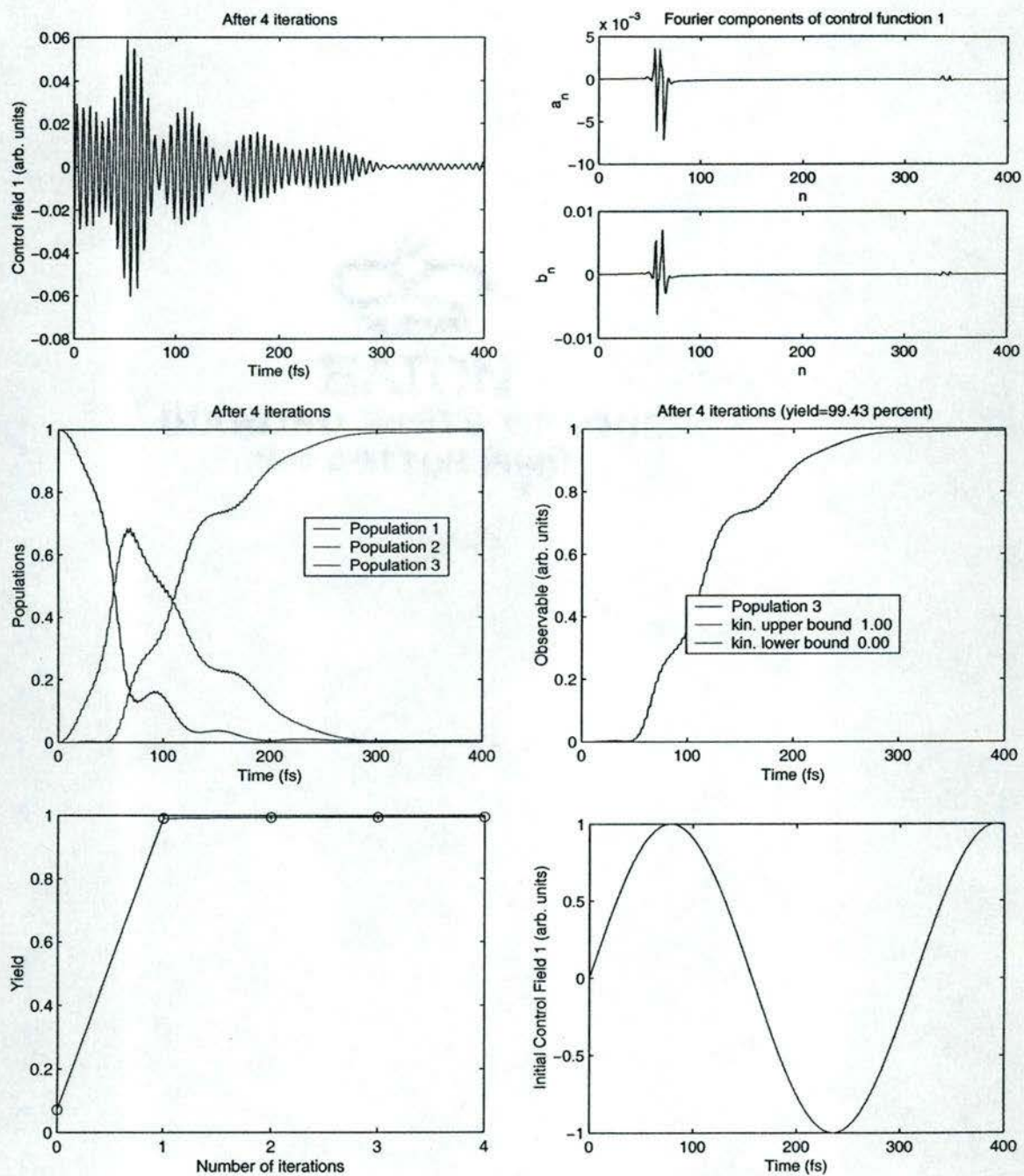


FIGURE 17: Maximization of the top-level population for a three-level system initially in the ground state with control parameters $J = 400$, $\lambda = 12$

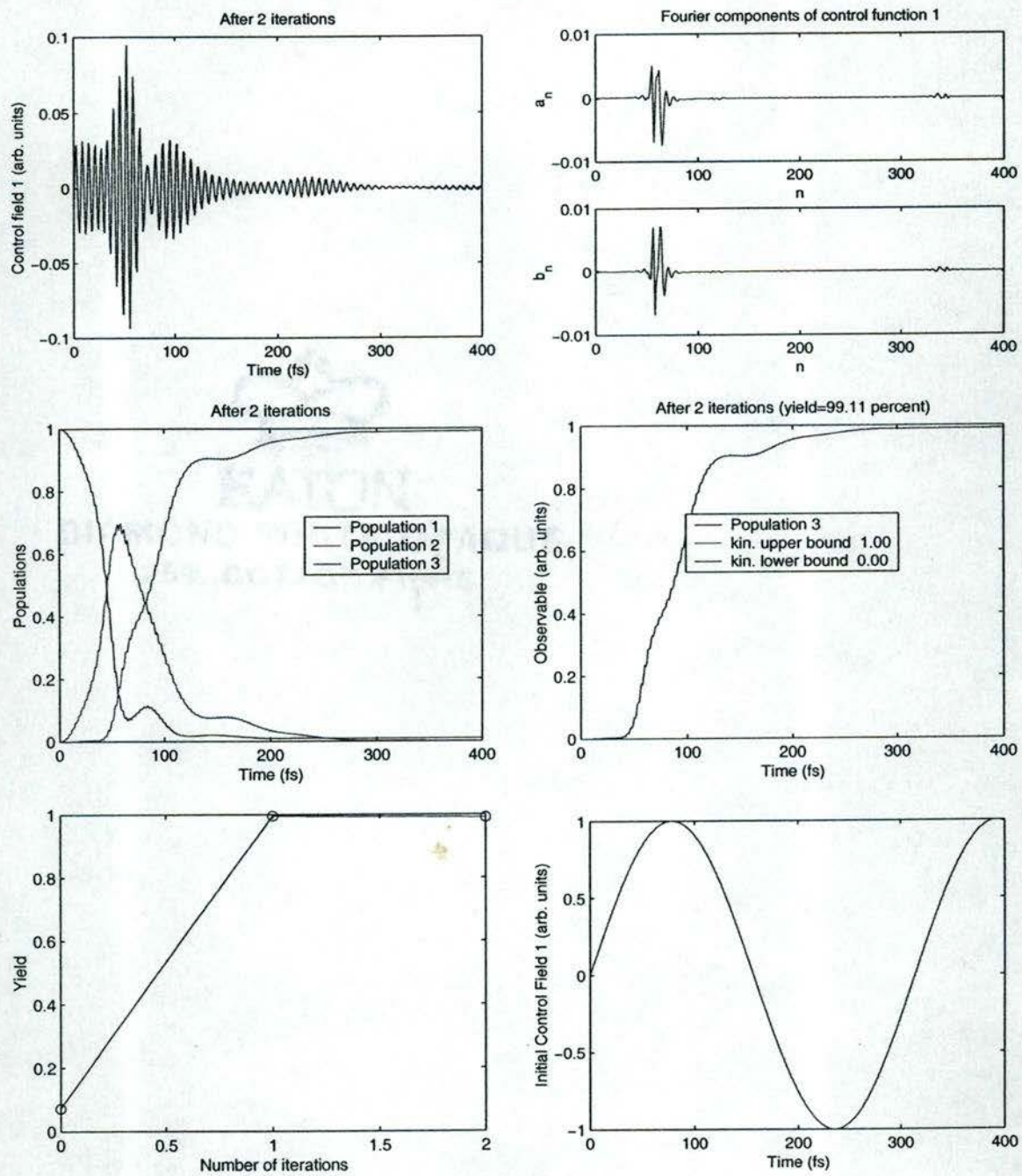


FIGURE 18: Maximization of the top-level population for a three-level system initially in the ground state with control parameters $J = 4000$, $\lambda = 30$

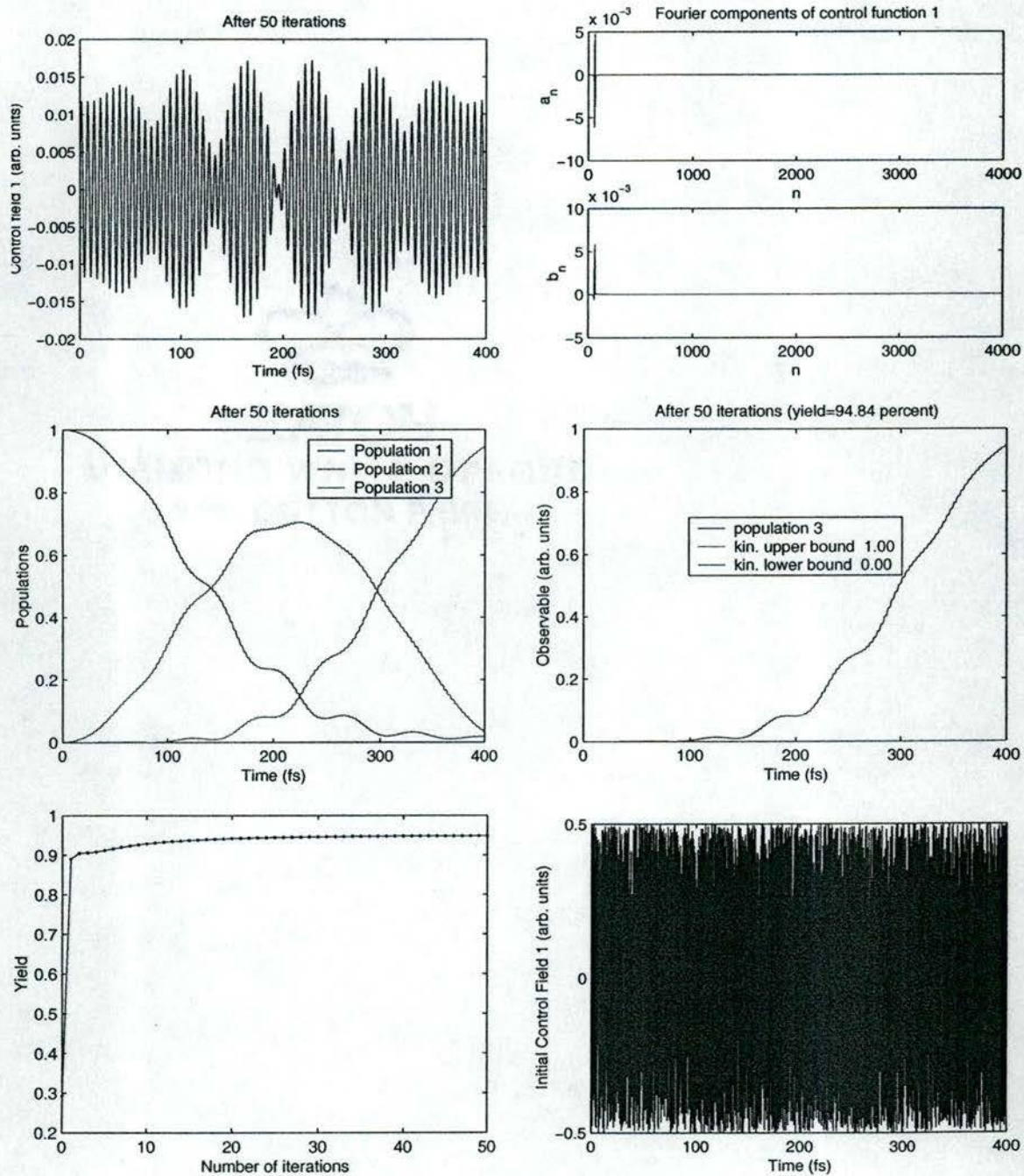


FIGURE 19: Maximization of the top-level population for a three-level system initially in the ground state with control parameters $J = 400$, $\lambda = 4$

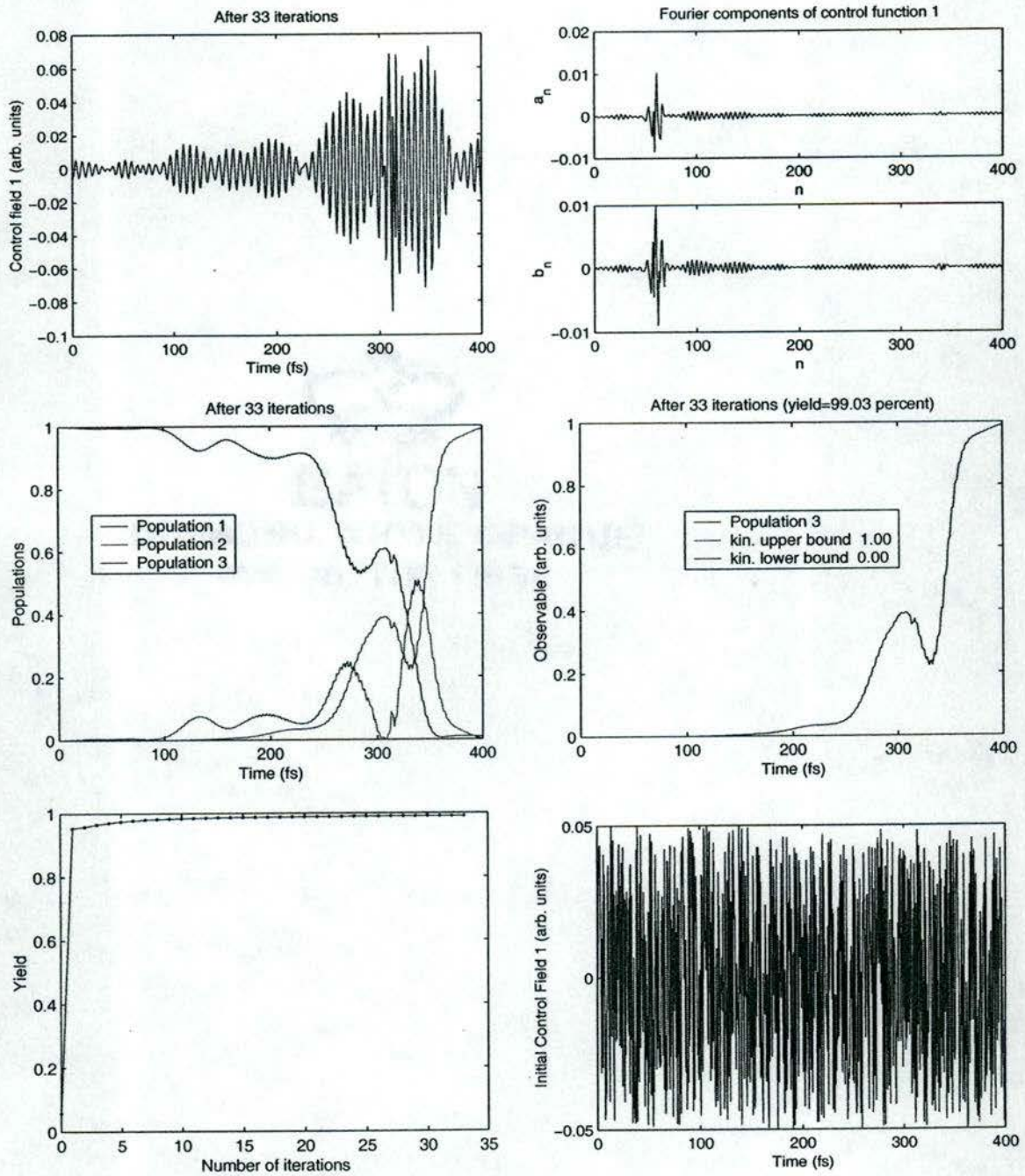


FIGURE 20: Maximization of the top-level population for a three-level system initially in the ground state with control parameters $J = 400$, $\lambda = 8$

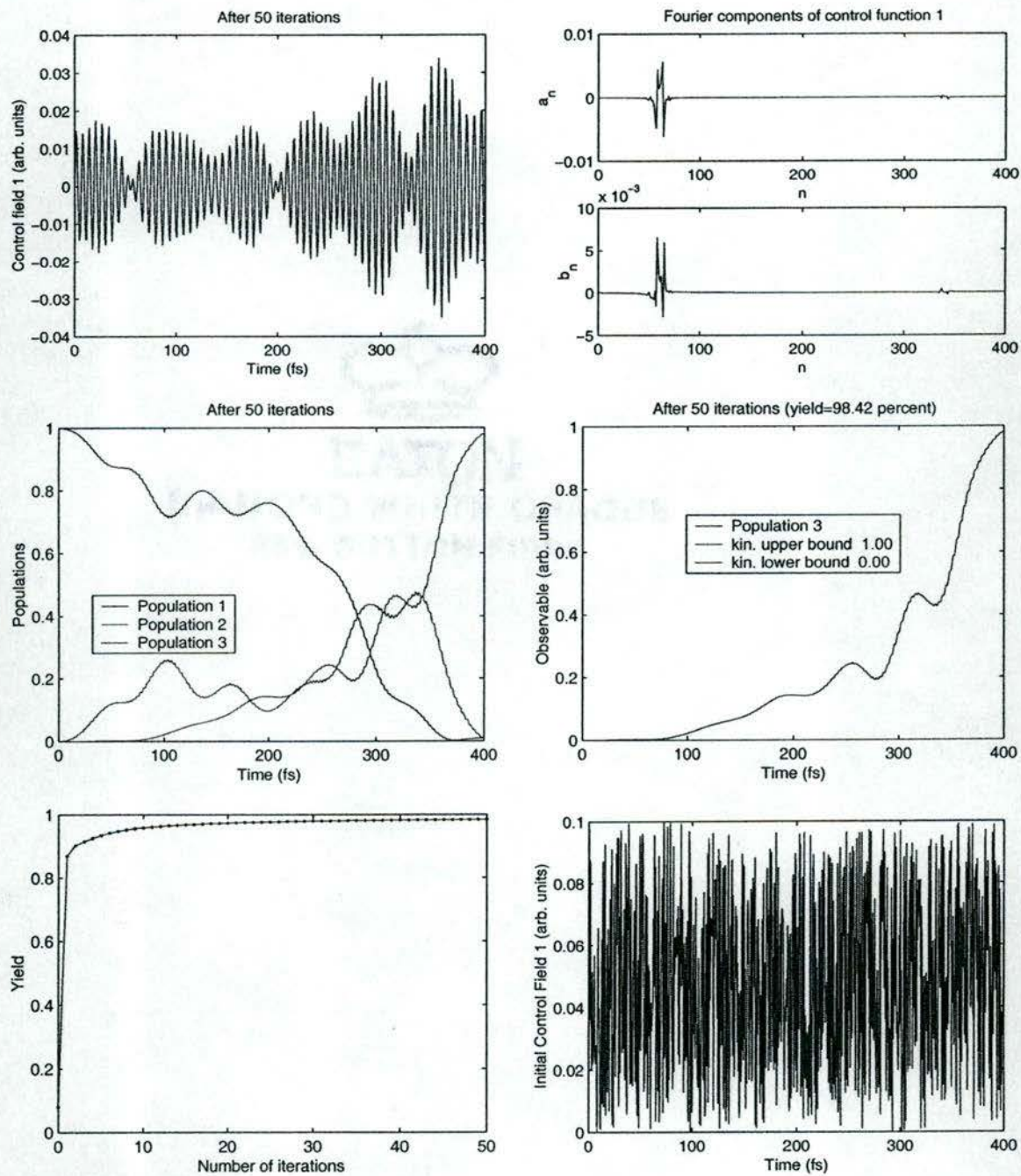


FIGURE 21: Maximization of the top-level population for a dissipative three-level system initially in the ground state with control parameters $J = 800$, $\lambda = 10$

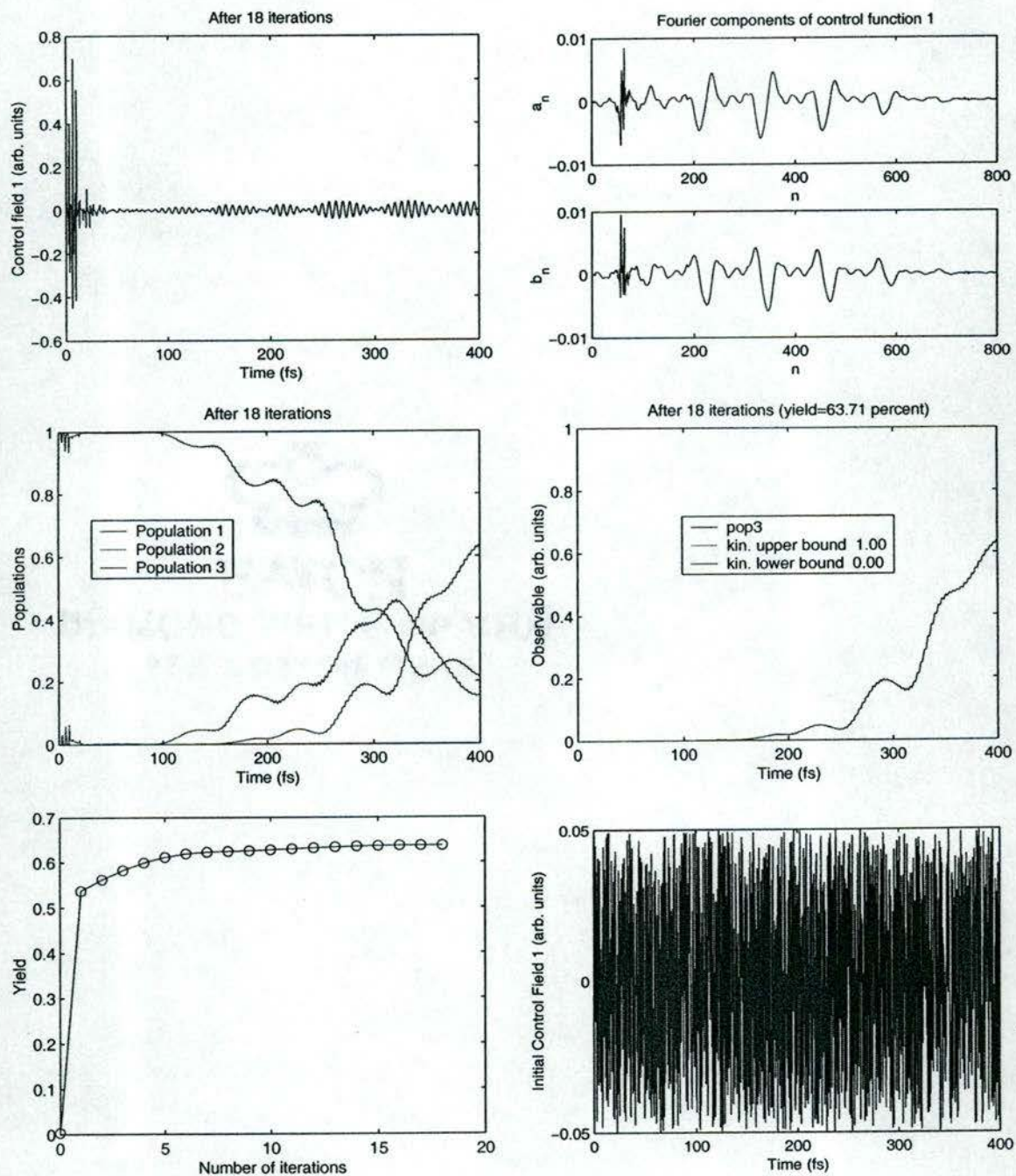


FIGURE 22: Maximization of the top-level population for a dissipative three-level system initially in the ground state with control parameters $J = 800$, $\lambda = 10$

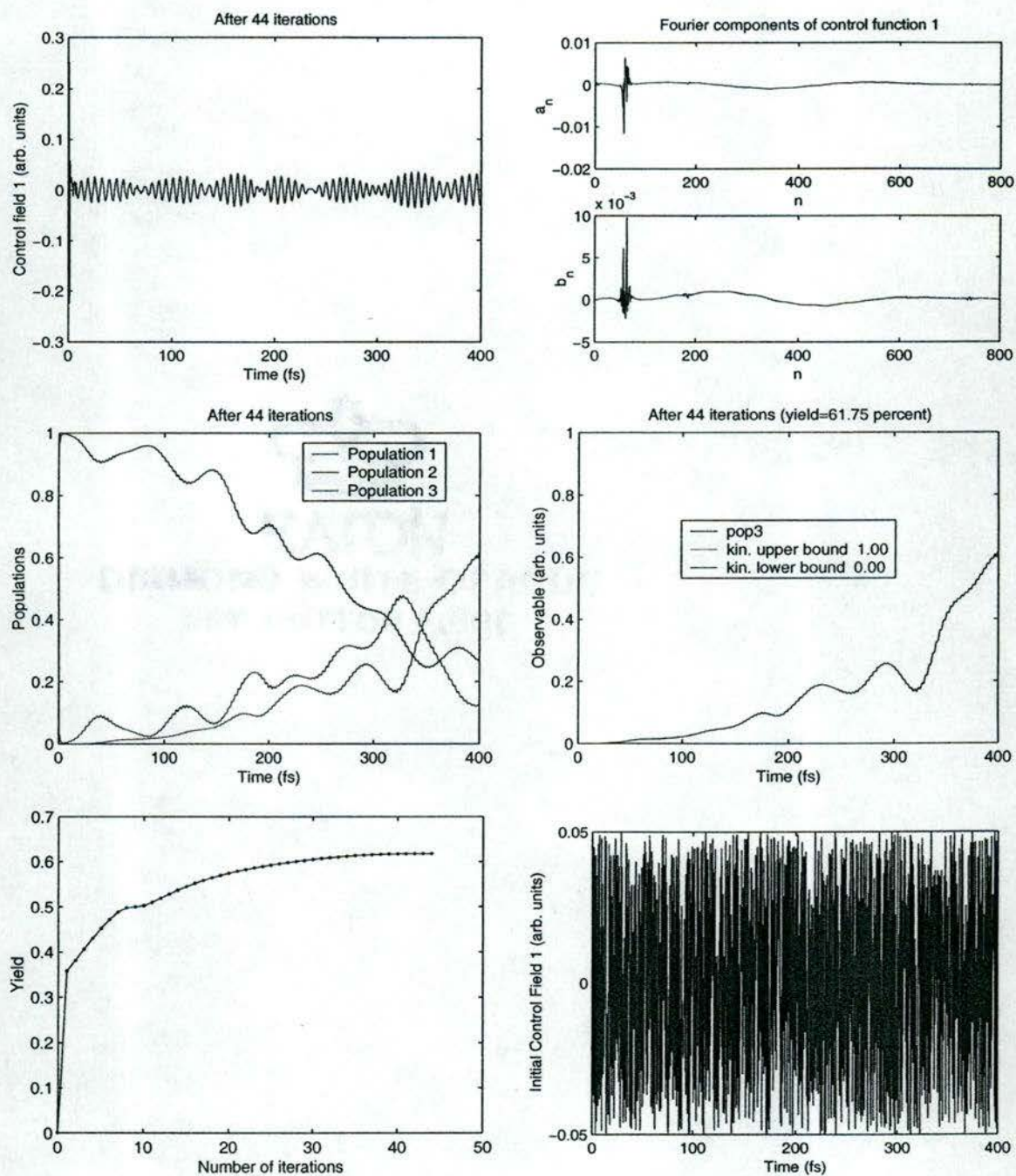
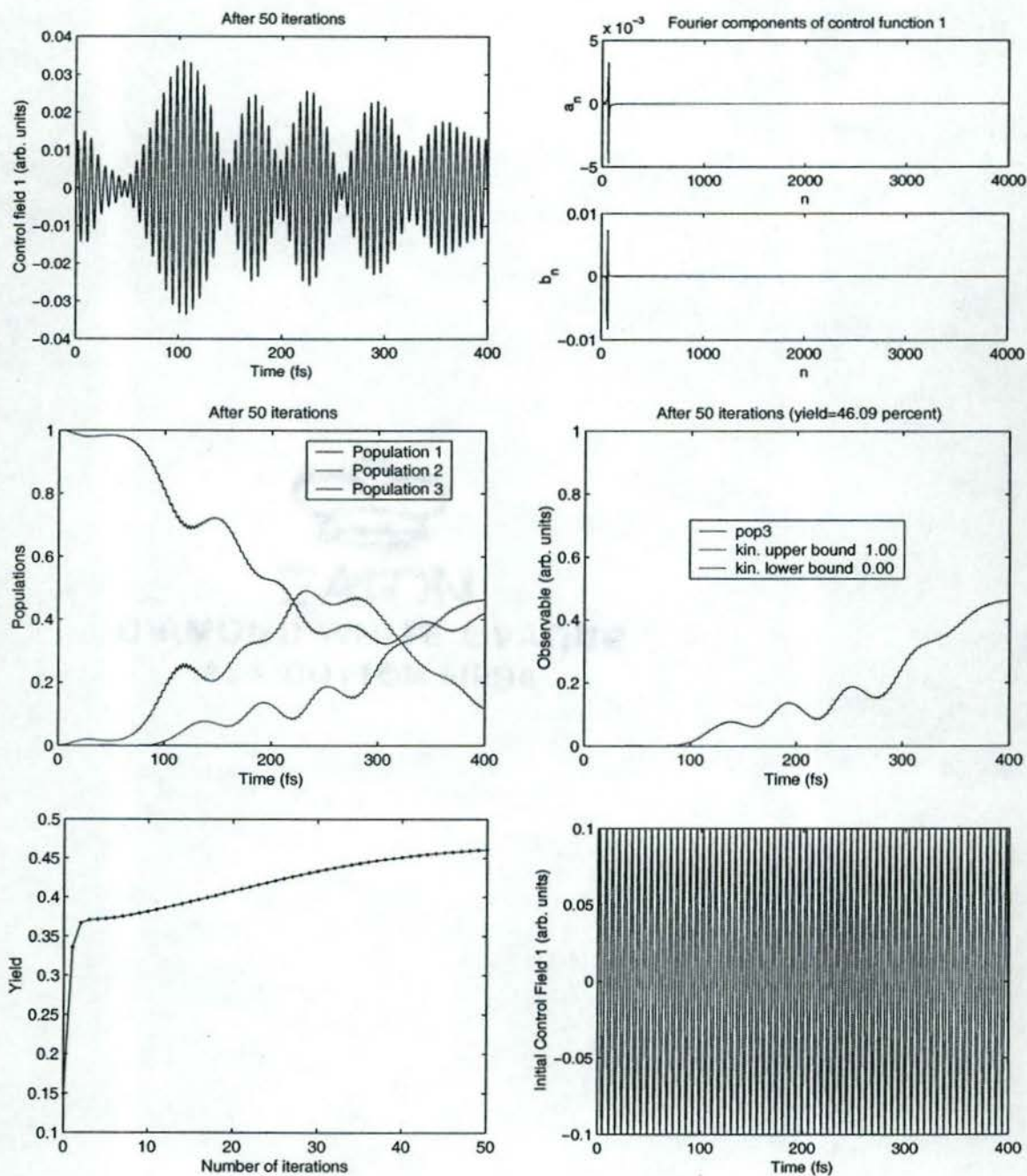


FIGURE 23: Maximization of the top-level population for a dissipative three-level system initially in the ground state with control parameters $J = 4000$, $\lambda = 30$



CHAPTER VI

CONCLUSION

In this dissertation we have addressed many issues pertinent to the theory of control of quantum processes. Yet, there are many open questions that remain to be investigated.

We used the kinematical constraints on the dynamical evolution of Hamiltonian systems to derive universal bounds on the expectation value of observables for non-dissipative quantum systems and showed that these bounds are dynamically realizable if the system is completely controllable. However, very little is known about dynamically attainable bounds on the expectation value of observables for dissipative systems, or even for Hamiltonian systems that fail to be completely controllable. Answering these questions requires understanding of the structure of the Lie algebra and the accessible sets, as well as how dissipation affects the dynamics of the system studied.

Another relevant issue is the mathematical structure of the controls. We simply assumed that the controls are bounded measurable functions. However, this is only a bare-minimum requirement. In general, there will be physical or experimental constraints on the control that not only restrict the norm of the control but also the pulse shape and the frequency components. Our limited numerical experiments suggest that small perturbations of the control function usually do not lead to drastic changes in the evolution of the system or the expectation value of the observable at the target time. However, the sensitivity of the yield to modifications of the control function is an important practical issue that warrants further study.

Related to this problem, is the question of how restrictions on the structure of controls affect the controllability of the system, or the time required to achieve the aim of control, or perhaps, to which extent the aim of control can be achieved in a given, fixed amount of time.

Last but not least, all our computations and studies are based on simple models

of actual physical systems of interest. The very uncertainty about the applicability and accuracy of these models presents a formidable challenge. The solution to problems like this lies most likely in the development of learning algorithms that do not require precise knowledge about the model system. Significant work has been done in this area (e.g., [28] and references therein) but many questions remain. Ultimately, perhaps, a combination of learning algorithms, control theory and experimental feedback might provide us with the feedback required to improve our models of the systems we wish to control.

APPENDIX A

INTERACTIVE QUANTUM CONTROL MATLAB MAIN PROGRAM

```

function IQC;
% ICT -- an interactive quantum control program -- determines kinematical bounds
% on the observable, checks controllability and computes optimal controls.

Init;
% IQC main menu
while 1,
s=menu('',MITEM);
switch s,
case 1, %   InputSystemData;
    [sysName,H,M,rho0,A,obs,t0,tF,gd,g,KB1,KB2]=InputSystemData(H,M,rho0,A,...
                                                                obs,t0,tF,gd,g,KB1,KB2);
case 2, %   LoadSystemData;
    [sysName,H,M,rho0,A,obs,t0,tF,gd,g,KB1,KB2,f0]=LoadSystemData(H,M,rho0,...
                                                                A,obs,t0,tF,gd,g,KB1,KB2);
case 3, %   DisplaySystemData;
    if isempty(H{1}) | isempty(A),
        msgbox('Insufficient input -- load or enter system data first');
    else
        DisplaySystemData(sysName,H,M,rho0,A,obs,t0,tF,gd,g,KB1,KB2,rn,...
                                                                controllable);
    end;
case 4, %   Modify control parameters
    [lambda,J,f0,delta,Nmax,debug]=ModifyCtrlParam(lambda,J,f0,delta,Nmax,debug);
case 5, %   Determine kinematical bounds
    if ~isempty(A) | ~isempty(rho0),
        if ~isempty(KB1) | ~isempty(KB2),
            buttonName=questdlg('Bounds already defined. Do you really want to ...
                                proceed and overwrite the existing bounds?','',...
                                'Yes','No','No');

            switch buttonName,
            case 'Yes', % Determine kinematical bounds
                [KB1,KB2]=KinBounds(A,rho0,length(H{1}));
            case 'No',
                msgbox('Bounds not overwritten');
            end;
        else
            [KB1,KB2]=KinBounds(A,rho0,length(H{1}));
        end;
    else
        msgbox('Insufficient input -- load or enter system data first');
    end;
case 6, %   Check controllability
    if isempty(H{1}),
        msgbox('Insufficient input -- load or enter system data first');
    else

```

```

M=length(H)-1;
N=length(H{1});
[rn,W]=dimLie(H,M,N);
controllable=(rn==N*N);
end;
case 7, % Optimal control, etc.
M=length(H)-1;
N=length(H{1});
figYield=5;
figFourier=6;
if isempty(f0) | (length(f0)~=2*J+1),
    f0=(rand(M,2*J+1)-0.5)*0.1
end;
if isempty(A)|isempty(rho0)|isempty(H{1})|isempty(H{2})|isempty(lambda)
    msgbox('Insufficient input -- load or enter system data and control ...
           parameters first');
else
    % If Liouville operator not yet defined, compute it now.
    if ~(exist('L','var')),
        L=cell(1,M+1);
        for m=1:M+1,
            L{m}=liouv(H{m});
        end;
    end;
    if isempty(KB2),
        [KB1,KB2]=KinBounds(A,rho0,length(H{1}));
    end;
    % convert A matrix to Liouville vector if necessary
    A=reshape(A,N*N,1);
    % convert rho0 matrix to Liouville vector if necessary
    rho0=reshape(rho0,N*N,1);
    % Numerically construct control and determine the populations and
    % evolution of the observable
    if ~isempty(gd),
        Gamma=dissipation(g,gd,N);
        [f,yield,Mf,Mp,Mo]=ZRcontrolD(f0,rho0,A,obs,L,Gamma,lambda,KB1,KB2,...
                                     t0,tF,J,delta,Nmax,debug,POS,PAPERPOS);
    else
        [f,yield,Mf,Mp,Mo]=ZRcontrol(f0,rho0,A,obs,L,lambda,KB1,KB2,t0,tF,...
                                    J,delta,Nmax,debug,POS,PAPERPOS);
    end;
    yieldplot(yield,figYield,sprintf('%s, lambda=%i',sysName,lambda),POS,...
              PAPERPOS);
    [a,b,ft]=fouriercomp(f,figFourier,POS,PAPERPOS);
end;
case 8,
M=length(H)-1;
N=length(H{1});
if isempty(f0) | (length(f0)~=2*J+1),
    f0=(rand(M,2*J+1)-0.5)*0.1
end;

```

```

if isempty(A)|isempty(rho0)|isempty(H{1})|isempty(H{2})|isempty(lambda)
    msgbox('Insufficient input -- load or enter system data and control ...
           parameters first');
else
    if ~(exist('L','var')),
        % If Liouville operator not yet defined, compute it now.
        L=cell(1,M+1);
        for m=1:M+1,
            L{m}=liouv(H{m});
        end;
    end;
    if isempty(KB2),
        [KB1,KB2]=KinBounds(A,rho0,length(H{1}));
    end;
    % convert A matrix to Liouville vector if necessary
    A=reshape(A,N*N,1);
    rho0=reshape(rho0,N*N,1);
    % convert rho0 matrix to Liouville vector if necessary
    if ~isempty(gd),
        Gamma=dissipation(g,gd,N);
    else
        Gamma=zeros(size(L{1}));
    end;
    LambdaRange(f0,rho0,A,obs,L,Gamma,lambda,KB1,KB2,t0,tF,J,delta,Nmax);
end;
case 9,    PlayMovie;
case 10,   VisualLambdaRange(POS,PAPERPOS);
case 11,   % save data, movies and figures
    if exist('f','var')==0 | isempty(H{1}) | isempty(lambda)
        msgbox('no data to save');
    else % check controllability, compute kinematical bounds if necessary
        % and save data
        if isempty(controllable),
            [rn,W]=dimLie(H,M,N);
            controllable=(rn==N*N);
        end;
        if isempty(KB2) | isempty(KB1),
            [KB1,KB2]=KinBounds(A,rho0,length(H{1}));
        end;
        SaveData(J,lambda,f0,KB1,KB2,controllable,rn,f,yield,ft,a,b,Mf,Mp,Mo,POS);
    end;
case 12,
    sprintf('Please type return <ENTER> to return to the menu')
    keyboard
case 13,
    clear;          % clear all workspace variables
    Init;          % re-initialize workspace
    close('all'); % close all figure windows
case 14, break;
end;
end;

```

APPENDIX B

MATLAB SUBROUTINE TO DETERMINE KINEMATICAL BOUNDS

```
function [KB1,KB2]=KinBounds(A,rho0,N);
% function [KB1,KB2]=KinBounds(A,rho0,N)
% INPUT:
% A:    matrix representation of observable
% rho0: matrix representation of initial density matrix
% N:    dim. of Hilbert space of pure states
%
% OUTPUT:
% KB1, KB2: kinematical upper and lower bounds
%
ea=sort(eig(reshape(A,N,N)));
er=sort(eig(reshape(rho0,N,N)));
KB1=ea'*er(N:-1:1);
KB2=ea'*er;
```

APPENDIX C
MATLAB SUBROUTINE TO DETERMINE CONTROLLABILITY

```

function [rn,historyW]=dimLie(H,M,N);
% function [rn,historyW]=dimLie(H,M,N);
% INPUT:
% H={H_0,H_1,...H_M} cell array of Hamiltonians
% M: number of control fields
% N: dim. of Hilbert space of pure states
%
% OUTPUT:
% rn: dim. of the Lie algebra
% historyW: cell array of matrices W{n}
%
W=[];
ro=0;
for m=1:M+1,
    W=[W reshape(H{m},N*N,1)];
end;
W=orth(W);
rn=rank(W);
n=1;
while (rn-ro)~=0,
    for l=1:rn, % note l=ro+1:rn does not seem to work with orth(W)
        h1=reshape(W(:,l),N,N);
        for j=1:l-1,
            h2=reshape(W(:,j),N,N);
            h3=h2*h1-h1*h2;
            W=[W h3(1:N*N)'];
        end
    end
    W=orth(W);
    historyW{n}=W;
    ro=rn;
    rn=rank(W);
    n=n+1;
end;

```

APPENDIX D

MATLAB SUBROUTINE TO FIND OPTIMAL CONTROL

```

function [f,yield,Mf,Mp,Mo]=ZRcontrolD(f0,rho0,A,obs,L,Gamma,lambda,KB1,KB2,...
                                     t0,tF,J,delta,Nmax,debug,POS,PAPERPOS,VISUAL);
%
% The function [f,yield,Mf,Mp,Mo,POS]=ZRcontrolD(f0,rho0,A,L,Gamma,lambda,...
%                                     KB1,KB2,t0,tF,J,delta,Nmax,debug);
% uses the generalized Zhu-Rabitz algorithm to compute an optimal control.
%
% INPUT:
% f0:      Initial guess for the control field;
%          (2J+1)-vector with f0(j)=f_0(t0+dt*(j-1)/2).
% rho0:    Liouville vector representing initial state; NL-column vector
% A:       Liouville vector representing target state; NL-column vector
% L:       M+1 cell array of Liouville (super)operators (i.e., NLxNL matrices)
% Gamma:   dissipation Liouville operator
% lambda:  Parameter (see variational functional)
% KB1:     kinematical lower bound for expectation value of observable
% KB2:     kinematical upper bound for expectation value of observable
% t0,tF:   Initial and final time
% J:       Number of subintervals; determines time-step dt=(tF-t0)/J
% delta:   convergence criterion
% Nmax:    maximum number of iterations;
% debug is a boolean variable; set to 1 for debug mode
% POS:     cell array specifying the figure window positions and sizes.
% PAPERPOS: cell array specifying the figure paper positions and sizes.
% VISUAL:  0 (no graphics) or 1 (graphics), default 1
%
% OUTPUT
% f:       (2J+1)-vector representing the optimal control;
%          f(m,j)=f_m(t0+dt*(j-1)/2)
% yield:   relative yield at the target time
% Mf,Mp,Mo are movies recording the control process

if ~exist('VISUAL','var'),
    VISUAL=1;      % make visual output default
end;
NL=length(rho0); % dimension of Liouville space
I=[1:NL];       % index range
dt=(tF-t0)/J;   % time step
rhov=zeros(NL,J+1); % The jth column of rhov contains rhov(t_0+(j-1)dt)
Av=zeros(NL,J+1); % The jth column of Av contains rhov(t_0+(j-1)dt)

M=length(L)-1; % Number of control fields
f=zeros(M,2*J+1); % The desired control; f(m,j)= f_m(t0+(j-1)dt)
V=cell(1,M+1);
E=cell(1,M+1);
e=cell(1,M+1);

```

```

LOm=cell(1,M+1);
for m=1:M+1,
    [V{m},E{m}]=eig(L{m});
    % The columns of V{m} are the normalized eigenvectors of L{m}
    e{m}=diag(E{m});
    % e{m} is a column vector containing the corresponding eigenvalues
end;
U0=prop(NL,V{1},e{1},1,dt/2);
UD=expm(-Gamma*dt/2);
UD2=expm(Gamma'*dt/2);
for m=1:M;
    LOm{m}=L{1}*L{m+1}-L{m+1}*L{1}; % LOm{m}=L0*Lm-Lm*L0
end;

stop=0;
Oold=0;
fold=f0;
n=0; % 0th iteration
rhov(:,1)=rho0;
O(1) =A'*rho0;
f =f0;
for j=1:J,
    U=eye(NL);
    for m=M:-1:1,
        Um=prop(NL,V{m+1},e{m+1}/2,f(m,2*j),dt);
        U=Um*U*Um;
    end;
    rhov(:,j+1)=UD*U0*U*U0*UD*rhov(:,j);
    O(j+1) =A'*rhov(:,j+1);
end;
yield=O(J+1)/KB2;

t1 =[t0:dt:tF];
dt2=dt/2;
t2 =[t0:dt2:tF];
N =sqrt(NL);
%keyboard
if VISUAL,
    [Mf,Mp,Mo]=visualize1m(N,t2,f,f0,t1,rhov,Av,0,KB1,KB2,obs,Nmax,debug,...
        POS,PAPERPOS);
end;
while stop==0, %nth iteration
    n=n+1;
    Av(:,J+1)=A; % step 1: compute Av^{(n)}
    for j=J:-1:1,
        U=eye(NL);
        for m=M:-1:1,
            fi=(-i/lambda(m))*(Av(:,j+1)')*L{m+1}*rhov(:,j+1);
            fi=fi-dt/(2*lambda(m))*(Av(:,j+1)')*LOm{m}*rhov(:,j+1);
            Um=prop(NL,V{m+1},e{m+1}/2,real(fi),dt);
            U=(Um')*U*(Um');
        end;
    end;
end;

```

```

end;
Av(:,j)=UD2*(U0')*U*(U0')*UD2*Av(:,j+1);
end;
rhov(:,1)=rho0; % step 2: compute new rhov^{(n)}
O(1)=A'*rho0;
for j=1:J,
    U=eye(NL);
    for m=M:-1:1,
        f(m,2*j-1)=(-i/lambda(m))*(Av(:,j)')*L{m+1}*rhov(:,j);
        f(m,2*j) =f(m,2*j-1)+dt/(2*lambda(m))*(Av(:,j)')*L0m{m}*rhov(:,j);
        Um=prop(NL,V{m+1},e{m+1}/2,real(f(m,2*j)),dt);
        U=Um*U*Um;
    end;
    rhov(:,j+1)=UD*U0*U*U0*UD*rhov(:,j);
    O(j+1)=A'*rhov(:,j+1);
end;
for m=1:M,
    f(m,2*J+1)=-i*(Av(:,J+1)')*L{m+1}*rhov(:,J+1)/lambda(m);
end;
stop=+(n>=Nmax)+(O(J+1)-Oold<delta);
% stop if n>=Nmax or O(J+1)-Oold<delta
if (O(J+1)-Oold)<0,
    f=fold;
end;
if VISUAL,
    [Mf,Mp,Mo]=visualize1m(N,t2,f,t1,rhov,Av,O,KB1,KB2,obs,Mf,Mp,Mo,n,debug);
end;
yield=[yield, O(J+1)/KB2];
Oold=O(J+1);
fold=f;
%keyboard
end;

```

```

function [Mf,Mp,Mo]=visualize1m(N,t1,f,f0,t2,rhov,Av,O,KB1,KB2,obs,Nmax,...
                                         debug,POS,PAPERPOS);
[Mf,Mp,Mo]=visualize1m(N,t1,f,f0,t2,rhov,Av,O,KB1,KB2,obs,Nmax,debug,...
                                         POS,PAPERPOS);

```

```

J=length(t2)-1;
TITLE=sprintf('After %i iterations',0);
PLEGEND=cell(1,N);
OLEGEND=cell(1,3);
OLEGEND{1}=sprintf('%s',obs);
OLEGEND{2}=sprintf('kin. upper bound %5.2f',KB2);
OLEGEND{3}=sprintf('kin. lower bound %5.2f',KB1);

```

```

%old fixed figure position
%POS{1}=[320 950 350 250];
%POS{2}=[670 950 350 250];
%POS{3}=[1020 950 350 250];

```

```

%POS{4}=[670 190 700 350];

for index=1:N,
    PLEGEND{index}=sprintf('Population %i',index);
end;
H1=figure(1);
    set(H1,'Position',POS{1});
    set(H1,'PaperPosition',PAPERPOS{1});
    set(H1,'Name','Fig. 1: Control Field(s)');
    Mf=moviein(Nmax+1);
    [M,dummy]=size(f);
    for m=1:M,
        subplot(M,1,m);
        plot(t1,real(f(m,:)));
        YLABEL=sprintf('Control Field %i (arb. units)',m);
        xlabel('Time (fs)');
        ylabel(YLABEL);
        title(TITLE);
    end;
    Mf(:,1)=getframe(H1);
H2=figure(2);
    set(H2,'Position',POS{2});
    set(H2,'PaperPosition',PAPERPOS{1});
    set(H2,'Name','Fig. 2: Evolution of the Populations');
    Mp=moviein(Nmax+1);
    plot(t2,real(rhov([1:N+1:N*N],:)));
    title(TITLE);
    xlabel('Time (fs)');
    ylabel('Populations');
    legend(PLEGEND,0);
    Mp(:,1)=getframe(H2);
H3=figure(3);
    set(H3,'Position',POS{3});
    set(H3,'PaperPosition',PAPERPOS{1});
    set(H3,'Name','Fig. 3: Evolution of the Observable');
    Mo=moviein(Nmax+1);
    plot(t2,real(0),t2,KB2*ones(size(t2)),t2,KB1*ones(size(t2)));
    xlabel('Time (fs)');
    ylabel('Observable (arb. units)');
    title(TITLE);
    legend(OLEGEND,0);
    Mo(:,1)=getframe(H3);
if debug==1,
    H4=figure(4);
    set(H4,'Position',POS{4});
    set(H4,'PaperPosition',PAPERPOS{4});
    set(H4,'Name','          Fig. 4: Other information          ');
end;
if ~isempty(f0),
    H7=figure(7);
    set(H7,'Position',POS{7});

```

```

set(H7,'PaperPosition',PAPERPOS{7});
set(H7,'Name','Fig. 7: Initial Field f_0');
for m=1:M,
    subplot(M,1,m);
    plot(t1,real(f0(m,:)));
    YLABEL=sprintf('Initial Control Field %i (arb. units)',m);
    xlabel('Time (fs)');
    ylabel(YLABEL);
end;
end;

function [Mf,Mp,Mo]=visualizem(N,t1,f,t2,rhov,Av,0,KB1,KB2,obs,Mf,Mp,Mo,n,debug);
% function visualizem(N,t1,f,t2,rhov,Av,0,KB1,KB2,obs,Mf,Mp,Mo,n,debug);
%
J=length(t2)-1;
TITLE=sprintf('After %i iterations',n);
PLEGEND=cell(1,N);
for index=1:N,
    PLEGEND{index}=sprintf('Population %i',index);
end;
OLEGEND=cell(1,3);
OLEGEND{1}=sprintf('%s',obs);
OLEGEND{2}=sprintf('kin. upper bound %5.2f',KB2);
OLEGEND{3}=sprintf('kin. lower bound %5.2f',KB1);
H1=figure(1);
[M,dummy]=size(f);
for m=1:M,
    subplot(M,1,m);
    plot(t1,real(f(m,:)));
    YLABEL=sprintf('Control field %i (arb. units)',m);
    title(TITLE);
    xlabel('Time (fs)');
    ylabel(YLABEL);
end;
Mf(:,n+1)=getframe(H1);
H2=figure(2);
plot(t2,real(rhov([1:N+1:N*N],:)));
title(TITLE);
xlabel('Time (fs)');
ylabel('Populations');
legend(PLEGEND,0);
Mp(:,n+1)=getframe(H2);
H3=figure(3);
plot(t2,real(0),t2,KB2*ones(size(t2)),t2,KB1*ones(size(t2)));
TITLEB=sprintf('After %i iterations (yield=%4.2f percent)',n,100*0(J+1)/KB2);
title(TITLEB);
xlabel('Time (fs)');
ylabel('Observable (arb. units)');
legend(OLEGEND,0);

```

```
Mo(:,n+1)=getframe(H3);
if debug==1,
figure(4);
subplot(2,2,1), plot(t2,sum(conj(rhov).*rhov));
xlabel('Time (fs)');
ylabel('Norm of rhov');
title(TITLE);
subplot(2,2,2), plot(t2,sum(conj(Av).*Av));
xlabel('Time (fs)');
ylabel('Norm of Av');
title(TITLE);
subplot(2,2,3), plot(t2,sum(conj(Av).*rhov));
xlabel('Time (fs)');
ylabel('Av*rhov');
title(TITLE);
subplot(2,2,4), plot(t1,imag(f));
xlabel('Time (fs)');
ylabel('Control Field, imag. part (arb. units)');
title(TITLE);
end;
```

APPENDIX E
AUXILLARY SUBROUTINES

```
H=cell(1);
rho0=[];
obs=[];
A=[];
t0=[];
tF=[];
gd=[];
g=[];
Gamma=[];
KB1=[];
KB2=[];
rn=[];
controllable=[];
N=[];
M=[];
lambda=[];
J=[];
f0=[];
delta=1e-8;
Nmax=20;
debug=0;

FONTSIZE=8;
%new screen-size dependend figure positions
screen=get(0,'ScreenSize');
w=screen(3);
h=screen(4);
% virtual screen / hell settings
POS{1}=[0.180*w 0.72*h 0.22*w 0.22*h];
POS{2}=[0.405*w 0.72*h 0.22*w 0.22*h];
POS{3}=[0.630*w 0.72*h 0.22*w 0.22*h];
POS{4}=[0.405*w 0.109*h 0.44*w 0.27*h];
POS{5}=[0.180*w 0.436*h 0.22*w 0.22*h];
POS{6}=[0.405*w 0.436*h 0.44*w 0.22*h];
POS{7}=[0.180*w 0.159*h 0.22*w 0.22*h];
% no virtual screen / cone settings
%POS{1}=[0.090*w 0.67*h 0.25*w 0.28*h];
%POS{2}=[0.345*w 0.67*h 0.25*w 0.28*h];
%POS{3}=[0.600*w 0.67*h 0.25*w 0.28*h];
%POS{5}=[0.090*w 0.35*h 0.25*w 0.28*h];
%POS{6}=[0.345*w 0.35*h 0.50*w 0.28*h];
%POS{7}=[0.090*w 0.05*h 0.25*w 0.28*h];
%POS{4}=[0.345*w 0.05*h 0.50*w 0.28*h];
%
% paper positions
PAPERPOS{1}=[2 4 4.6666 3.3333];
```

```

PAPERPOS{2}=[2 4 4.6666 3.3333];
PAPERPOS{3}=[2 4 4.6666 3.3333];
PAPERPOS{4}=[2 4 7 6.5];
PAPERPOS{5}=[2 4 4.6666 3.3333];
PAPERPOS{6}=[2 4 4.6666 3.3333];
PAPERPOS{7}=[2 4 4.6666 3.3333];
MITEM{1}='Enter or modify control system data';
MITEM{2}='Load control system data from disk';
MITEM{3}='Display control system data';
MITEM{4}='Modify control parameters';
MITEM{5}='Determine kinematical bounds';
MITEM{6}='Check controllability';
MITEM{7}='Find optimal control, populations and evolution of the observable';
MITEM{8}='Compute optimal control and yield for a range of lambda-values';
MITEM{9}='Select a movie to play';
MITEM{10}='Visualize optimal control vs. lambda';
MITEM{11}='Save data and print figures to disk';
MITEM{12}='Command window';
MITEM{13}='Clean up workspace (i.e., clear variables and close figures)';
MITEM{14}='Quit this program';

function [sysName,H,M,rho0,A,obs,t0,tF,gd,g,KB1,KB2]=InputSystemData(H,M,...
                                                                    rho0,A,obs,t0,tF,gd,g,KB1,KB2);
promptA{1}='System name (please no spaces or special characters):'
promptA{2}='Number of independent control fields:';
answerA=inputdlg(promptA)
if isempty(answerA),
    return;
end;
sysName=answerA{1};
M=str2num(answerA{2});

TITLE=sprintf('System %s',sysName);
if ~isempty(H{1}),
    prompt{1}=sprintf('Internal Hamiltonian %s',mat2str(H{1}));
    for m=1:length(H)-1,
        prompt{m+1}=sprintf('Interaction Hamiltonian %i: %s',m,mat2str(H{m+1}));
    end;
    for m=length(H):M,
        prompt{m+1}=sprintf('Interaction Hamiltonian for field %i',m);
    end;
else
    prompt{1}=sprintf('Internal Hamiltonian');
    for m=1:M,
        prompt{m+1}=sprintf('Interaction Hamiltonian for field %i',m);
    end;
end;
if ~isempty(rho0),
    prompt{M+2}=sprintf('Density matrix for initial state rho_0=%s',mat2str(rho0));

```

```

else
    prompt{M+2}='Density matrix for initial state rho_0: ';
end;
if ~isempty(obs),
    prompt{M+3}=sprintf('Observable (name as you wish it to appear on plots, ...
                        etc.): %s',obs);
else
    prompt{M+3}='Observable (name as you wish it to appear on plots, etc.): ';
end;
if ~isempty(A),
    prompt{M+4}=sprintf('Matrix representation of observable %s:',mat2str(A));
else
    prompt{M+4}='Matrix representation of observable: ';
end;
if ~isempty(t0),
    prompt{M+5}=sprintf('Initial time t_0=%i:',t0);
else
    prompt{M+5}='Initial time t_0: ';
end;
if ~isempty(tF),
    prompt{M+6}=sprintf('Final time t_F=%i:',tF);
else
    prompt{M+6}='Final time tF';
end;
if ~isempty(gd),
    prompt{M+7}=sprintf('Dephasing operator: gd=%s\n ...
                        Leave blank if no dephasing',mat2str(gd));
else
    prompt{M+7}=sprintf('Dephasing operator: undefined\n ...
                        Leave blank if no dephasing');
end;
if ~isempty(g),
    prompt{M+8}=sprintf('Population relaxation operator: g=%s\n ...
                        Leave blank if no population relaxation',mat2str(g));
else
    prompt{M+8}=sprintf('Population relaxation operator: undefined\n ...
                        Leave blank if no population relaxation');
end;
if ~isempty(KB1),
    prompt{M+9}=sprintf('Lower bound for observable: %f',KB1);
else
    prompt{M+9}=sprintf('Lower bound for observable (optional): undefined');
end;
if ~isempty(KB2),
    prompt{M+10}=sprintf('Upper bound for observable: %f',KB2);
else
    prompt{M+10}=sprintf('Upper bound for observable (optional): undefined');
end
answer=inputdlg(prompt,TITLE)

if isempty(answer)          % return to menu

```

```

    disp('answer is empty');
    return;
end;

if isempty(H{1}) ! ~isempty(str2num(answer{1})),
    H{1}=str2num(answer{1});
end;
while isempty(H{1}),
    res=inputdlg('Please enter valid Hamiltonian H_0');
    H{1}=str2num(res{1});
end;
N=length(H{1});

for m=1:M,
    if isempty(H{m+1}) ! ~isempty(str2num(answer{m+1})),
        H{m+1}=str2num(answer{m+1});
    end;
    while isempty(H{m+1}),
        res=inputdlg(sprintf('Please enter valid Hamiltonian H_%i',m));
        H{m+1}=str2num(res{1});
    end;
end;

if isempty(rho0) | ~isempty(str2num(answer{M+2})),
    rho0=str2num(answer{M+2});
end;
while isempty(rho0),
    res=inputdlg('Please enter valid initial density matrix');
    rho0=str2num(res{1});
end;

if isempty(obs) | ~isempty(answer{M+3}),
    obs=answer{M+3};
end;

if isempty(A) | ~isempty(str2num(answer{M+4})),
    A=str2num(answer{M+4});
end;
while isempty(A),
    res=inputdlg('Please enter valid observable matrix');
    A=str2num(res{1});
end;

if isempty(t0) | ~isempty(str2num(answer{M+5})),
    t0=str2num(answer{M+5});
end;
while isempty(t0),
    res=inputdlg('Please enter valid initial time');
    t0=str2num(res{1});
end;

```

```

if isempty(tF) | ~isempty(str2num(answer{M+6})),
    tF=str2num(answer{M+6});
end;
while isempty(tF),
    res=inputdlg('Please enter valid target time');
    tF=str2num(res{1});
end;
save(sysName,'H','rho0','obs','A','t0','tF');

%Optional arguments:

if ~isempty(answer{M+7}),
    gd=str2num(answer{M+7});
    while isempty(gd)
        res=inputdlg('Please enter valid dephasing matrix!');
        gd=str2num(res{1});
    end;
    save(sysName,'gd','-APPEND');
elseif exist('gd','var'),
    save(sysName,'gd','-APPEND');
end;

if ~isempty(answer{M+8}),
    g=str2num(answer{M+8});
    while isempty(g)
        res=inputdlg('Please enter valid population relaxation matrix!');
        g=str2num(res{1});
    end;
    save(sysName,'g','-APPEND');
elseif exist('g','var'),
    save(sysName,'g','-APPEND');
end;

if ~isempty(answer{M+9}),
    KB1=str2num(answer{M+9});
    while isempty(KB1)
        res=inputdlg('Please enter valid lower bound!');
        KB1=str2num(res{1});
    end;
    save(sysName,'KB1','-APPEND');
elseif exist('KB1','var'),
    save(sysName,'KB1','-APPEND');
end;

if ~isempty(answer{M+10}),
    KB2=str2num(answer{M+10});
    while isempty(KB2)
        res=inputdlg('Please enter valid upper bound!');
        KB2=str2num(res{1});
    end;
    save(sysName,'KB2','-APPEND');

```

```

elseif exist('KB2','var'),
    save(sysName,'KB2','-APPEND');
end;

```

```

function [sysName,H,M,rho0,A,obs,t0,tF,gd,g,KB1,KB2,f0]=LoadSystemData(H,M,...
                                                                    \rho0,A,obs,t0,tF,gd,g,KB1,KB2);

[datafile,pathname]=uigetfile('*.mat');
if (datafile~=0),
    load(sprintf('%s%s%s',pathname,filesep,datafile));
    sysName=datafile(1:findstr('.mat',datafile)-1);
    M=length(H)-1;
end;

```

```

function DisplaySystemData(sysName,H,M,rho0,A,obs,t0,tF,gd,g,KB1,KB2,rn,...
                                                                    controllable);

TITLE=sprintf('System %s',sysName);
prompt{1}=sprintf('Internal Hamiltonian %s',mat2str(H{1}));
for m=1:M,
    prompt{m+1}=sprintf('Interaction Hamiltonian %i: %s',m,mat2str(H{m+1}));
end;
prompt{M+2}=sprintf('Density matrix for initial state rho_0=%s',mat2str(rho0));
prompt{M+3}=sprintf('Observable A=%s (%s)',mat2str(A),obs);
prompt{M+4}=sprintf('Initial time t_0=%i',t0);
prompt{M+5}=sprintf('Final time t_F=%i',tF);
if exist('gd','var'),
    prompt{M+6}=sprintf('Dephasing operator: gd=%s',mat2str(gd));
else
    prompt{M+6}=sprintf('Dephasing operator: undefined');
end;
if exist('g','var'),
    prompt{M+7}=sprintf('Population relaxation operator: g=%s',mat2str(g));
else
    prompt{M+7}=sprintf('Population relaxation operator: undefined');
end;
if exist('KB1','var'),
    prompt{M+8}=sprintf('Lower bound for observable: %f',KB1);
else
    prompt{M+8}=sprintf('Lower bound for observable: undefined');
end;
if exist('KB2','var')
    prompt{M+9}=sprintf('Upper bound for observable: %f',KB2);
else
    prompt{M+9}=sprintf('Upper bound for observable: undefined');
end
if ~isempty(controllable),

```

```

    if controllable==0,
        prompt{M+10}=sprintf('not controllable (dim. of Lie alg.=%i)',rn);
    else
        prompt{M+10}=sprintf('controllable');
    end;
end;
msgbox(prompt);

function [lambda,J,f0,delta,Nmax,debug]=ModifyCtrlParam(lambda,J,f0,delta,...
                                                    Nmax,debug);

if ~isempty(J),
    prompt{1}=sprintf('Time grid constant J=%i',J);
else
    prompt{1}=sprintf('Time grid constant J=');
end;
if ~isempty(lambda),
    prompt{2}=sprintf('Control parameter lambda=%i',lambda);
else
    prompt{2}=sprintf('Control parameter lambda=');
end;
%if ~isempty(f0),
%    prompt{3}=sprintf('Initial control (2J+1 samples) f_0=%s',mat2str(f0));
%else
    prompt{3}=sprintf('Initial control f_0');
%end;
prompt{4}=sprintf('delta=%f',delta);
prompt{5}=sprintf('Maximum number of iterations N_max=%i',Nmax);
prompt{6}=sprintf('compute norm of rhov, Av, etc., (Yes=1,No=0) [%i]',debug);
answer=inputdlg(prompt);

if isempty(J) | ~isempty(str2num(answer{1})),
    J=str2num(answer{1});
end;
while isempty(J),
    res=inputdlg('Please enter valid J');
    J=str2num(res{1});
end;

if isempty(lambda) | ~isempty(str2num(answer{2})),
    lambda=str2num(answer{2});
end;
while isempty(lambda),
    res=inputdlg('Please enter valid lambda');
    lambda=str2num(res{1});
end;

if ~isempty(str2num(answer{3})),
    if length(str2num(answer{3}))~=2*J+1,
        msgbox('invalid f0 -- ignored');
    end;
end;

```

```

else
    f0=str2num(answer{3});
end;
end;

if ~isempty(str2num(answer{4})),
    delta=str2num(answer{4});
end;

if ~isempty(str2num(answer{5})),
    Nmax=str2num(answer{5});
end;

if isequal(str2num(answer{6}),1),
    debug=1;
end;

```

```

function L=liouv(H);
[r,c]=size(H);
if (r==c) & (H==H'),
    N=r;
    L=zeros(N*N,N*N);
    for j=1:N,
        for k=1:N,
            for m=1:N,
                for n=1:N,
                    r=(j-1)*N+k;
                    s=(m-1)*N+n;
                    L(r,s)=H(j,m)*(k==n)-conj(H(k,n))*(j==m);
                end;
            end;
        end;
    end;
else
    sprintf('Invalid Hamiltonian')
end;

```

```

function G=dissipation(gamma,gammad,N);
G=zeros(N^2);
for l=1:N,
    for k=1:N,
        if (k~=1),
            G(k+(l-1)*N,k+(l-1)*N)=gammad(k,l);
        else
            for m=1:N,
                G(k+(k-1)*N,m+(m-1)*N)=G(k+(k-1)*N,m+(m-1)*N)-gamma(k,m);
            end;
        end;
    end;
end;

```

```

        G(k+(k-1)*N,k+(k-1)*N)=G(k+(k-1)*N,k+(k-1)*N)+gamma(m,k);
    end;
end;
end;
end;

```

```

function yieldplot(yield,figNo,TITLE,POS,PAPERPOS);
figure(figNo);
set(figNo,'Position',POS{figNo});
set(figNo,'PaperPosition',PAPERPOS{figNo});
set(figNo,'Name',sprintf('Fig. %i: %s',figNo,TITLE));
n=length(yield);
if n<26,
    plot([0:n-1],real(yield),'-bo');
else
    plot([0:n-1],real(yield),'-b. ');
end;
xlabel('Number of iterations');
ylabel('Yield');

```

```

function [a,b,ft]=fouriercomp(f,figNo,POS,PAPERPOS);
figure(figNo);
[M,N]=size(f); % N=2J+1;
POS{6}(4)=POS{6}(4)*M;
PAPERPOS{6}(4)=PAPERPOS{6}(4)*M;
set(figNo,'Position',POS{6});
set(figNo,'PaperPosition',PAPERPOS{6});
set(figNo,'Name',sprintf('Fig. %i: Fourier components',figNo));
I=[2:floor(N/2)+1];
for m=1:M,
    ft(m,:)=fft(real(f(m,:)));
    a(m,:)=[ft(m,1)/N, 2*real(ft(m,I))/N];
    b(m,:)=-2*imag(ft(m,I))/N;
    subplot(2*M,1,2*m-1);
    plot([0:floor(N/2)],a);
    set(gca,'FontSize',8);
    xlabel('n','FontSize',8);
    ylabel('a_n','FontSize',8);
    TITLE=sprintf('Fourier components of control function %i',m)
    title(TITLE,'FontSize',8);
    subplot(2*M,1,2*m);
    plot([1:floor(N/2)],b);
    set(gca,'FontSize',8);
    xlabel('n','FontSize',8);
    ylabel('b_n','FontSize',8);
end

```

```

function PlayMovie;
[moviefile,pathname]=uigetfile('*.mat')
if moviefile==0,
    return;
elseif ~exist(sprintf('%s/%s',pathname,moviefile),'file'),
    return;
end;
load(sprintf('%s/%s',pathname,moviefile),'Mf','Mp','Mo','POS');
if ~exist('POS','var'),
    screen=get(0,'ScreenSize');
    w=screen(3);
    h=screen(4);
    POS{1}=[0.180*w 0.72*h 0.22*w 0.22*h];
    POS{2}=[0.405*w 0.72*h 0.22*w 0.22*h];
    POS{3}=[0.630*w 0.72*h 0.22*w 0.22*h];
end;
ans=inputdlg({'How many frames per second? (Default=1)',...
             'How often? (Default=1)'});
if isempty(ans),
    return;
else
    if isempty(str2num(ans{1})),
        fps=1;
    else
        fps=str2num(ans{1});
    end;
    if isempty(str2num(ans{2})),
        repeat=1;
    else
        repeat=str2num(ans{2});
    end;
end;
H1=figure(1),clf;
set(H1,'Position',POS{1});
movie(H1,Mf,repeat,fps,[0 0 0 0]);
[FIELD,FMAP]=frame2im(Mf(length(Mf)));
axes('Position',[0 0 1 1]), image(FIELD), colormap(FMAP), axis off;
H2=figure(2),clf;
set(H2,'Position',POS{2});
movie(H2,Mp,repeat,fps,[0 0 0 0]);
[POP,PMAP]=frame2im(Mp(length(Mp)));
axes('Position',[0 0 1 1]), image(POP), colormap(PMAP), axis off;
H3=figure(3),clf;
set(H3,'Position',POS{3});
movie(H3,Mo,repeat,fps,[0 0 0 0]);
[OBS,OMAP]=frame2im(Mo(length(Mo)));
axes('Position',[0 0 1 1]), image(OBS), colormap(OMAP), axis off;

```

```
function [f,yield]=LambdaRange(f0,rho0,A,obs,L,Gamma,lambda,KB1,KB2,t0,tF,J,...
```

delta,Nmax);

```
ans=inputdlg('Enter lambda values:');
if isempty(ans),
    return;
elseif isempty(str2num(ans{1})),
    sprintf('Invalid lambda');
    return;
else
    lambda=str2num(ans{1});
end;
[fname,fpath]=uiputfile('*.mat');
for n=1:length(lambda),
    l=lambda(:,n);
    [f{n},yield{n}]=ZRcontrol(f0,rho0,A,obs,L,l,KB1,KB2,t0,tF,J,delta,Nmax,...
                                0,0,0,0);
end;
t=[t0:(tF-t0)/(2*J):tF];
save(sprintf('%s/%s',fpath,fname),'t','f','yield','lambda');
```

```
function VisualLambdaRange(POS,PAPERPOS);
[fname,fpath]=uigetfile('*.mat');
load(sprintf('%s/%s',fpath,fname),'t','f','yield','lambda');
H1=figure(1);
set(H1,'Position',POS{1});
set(H1,'PaperPosition',PAPERPOS{1});
H5=figure(5);
set(H5,'Position',POS{5});
set(H5,'PaperPosition',PAPERPOS{5});
y=[];
figure(1);
for n=1:length(lambda),
    plot(t,f{n}),
    xlabel('Time (fs)'),
    ylabel(sprintf('Field after %i iterations (arb. units)',length(yield{n})-1)),
    title(sprintf('lambda=%f',lambda(n))),
    waitforbuttonpress,
    y=[y real(yield{n}(length(yield{n})))];
end;
figure(5);
plot(lambda,y);
xlabel('lambda');
ylabel('Yield');
```

BIBLIOGRAPHY

- [1] W. Warren, H. Rabitz, and M. Dahleh, *Science* 259, 1581 (1993).
- [2] S. Chelkowski, A. Bandrauk, and P. B. Corkum, *Phys. Rev. Letters* 65, 2355 (1990).
- [3] S. Chelkowski and A. D. Bandrauk, *Phys. Rev. A* 41, 6480 (1990).
- [4] M. E. Goggin and P. W. Milonni, *Phys. Rev. A* 37, 796 (1988).
- [5] V. S. Letokhov, *Nonlinear Laser Chemistry* (Springer Verlag, Berlin, 1983), chap. 5.
- [6] N. Bloembergen and A. H. Zewail, *J. Chem. Phys.* 88, 5459 (1984).
- [7] J. von Neumann, *Mathematical Foundations of Quantum Mechanics* (Princeton University Press, Princeton, New Jersey, 1955).
- [8] Y. Yan *et al.*, *J. Phys. Chem.* 97, 2320 (1993).
- [9] P. Gaspard and P. van Ede van der Pals, in *Towards the Harnessing of Chaos*, edited by M. Yamaguti (Elsevier Science, B.V., 1994), p. 205.
- [10] K. G. Kim and M. D. Girardeau, *Phys. Rev. A* 52, R891 (1995).
- [11] W. Zhu and H. Rabitz, *J. Chem. Phys.* 109, 385 (1998).
- [12] H. Rabitz, in *Few-Body Problems in Physics* (AIP Conf. Proc., Am. Inst. Phys., 1995), Vol. 334, p. 160.
- [13] S. H. Tersigni, P. Gaspard, and S. A. Rice, *J. Chem. Phys.* 93, 1670 (1990).
- [14] R. Kosloff *et al.*, *J. Chem. Phys.* 139, 201 (1989).
- [15] R. Balian and M. Vénéroni, *Phys. Rev. Lett.* 47, 1353 (1981).
- [16] M. D. Girardeau, S. G. Schirmer, J. V. Leahy, and R. M. Koch, *Phys. Rev. A* 58, 2684 (1998).
- [17] M. Girardeau, M. Ina, S. Schirmer, and T. Gulsrud, *Phys. Rev. A* 55, R1565 (1997).
- [18] S. G. Schirmer, M. D. Girardeau, and J. V. Leahy, *Phys. Rev. A* 61, ? (2000).
- [19] V. Ramakrisna *et al.*, *Phys. Rev. A* 51, 960 (1995).

- [20] A. G. Butkovskiy and Y. I. Saimolenko, *Control of Quantum-Mechanical Processes and Systems* (Kluwer Academic, Dordrecht, 1990).
- [21] V. Jurdjevic and H. J. Sussmann, *J. Diff. Eq.* 12, 313 (1972).
- [22] S. Shi and H. Rabitz, *Comp. Phys. Comm.* 63, 71 (1991).
- [23] J. E. Combariza, B. Just, J. Manz, and G. K. Paramonov, *J. Phys. Chem.* 95, 10351 (1991).
- [24] J. Somloi, V. A. Kazakov, and D. J. Tannor, *Chem. Phys.* 172, 85 (1993).
- [25] M. Ina, Ph.D. thesis, University of Oregon, 1996.
- [26] Y. Ohtsuki, W. Zhu, and H. Rabitz, *J. Chem. Phys.* 110, 9825 (1999).
- [27] M. Suzuki, *Physics Letters A* 146, 319 (1990).
- [28] M. Q. Phan and H. Rabitz, *J. Chem. Phys.* 110, 34 (1999).